Studies on the Regulation Mechanism of Ligand Binding Reactions in Heme Proteins(Dissertation_全文)

AUTHOR(S):

Uchida, Takeshi

STUDIES ON THE REGULATION MECHANISM OF LIGAND BINDING REACTIONS IN HEME PROTEINS

TAKESHI UCHIDA

1998

STUDIES ON THE REGULATION MECHANISM OF LIGAND BINDING REACTIONS IN HEME PROTEINS

TAKESHI UCHIDA

Department of Molecular Engineering
Graduate School of Engineering
Kyoto University

1998

PREFACE

Structures of proteins in solutions are not rigid as the crystal structure revealed, but are fluctuating and flexible. Proteins under physiological condition are supposed to have a substantial number of conformational substates and transitions from one substate to another are also induced, breaking and reforming non-covalent bonds and changing the structure continuously. Such structural transitions in the conformational substates are referred to as protein dynamics. The experimental description of the protein dynamics and discovery of new relations to biological function have fascinated many researchers in biological science. One of the clues for these difficult tasks may come from studies on ligand binding to heme proteins, bearing the common active site, heme, as the reaction center, since the ligand binding reaction of hemoproteins have been subjects of extensive studies in biophysical chemistry. However, the factors which regulate the ligand binding reaction have not been completely understood yet and essential problems to be solved have still remained. In this thesis, combined with site-directed mutagenesis, the author applied various techniques of the spectroscopies to the ligand binding in myoglobin, which is one of the small hemoproteins and can reversibly bind some gaseous ligand such as oxygen and carbon monoxide, to elucidate the molecular mechanism for the dynamics in the ligand binding of hemoproteins.

This thesis contains collected papers and discussions of the author's study at Department of Molecular Engineering, Graduate School of Engineering, Kyoto University, 1992-1998, and is divided into five parts. Part I contains a survey of hemoproteins and affords sufficient background and significance of these studies. Part II deals with the restriction of the protein dynamics in the ligand binding for myoglobin and revealed the significance of protein dynamics in the ligand entry process. In part III, the hydrophobicity in the heme pocket and electrostatic interaction between the distal histidine and amino acid inside the heme pocket were examined as key factors for the ligand binding reaction in myoglobin. It was made clear that the heme pocket structure is related to the bond formation process. Part IV provides studies on the dynamics of a protein other than myoglobin. CO binding kinetics of a new heme-containing transcriptional activator, CooA, has been investigated to clarify the activation mechanism induced by CO binding. Finally,

summary and general aspects of the present work are discussed in Part V.

ACKNOWLEDGMENTS

It is author's pleasure to acknowledge profound indebtedness to Professor Isao Morishima for his continual guidance, criticism, and encouragement. The author also wishes to express his sincere gratitude to Associate professor Koichiro Ishimori and Dr. Takahashi for their guidance and fruitful discussions throughout the course of this study. He would like to acknowledge Professor Yoshihito Watanabe for his valuable discussion

It should be emphasized that the studies in this thesis have required the cooperation with a number of groups of investigation. Grateful acknowledgment is Dr. Yoshitsugu Shiro and Professor Tetsuro Iizuka (laser photolysis measurement), Dr. Yoshinao Wada (FAB-mass measurements), Professor Teizo Kitagawa (resonance Raman measurements). The author is also obliged to Dr. Unno for his valuable suggestion and warmhearted encouragement.

This work would not have been possible without help of the colleagues in the molecular design group. Mr. Haruto Ishikawa participated in some of the work presented here are greatly appreciated. The author is also indebted to Drs. Shinji Ozawa, Shingo Nagano, and Keisuke Wakasugi, and Messrs. Masakazu Hashimoto, Hiroshi Tsurumaki, Kenji Machii, Masaaki Aoki, Eigo Sakamoto, Toshitaka Matsui, Kenji Inaba, Tatsuya Murakami, Taro Ichikawa, Motomasa Tanaka, Yoshio Goto, Mitihiro Izuta, Takaki Hatsui, Yoichi Sugiyama, Siro Yoshioka, Jin Nakatani, Masahiro Yamada, Hirotaka Kataoka, Atushi Morimoto, Masaki Ihara, Mitsuru Murata, Yoshiaki Furukawa, Shuji Akiyama, Norihiro Maeda, Jun Inoue, Hiroaki Tanioka, Manabu Teramoto, and Misses. Keiko Matsuda and Shino Kondo. He is also grateful to Mr. Haruyuki Harada for assistance in the NMR measurements.

Finally, the author expresses his sincere gratitude to his family for their unfailing understanding and affectionate encouragement.

January , 1998
Kyoto
Takeshi Uchida

LIST OF PUBLICATION

PART II

CHAPTER 1. The Effects of the Intramolecular Disulfide Bond on Ligand Binding Dynamics in Myoglobin
Uchida, T., Unno, M., Ishimori, K., and Morishima, I. (1997)
Biochemistry **36,** 324-332.

CHAPTER 2. Unusual Pressure Effects on Carbon Monoxide Rebinding to the Human Myoglobin Leucine29 Mutant
Uchida, T., Ishimori, K., & Morishima, I.
Submitted for publication. (*J. Biol. Chem.*).

PART III

CHAPTER 1. The Effects of Hydrophobicity of Heme Pocket on the Ligand Binding Dynamics in Myoglobin as Studied with Leucine29 Mutants
Uchida, T., Ishimori, K., & Morishima, I. (1997)
J. Biol. Chem. **272,** 30108-30114

CHAPTER 2. The Role of Interaction between Distal Histidine and Thr67 on the Ligand Binding Dynamics in Myoglobin
Uchida, T., Nagano, S., Ishimori, K., & Morishima, I.
Submitted for publication. (*Biochemistry*)

PART IV

CHAPTER 1. Coordination Structure of CO to the Transcriptional Activator, CooA, Studied by Resonance Raman Spectroscopy and Ligand Binding Kinetics
Uchida, T., Takahashi, S., Ishimori, K., Morishima, I., Ohkubo, K., Nakajima, H., and Aono, S.
Submitted for publication. (*J. Biol. Chem.*).

CHAPTER 2. A kinetic Study of CO Binding to a CO-sensing Transcriptional Activator, CooA by Flash Photolysis
Uchida, T., Takahashi, S., Ishimori, K., Morishima, I., Ohkubo, K., Nakajima, H., and Aono, S.
Submitted for publication. (*J. Biol. Chem.*).

CONTENTS

PART I.

GENERAL INTRODUCTION

GENERAL INTRODUCTION

Proteins are the most abundant macromolecules in living cells and occur in all the cells and all parts of cells. To understand cellular processes, knowledge of the three-dimensional structures of proteins is vital. X-ray diffraction has provided detailed informations on the relationship between the structure and function. However, proteins in solutions are not in rigid structures as the x-ray diffraction revealed, but are substantially fluctuating systems. In solution, protein consists of a number of conformational substates and transitions between the conformational substates occur (Ansari et al., 1985; Ehrenberg et al., 1987; Frauenfelder et al., 1988, 1991). Since proteins have such a large number of nearly isoenergetic but slight different structures, the side chains of the amino acids can be in slightly different positions, rotation about single bonds, or shifts of hydrogen bonds may occur, which leads to unexpected reactivity of proteins based on the crystal structure. These transitions between the conformational substates are referred to as protein dynamics. It is, therefore, significant and essential to understand the biological function of protein based on the protein dynamics as well as on the structures by x-ray diffraction studies.

One of the crucial reactions to understand how the protein dynamics of a protein affects its function, is the ligand binding to oxygen storage protein, myoglobin. Myoglobin is a simple monomeric protein which consists of 153 amino acid residues and has a molecular weight of 17800 dalton, and has also served as a model protein for ligand binding and substrate binding reactions. The main role of myoglobin is oxygen storage and myoglobin can reversibly bind dioxygen (O_2).

$$MbO_2 \rightleftharpoons Mb + O_2 \qquad (1)$$

The active binding site in myoglobin consists of an iron(II)-containing porphyrin, known as a heme. The heme iron is recessed some 10Å in the protein and buried by the polypeptide structure. As evident by the crystal structure of myoglobin, the protein is so densely packed that there are no obvious pathways from the protein surface into the ligand binding site to allow entrance and exit of O_2 from the solvent (Perutz, 1965; Takano, 1977) (Figure 1).

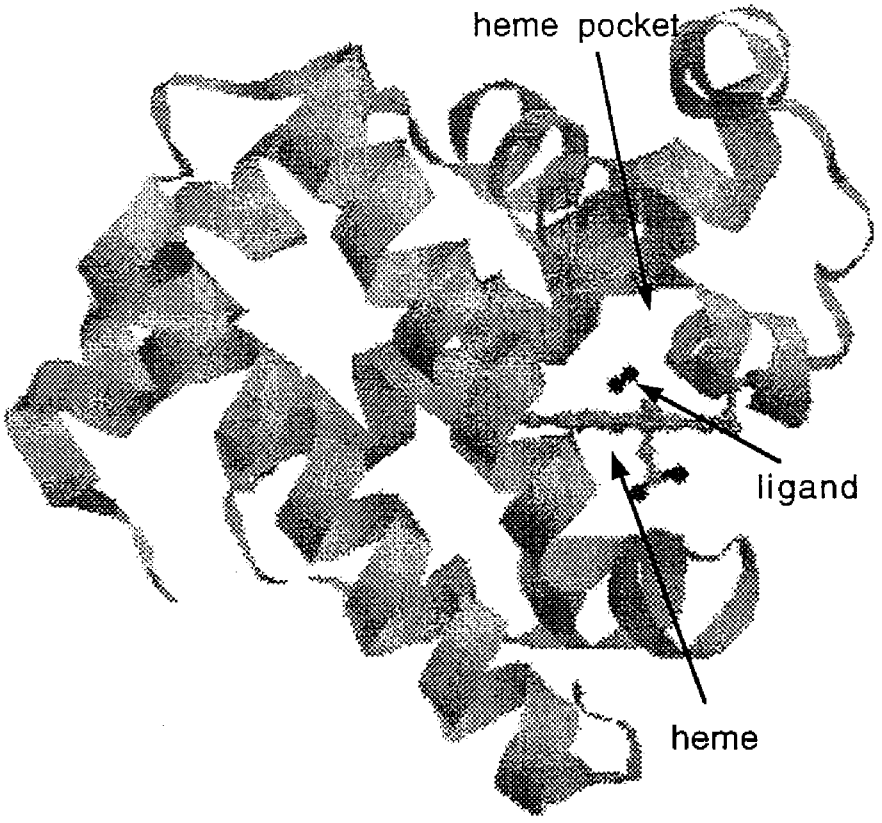

Figure 1: X-ray structure of oxymyoglobin (Phillips, 1980).

To investigate the role of the protein dynamics in the ligand binding to myoglobin, the author perturbed the protein dynamics by two approaches. One is introduction of an artificial intramolecular linkage into myoglobin as discussed in Part II. The author intended to restrict the protein dynamics by introducing an intramolecular covalent bridge into myoglobin to clarify the significance of the protein dynamics in the ligand binding (chapter 1 of Part II). In this mutant protein, an artificial S-S linkage was formed at the EF corner which is a hinge region of the E-, and F-helices (Figure 2). The E-helix contains the amino acid residues forming the distal heme pocket for the ligand binding, and the F-helix contains an axial ligand of the heme. This region showed a large B-factor of the x-ray crystal structure, which reflects the large structural fluctuations (Frauenfelder et al., 1979). Thus, perturbation of the fluctuations in this region would affect the ligand binding properties of myoglobin, which offers unique information for dynamics of the ligand binding.

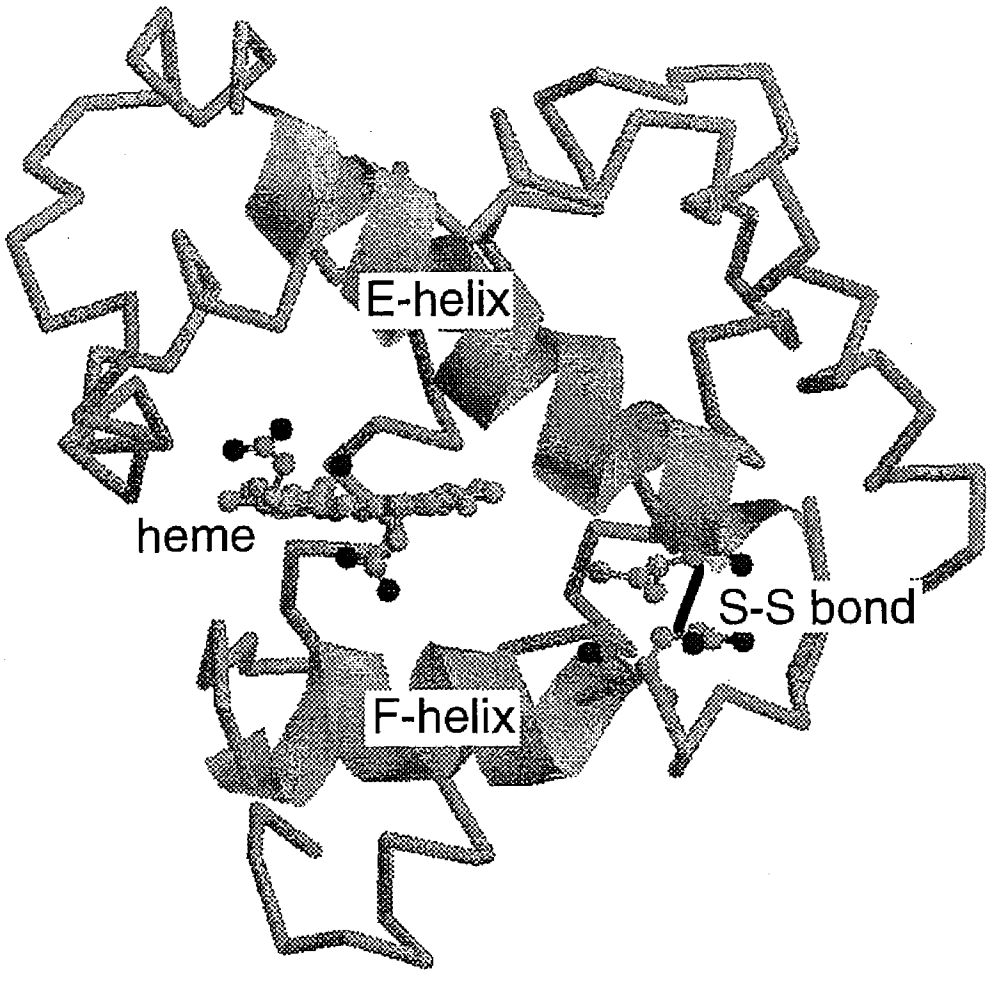

Figure 2: Introduction site of the S-S bond in myoglobin.

The second approach is an application of the hydrostatic pressure into the ligand binding kinetics. High pressure can affect a wide variety of biological processes (Zipp & Kauzmann, 1973; van Eldik et al., 1989; Lange et al., 1994; Gross & Jaenicke, 1994) and can be a powerful tool in the investigation of their mechanism (Frauenfelder et al., 1990; Mozhaev et al., 1994, 1996). The measurements of the pressure dependence of the ligand binding kinetics provide the activation volume ($\Delta V^{\neq}$) of the ligand binding reaction (the volume difference between the transition state and the ground state) according to,

$$\frac{\partial \ln k}{\partial P} = -\frac{\Delta V^{*}}{RT} \qquad (2)$$

Since the magnitude of the activation volume results from conformational changes accompanied with the reaction of the protein and also reflects the specific interactions of the transition state with ligands, the volume profile can give a wealth of information on dynamics of the ligand binding process. In chapter 2 of Part II, the author undertook the study of the ligand binding at high pressure to elucidate the role of protein dynamics in the ligand binding.

Protein dynamics of myoglobin would be also regulated by the heme environmental structure (Springer et al., 1994). The histidine located near the ligand binding site (distal histidine) has been considered as one of the crucial factors which would control the ligand binding dynamics. Removal of the imidazole ring in the distal histidine by the replacement with glycine increased the CO binding rate by 10-fold in myoglobin (Rohlfs et al., 1990; Carver et al., 1990), suggesting that the ligand binding is regulated by the steric hindrance of the distal histidine. However, the His→Leu substitution increased the CO binding rate by 50-fold despite of the steric hindrance of the side chain of Leu (Rohlfs et al., 1990; Carver et al., 1990). These findings indicate that the ligand binding was not regulated by the size at position 64, which allows us to speculate the contribution of other factors which would be also crucial for the ligand binding. Recently, non-coordinated water molecules hydrogen-bonded to the distal histidine in deoxy myoglobin were considered to inhibit the ligand movement into the distal pocket (Rohlfs et al., 1990; Quillin et al., 1993, 1995; Springer et al., 1994; Olson & Phillips, 1996, 1997). The 50-fold increase in the CO association rate by substitution of the distal histidine with apolar amino acid, Leu, would be attributed to loss of the non-coordinated water molecules (Rohlfs et al., 1990; Quillin et al., 1993) (Figure 3).

Thus, it is plausible that such water molecules can modulate the heme environmental structure to control the ligand binding in myoglobin. In chapter 1 of Part III, the author focused on the effects of hydrophobicity in the heme pocket on the ligand binding to myoglobin. The x-ray structure of myoglobin has shown that the active site of myoglobin is surrounded by the hydrophobic residues and the hydrophobic heme pocket is formed. Leu29 is one of the amino acids constructing the hydrophobic pocket and located at top of the heme pocket crevice (Figure 4). Replacement of the residue with less hydrophobic residue could reduce hydrophobicity in the heme pocket, which provides an information on the role of the hydrophobic heme pocket in the ligand binding for myoglobin.

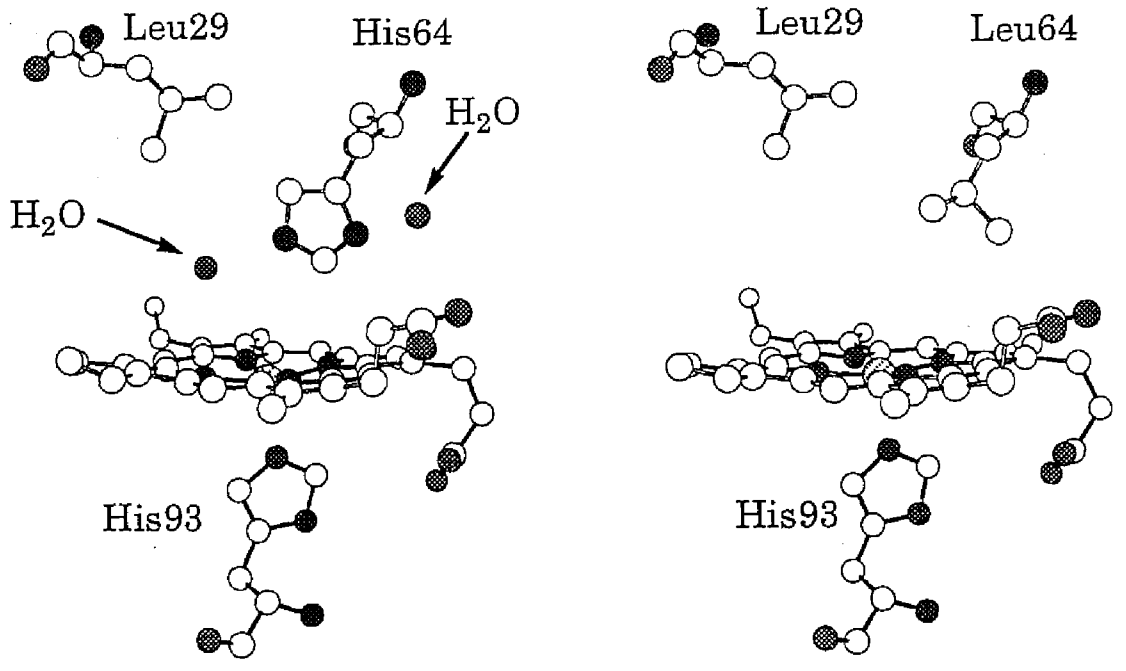

Figure 3: The heme environmental structures of deoxymyoglobins (Quillin et al., 1993). The heme and amino acid residues in the immediate of the heme pocket and water molecules in the heme pocket are shown. (A) wild type myoglobin (B) His64→Leu mutant myoglobin.

In chapter 2 of Part III, the possibility of the regulation of protein dynamics by the electrostatic interaction between the distal histidine and its adjacent residue, Thr67 (Figure 4) was investigated. The distal histidine forms a hydrogen bond with the amino acid residue, such as distal arginine, adjacent to the distal histidine in many peroxidase, which enhances the peroxidase activity (Poulos & Kraut, 1980; Finzel et al., 1984; Nagano et al., 1996). On the other hand, the corresponding amino acid residue adjacent to the distal histidine, Thr67, in myoglobin is not hydrogen bonded to the distal histidine. However, the recent mutational study of Thr67 in myoglobin has suggested the presence of electrostatic interaction between Thr67 and the distal histidine (Nagano et al., to be submitted). We investigated the effect of the electrostatic interaction between the distal histidine and Thr67 in the ligand binding properties and the polarity of the heme pocket through the non-coordinated water molecule.

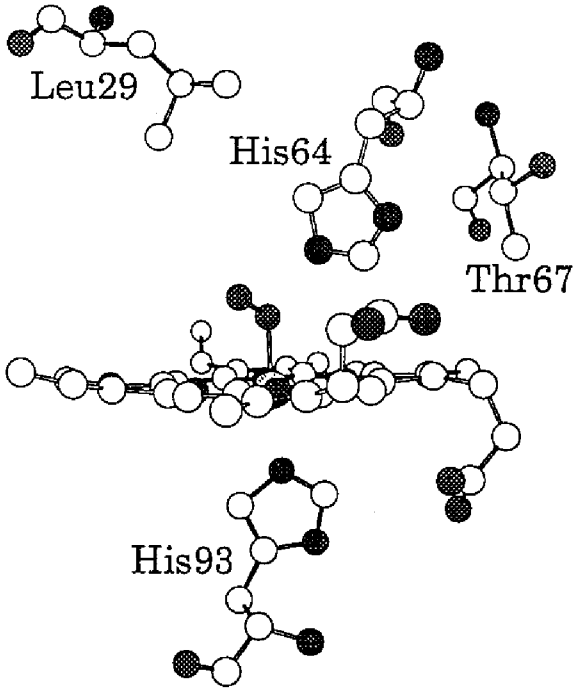

Figure 4: The heme environmental structure of oxymyoglobin (Phillips, 1980). The heme and selected amino acid residues in the presented studies are shown.

The dynamics of the ligand binding are not only essential for the storage and transport of the small gaseous ligand but also one of the key steps for the regulation mechanism in gene expression and signal transduction (Ignarro et al., 1982; Gilles-Gonzalez et al., 1991). CooA is the first heme protein which acts as a DNA-binding transcriptional activator (Aono et al., 1996; Shelver et al., 1997). Only in the presence of CO, CooA can specifically bind to the target DNA (Shelver et al., 1995, 1997; He et al., 1996). It has been accepted that CO binding to the ferrous CooA triggers the conformational changes to the specific DNA binding form. However, experimental evidence for the activation mechanism by CO has not yet been clear due to the lack of the information of the heme environmental structure. The author investigated the coordination structure of the heme iron and axial ligands of CooA by using electronic absorption and resonance Raman spectroscopies in chapter 1 of Part IV. In chapter 2 of Part IV, the author examined the CO binding to ferrous CooA to characterize the ligand binding mechanism and compare with that of myoglobin. These observations would provide us with several new insights into the transcription mechanism in the CooA system.

In this thesis, the author examined ligand binding kinetics of myoglobin and CooA to understand the role of protein dynamics in biological function by various spectroscopies and site-directed mutagenesis. The picture of the protein as rigid macromolecules represented by the x-ray and neutron diffraction techniques would reflect only one side of the picture of the protein acting in solution with fluctuating. To examine protein dynamics is closely related to the understanding of biological function.

REFERENCES

Aono, S., Nakajima, H., Saito, K., & Okada, M. (1996) *Biochem. Biophys. Res. Commun. 228*, 752-756.

Ansari, A., Berendzen, J., Bowne, S. F., Frauenfelder, H., Iben, I. E. T., Sauke, T. B., Shyamsunder, E., & Young, R. D. (1985) *Proc. Natl. Acad. Sci. U.S.A. 82*, 5000-5004.

Carver, T. E., Rohlfs, R. J., Olson, J. S., Gibson, Q. H., Blackmore, R. S., Springer, B. A., & Sligar, S. G. (1990) *J. Biol. Chem. 265*, 20007-20020.

Ehrenberg, A., Rigler, R., Graslund, A., & Nilsson, L. (1987) *Structure, Dynamics, and Function of Biomolecules*, New York, Springer.

Finzel, B. C., Poulos, T., & Kraut, J. (1984) *J. Biol. Chem. 259*, 13027-13036.

Frauenfelder, H., Petsko, G. A., & Tsernoglou, D. (1979) *Nature 280*, 558-563.

Frauenfelder, H., Park, K. D., & Young, R. D. (1988) *Annu. Rev. Biophys. Biophys. Chem. 17*, 451-479.

Frauenfelder, H., Alberding, N. A., Ansari, A., Braunstein, D., Cowen, B. R., Hong, M. K., Iben, I. E. T., Johnson, J. B., Lack, S., Marden, M. C., Mourant, J. R., Olmos, P., Reinisch, L., Scholl, R., Schulte, A., Shyamsunder, E., Sorensen, L. B., Steinback, P. J., Young, R. D., Xie, A., & Yue, K. T. (1990) *J. Phys. Chem. 94*, 1024-1037.

Frauenfelder, H., Sligar, S. G., & Wolynes, P. G. (1991) *Science 254*, 1598-1603.

Gilles-Gonzalez, M. A., Gonzalez, G., & Helinski, D. R. (1991) *Nature 350*, 170-172.

Gross, M., & Jaenicke, R. (1994) *Eur. J. Biochem. 221*, 617-630.He, Y., Shelver, D., Kerby, R. L., & Roberts, G. P. (1996) *J. Biol. Chem. 271*, 120-123.

He, Y., Shelver, D., Kerby, R. L., & Roberts, G. P. (1996) *J. Biol. Chem. 271*, 120-123.

Ignarro, L. J., Degnan, J. N., Baricos, W. H., Kadowitz, P. J., & Wolin, M. S. (1982) *Biochim. Biophys. Acta. 718*, 49-59.

Lange, R., Heiber-Langer, I., Bonfils, C., Fabre, I., Negishi, M., & Balny, C. (1994) *Biophys. J. 66*, 89-98.

Mozhaev, V. V., Heremans, K., Frank, J., Masson, P., & Balny, C. (1994) *TIBTECH 12*, 493-501.

Mozhaev, V. V., Heremans, K., Frank, J., Masson, P., & Balny, C. (1996) *Proteins 24*, 81-91.

Nagano, S., Tanaka, M., Ishomori, K., Watanabe, Y., & Morishima, I. (1996) *Biochemistry 35*, 14251-14258.

Olson, J. S., & Phillips Jr, G. N. (1996) *J. Biol. Chem. 271*, 17593-17596.

Olson, J. S., & Phillips Jr, G. N. (1997) *J. Biol. Inorg. Chem 2*, 544-552.

Perutz, M. F. (1965) *J. Mol. Biol. 13*, 646-668.

Phillips, S. E. V. (1980) *J. Mol. Biol. 142*, 531-554.

Poulos, T. L., & Kraut, J. (1980) *J. Biol. Chem. 255*, 8199-8205.

Quillin, M. L., Arduini, R. M., Olson, J. S., & Phillips Jr., G. N. (1993) *J. Mol. Biol. 234*, 140-155.

Quillin, M. L., Li, T. S., Olson, J. S., Phillips Jr, G. N., Dou, Y., Ikeda-Saito, M., Regan, R., Carlson, M., Gibson, Q. H., Li, H. Y., & Elber, R. (1995) *J. Mol. Biol. 245*, 416-436.

Rohlfs, R. J., Mathews, A. J., Carver, T. E., Olson, J. S., Springer, B. A., Egeberg, K. D., & Sligar, S. G. (1990) *J. Biol. Chem. 265*, 3168-3176.

Shelver, D., Kerby, R. L., He, Y., & Roberts, G. P. (1995) *J. Bacteriol. 177*, 2157-2163.

Shelver, D., Kerby, R. L., He, Y., & Roberts, G. P. (1997) *Proc. Natl. Acad. Sci. U.S.A. 94*, 11216-11220.

Springer, B. A., Sligar, S. G., Olson, J. S., & Phillips Jr., G. N. (1994) *Chem. Rev. 94*, 699-714.

Takano, T. (1977) *J. Mol. Biol. 110*, 537-584.

van Eldik, R., Asano, T., & le Noble, W. J. (1989) *Chem. Rev. 89*, 549-668.

Zipp, A., & Kauzmann, W. (1973) *Biochemistry 21*, 4217-4228.

PART II.

STUDIES ON PROTEIN DYNAMICS

CHAPTER 1.

The Effects of the Intramolecular Disulfide Bond on Ligand Binding Dynamics in Myoglobin

ABSTRACT

In order to investigate the effects of an intramolecular disulfide bond on protein structure and ligand binding dynamics in myoglobin, we prepared a mutant myoglobin having a disulfide bond at the EF corner by introducing two cysteine at the position of Ile75 and Glu85. Based on the spectral features of the mutant, the formation of the disulfide bond only affected minor structural deviations of the heme environmental structure in the carbonmonoxy form, whereas more substantial structural alterations were induced in the deoxygenated form. Laser photolysis experiments for carbon monoxide rebinding clearly showed that the artificial S–S bond accelerates the bimolecular rebinding rate from 1.0 $\mu M^{-1}s^{-1}$ to 1.8 $\mu M^{-1}s^{-1}$ and increases the geminate yield from 0.072 to 0.092. The ligand migration rate from solvent to heme pocket and the bond formation rate from heme pocket to heme iron also increased. The free energy diagram for the mutants indicates that the energy barrier for the bond formation was raised as well as that for the ligand migration by introduction of the disulfide bond. However, the effects of the disulfide linkage at the EF corner on the kinetic parameter is much smaller than those of the amino acid substitutions located in the heme cavity. We can conclude that the perturbation of the protein fluctuations by formation of the disulfide bond would be localized at the mutation site or the contributions from other regions and motions might be more important for the ligand binding dynamics.

INTRODUCTION

The protein fluctuation plays key roles not only in the protein folding, but also in the substrate-binding dynamics for many enzymes (Gurd & Rothgeb, 1979; Karplus & McCammon, 1983). X-ray structures of hemoproteins have shown that there are no ligand entry channels even for small molecules such as oxygen molecule or carbon monoxide (Takano, 1977; Phillips, 1980). This observation implies that the ligand binding process requires protein structural fluctuations. Although a number of the kinetic experiments over wide ranges of time and temperature have enabled us to investigate the effects of the protein fluctuation on the ligand binding dynamics of hemoproteins, molecular mechanisms for regulation of the ligand binding by the protein fluctuation are still unclear (Gibson et al., 1986; Austin et al., 1975; Henry et al., 1983; Olson et al., 1988; Frauenfelder et al., 1991; Steinback et al., 1991; Lambright et al., 1991; Tian et al., 1996).

To elucidate the effect of protein fluctuation on ligand binding, we introduced an artificial disulfide bond into myoglobin (Mb) which is a globular protein of about molecular weight 18000 and 153 amino acid residues and contains one protoheme. Intensive studies on the ligand binding kinetics of myoglobin (Springer et al., 1994 and references therein) have revealed the detailed mechanism of the ligand binding process on the time scales from the picosecond to second, which led myoglobin to be one of the most basic and conventional model systems to examine dynamic properties of proteins. However, most of the previous studies have focused on the regulation mechanism by single or some amino acid residues around the distal or proximal histidine and little attention has been paid to the protein fluctuation including global motion of helices of myoglobin in the ligand binding.

Disulfide bond, which is formed by the oxidation of a pair of cysteine, has been considered to be one of the major structural factors for the protein fluctuation (Kidera et al., 1992; Careaga & Falke, 1992; Daggett & Levitt, 1993; Jeng & Dyson, 1995). Previous studies have shown that introduction of artificial disulfide bonds into a protein molecule enhanced protein stability by lowering the entropy of the unfolding state and enthalpic stabilization of the folded state (Perry & Wetzel, 1984; Pantoliano et al., 1987; Matsumura et al., 1989; Kanaya et al., 1991; Gusev et al., 1991), indicating that a disulfide bond perturbs or restricts the protein fluctuations. Since the protein fluctuation should be essential to protein

function as well as to stabilize protein structure, introduction of disulfide bonds would be critical for the ligand binding dynamics in myoglobin.

Based on the temperature dependent X-ray diffraction, Frauenfelder et al. (1979) pointed out large mean-square displacement in the EF corner, F-helix and GH corner upon the ligand binding. These regions are close to heme and might be involved in a dynamic control mechanism in myoglobin and hemoglobin as suggested by Perutz (1965). Of these regions showing the large B-factor, we focused on the E- and F-helices, in which the proximal and distal histidines are located. As shown in the crystal structure (Takano, 1977; Phillips, 1980), the proximal histidine is the only amino acid residue with coordinating to the heme iron and the distal histidine directly interacts with the bound oxygen at the heme iron. Since the E- and F-helices would move away to let oxygen molecule migrate from solvent to the heme iron, restriction of the fluctuations of these two helices by formation of the disulfide bond would affect ligand binding properties of myoglobin and offer unique information for dynamics of the ligand binding.

In order to perturb the motion of the E- and F-helices, we mutated isoleucine-75 (Ile75) and glutamic acid-85 (Glu85) to cysteine to form a disulfide bond in the EF corner (Figure 1). Ile75 is located at the end of the E-helix and the position of Glu85 is the beginning of the F-helix. The distance between γ-methylene carbon of Ile75 and γ-carbonyl carbon of Glu85 is about 4.05 Å in the carbonmonoxy form (Cheng & Schoenborn, 1991), which is not so far from the length of a typical disulfide bond (2.0 Å) (Phillips, 1966), showing that Ile75 and Glu85 are one of the most appropriate amino acid pair to form an intramolecule disulfide bond between E- and F-helices. We examined the effects of the intramolecular disulfide bond on the static structure of the liganded and unliganded forms by various spectroscopies and the carbon monoxide binding properties of the mutant myoglobin in the absence and presence of the disulfide bond by laser photolysis under various hydrostatic pressure.

EXPERIMENTAL PROCEDURE

Reagents and Protein Preparation. Potassium ferricyanide, DTT[1], and sodium dithionite were purchased from Wako Pure Chemical Industries, Ltd.

The original expression vector of human myoglobin, pMb3 (pLcIIFXMb), is a gift from Varadarajan and Boxer (Varadarajan et al.,

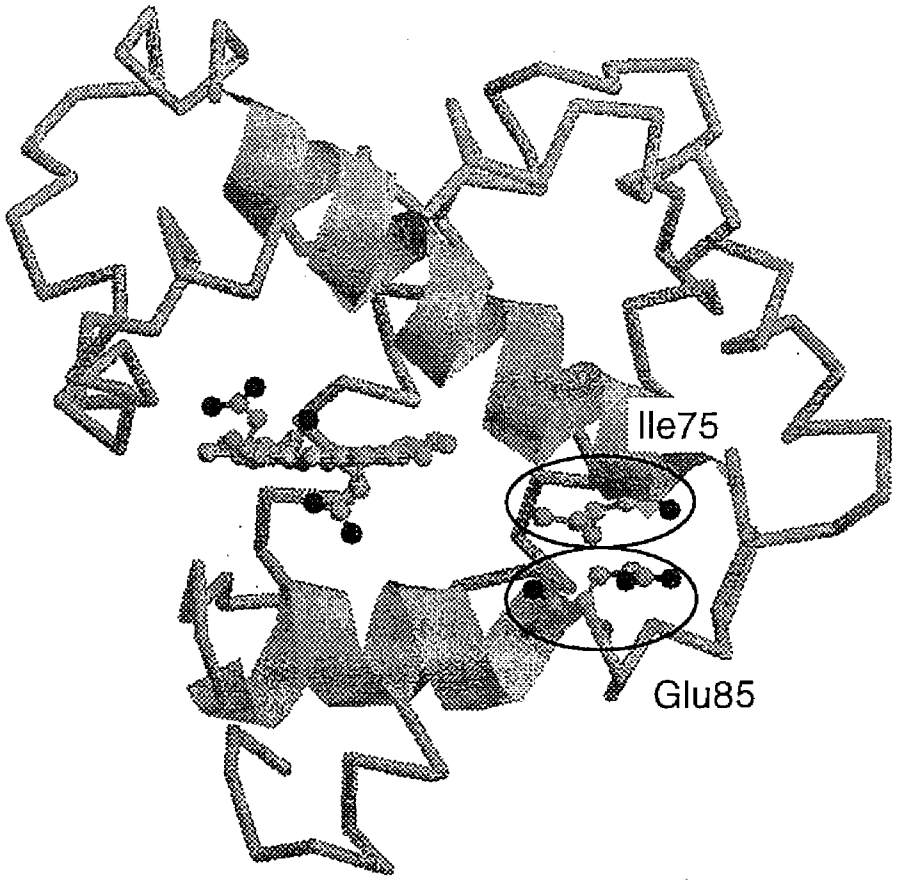

Figure 1. The introduction site of disulfide bond in human myoglobin. The mutated residues, Ile75 and Glu85, are circled. The E- and F-helices are described by ribbon model and the other part is described α-carbon backbone structure.

1985). The procedures for site-directed mutagenesis are described in previous papers (Kunkel 1985; Varadarajan et al., 1989; Adachi et al., 1992). DNA sequencing for the mutated myoglobin genes was performed by the Dyedeoxy Termination method using by ABI 373A DNA Sequencer and was analyzed by 373A DNA Sequencing system. Protein preparation and purification was followed by the method described previously (Varadarajan et al., 1989; Adachi et al., 1992).

The spectroscopic and functional properties of the recombinant wild type myoglobin[2] were indistinguishable from those of the native myoglobin (Varadarajan et al., 1989). The buffer solutions were 0.1 M sodium phosphate buffer, pH 7.0. The electronic absorption spectra of deoxy-, oxy- and carbonmonoxy forms of the mutants are similar to those of the wild type protein. The peak maxima did not shift for more than 1 nm by the mutation.

Oxidation and Reduction of the Disulfide Bond. To form the intramolecular disulfide bond in the mutant, the purified protein was oxidized by two equivalent potassium ferricyanide ($K_3[Fe(CN)_6]$) at 37 °C for 12 hr. Excess amount of ferricyanide was removed by a gel filtration column (Sephadex G-25) with 0.1 M sodium phosphate buffer at pH 7.0. By addition of a small amount of solid sodium dithionite, the heme iron was reduced to the ferrous state without the cleavage of the disulfide bond. To cleave the disulfide bond, the purified protein was incubated with 100 mM DTT, 1 mM EDTA at 37 °C for 12 hr under CO atmosphere.

Laser Photolysis Experiments. The method for milli-, and microsecond laser photolysis measurements are followed by the procedure previously reported (Adachi & Morishima, 1989; Adachi et al., 1992; Unno et al., 1994). A flashlamp-pumped dye laser with a half-peak duration of 300 ns (UNISOKU LA-501) was used. Rhodamine 6G (Kodak) in methanol was used to produce an excitation pulse at wavelength maximum of 590 nm. The probe light at 436 nm was focused onto the slit of monochromator (UNISOKU USP-501) and detected by a photomultiplier. A transient memory (GRAPHTEC TMR-80) was used to digitize the signal (50 ns/point, 4096 points), and data were transferred to a NEC PC-9801VX computer for further data analysis. The sample concentration was about 20 μM.

Ligand rebinding to the mutant and wild type myoglobins were analyzed by fitting to the following equation,

$$\Delta A_t = \Delta A_0 \exp(-k_{app}\, t) \tag{1}$$

where ΔA_t is the absorbance change at any time t, ΔA_0 is the total absorbance change (absorbance at $t = 0$ minus absorbance at $t = \infty$). k_{app} is the observed first-order rate constant and the k_{app} satisfies the following equation (Antonini & Brunori, 1971),

$$k_{app} = k_{on}[CO] \tag{2}$$

where k_{on} is the bimolecular ligand binding rate constant.

Over the narrow range of temperature (275 K–315 K) in these measurements, the overall rate constants showed a temperature dependence which obeys an Arrhenius law,

$$k_{on} = A \exp(-E_a/RT) \tag{3}$$

where E_a is the activation energy and A is the prefactor (Chatfield et al., 1990).

For the nanosecond laser photolysis experiments, we used 6-ns FWHM pulses from a Q-switched Nd:YAG laser for the experiment. The incident energy was about 10 mJ. The absorption changes were monitored by a continuous, weak probe beam from a 150-W xenon arc lamp passed through a monochromator. The probe wavelength was 440 nm. Signals were detected in transmission using a photomultiplier (Hamamatsu Photonics, R2949) and the transient signals were digitized using Iwatsu DS-8621 oscilloscope. Signals were averaged 150 to 240 times. The data were transferred to a NEC PC-9821Ae computer for further data analysis. No smoothing artifact affected the results of the following data analysis. The protein concentration was about 10 mM. The time courses were analyzed by fitting to the following equation,

$$\Delta A_t / \Delta A_0 = \phi_g \exp(-k_g t) + (1-\phi_g) \exp(-k_{on} t) \quad (4)$$

where k_g is the geminate rate constant, ϕ_g is the geminate yield, ΔA_0 is the total absorbance change (absorbance at $t = 0$ minus absorbance at $t = \infty$).

In this study, we assumed the simple three-state sequential scheme (Henry et al, 1983),

$$\mathrm{A\ (MbCO)} \underset{k_{BA}}{\overset{h\nu}{\rightleftharpoons}} \mathrm{B\ (Mb{\bullet\bullet\bullet}CO)} \underset{k_{SB}}{\overset{k_{BS}}{\rightleftharpoons}} \mathrm{C\ (Mb+CO)} \quad (5)$$

where the symbol A represents the liganded state in which CO is bounded to the heme iron (carbonmonoxy form), and S is unliganded form (deoxy form). B is a geminate state in which the iron-CO bond has been photolyzed but CO is still trapped within the protein (Henry et al., 1983; Lambright et al., 1989; Carver et al., 1990). The observable k_g (geminate rate constant), ϕ_g (geminate yield), and k_{on} (pseudo-first-order association rate constant) are related to the rate constants for the three-state sequential scheme (Lambright et al., 1989) by the equations,

$$k_g = k_{BA} + k_{BS} \quad (6)$$

$$\phi_g = k_{BA}/k_g = k_{BA}/(k_{BA}+k_{BS}) \quad (7)$$

$$k_{on} = k_{SB}\,\phi_g = k_{SB}\,k_{BA}/(k_{BA}+k_{BS}) \quad (8)$$

$$k_{off} = k_{AB}\,(1-\phi_g) \quad (9)$$

Since we defined the activation energy as expressed by equation 3 it is presumed that the pre-exponential factor, A, of each step was equal to each other, which is adequate in our case (Carver et al., 1990). The absolute values of the pre-exponential factor do not affect the differences between the barrier height for the mutants (Carver et al., 1990).

Laser Photolysis Measurement under Various Pressure and Temperature. The method for milli-, and microsecond laser photolysis measurements under various pressure have been described in our previous papers (Adachi & Morishima, 1889; Unno et al., 1990, 1991, 1994). All experiments under high pressure were performed in 0.1 M Tris-HCl buffer pH 7.8. The pH of Tris buffer has been shown to be independent of pressure up to 200 MPa (Newmann et al., 1973). The activation volume is given by the equation,

$$\Delta V^{\neq} = -RT\left(\frac{\partial(\ln k_p / k_1)}{\partial P}\right)_T \quad (10)$$

where R is the gas constant (= 8.314 J K^{-1} mol^{-1}), T is absolute temperature and k_1 and k_p are observed first-order rate constants at 0.1 and P MPa, respectively. The slopes of the plot of ln k_p/k_1 versus pressure for the mutant myoglobins at atmospheric pressure were calculated by the optimized second order polynomial function.

Dissociation Constant of Carbon Monoxide. The kinetics measurements of the CO dissociation rates were carried out with a UV/visible spectrometer (SHIMADZU UV-2200). k_{off} was determined by analyzing the replacement reaction in which ligated CO was replaced by NO as described in detail by Lambright et al. (1989). The concentrated myoglobin stocks were converted to the carbonmonoxy form by stirring under CO followed by reduction with sodium dithionite. NO saturated buffer (100 mM sodium phosphate for pH 7.0) was prepared by bubbling NO through 3 ml of buffer in a sealed 1 cm path-length UV cell. About 20 ml of the concentrated MbCO solution was then injected into the cell at 20 °C, and the reaction was followed by monitoring the absorbance at 454 nm. The decay was fit to a single exponential using a non-linear least-squares fitting.

The free energy change for the ligand binding in the deoxy and geminate states is calculated by the following equations, (11) and (12) (Antonini & Brunori, 1971),

$$\Delta G = -RT \ln K_{CO} \quad (11)$$

$$\Delta\Delta G = -RT \ln \{K_{CO}(S\text{–}S)/K_{CO}(SH)\} \quad (12)$$

where K_{CO} is the equilibrium constant for CO binding (k_{on}/k_{off}).

Infrared Absorpton Spectra. The infrared spectra were measured at 1 cm^{-1} resolution on a Bio-Rad FTS-30 spectrophotometer. The sample concentration was about 1 mM. A small amount of sodium dithionite was added to remove residual oxygen just prior to recording the infrared spectra. Approximately 40 μl of carbonmonoxy myoglobin solution was loaded into a CaF_2 cell with 0.1 mm path length. We used equimolar amount of wild type aquomet myoglobin as a reference. Each spectrum was an average of 512 scans. To determine the peak positions and line width, we fitted the experimental data with a linear combination of three independent Gaussian line shapes (Caughey et al., 1981).

NMR Spectroscopy. ^{1}H-NMR spectra were recorded using a GE OMEGA 500 spectrometer equipped with a SUN 3 workstation. Hyperfine-shifted NMR spectra were obtained with 8K data transform of 125 kHz and 7.0 ms 90° pulse by using a conventional WEFT pulse sequence (180-τ-90 acquire) in order to minimize the strong solvent resonances in H_2O solution. A careful setting of the τ value (typically 120–130 ms) can completely eliminate the H_2O signal under rapid repetition of the sequence. We also used a PRESAT pulse sequence with a 1 s presaturation pulse to suppress the residual water resonance. The probe temperature was 23 ± 0.5 °C. The concentration of the sample was about 1 mM in 100 mM sodium phosphate, pD 7.0, and the volume was about 500 μl. Proton shifts were referenced with respected to the signal of the proton resonance of tetramethylsilane (TMS).

RESULTS

Formation and Cleavage of the Disulfide Bond. Figure 2 shows the SDS-polyacrylamide gel electrophoresis (SDS-PAGE) under non-reducing conditions. Since a protein containing an intramolecular disulfide linkage has a smaller radius of gyration and migrates further down the gel (Pollitt & Zalkin, 1983; Perry & Wetzel, 1984), the formation and

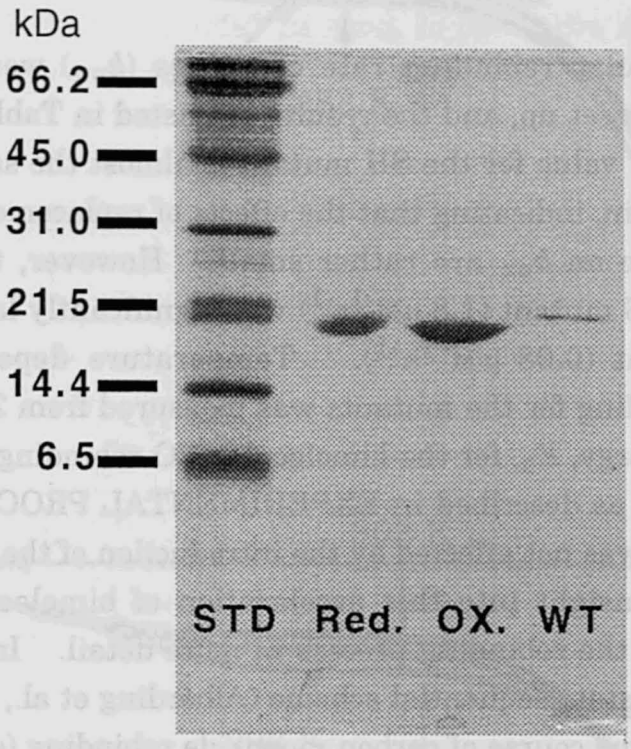

Figure 2. SDS-PAGE analysis of the S–S and SH mutants. **STD** is the molecular weight standard; **WT** is wild type human myoglobin; **Ox.** is the S–S mutant (oxidized 75C/85C); **Red.** is the SH mutant (reduced 75C/85C). Each lane contains 0.5 μg protein.

cleavage of a disulfide bond was detected under these conditions. As illustrated in Figure 2, the S–S mutant (the mutant having the disulfide bond between Cys75 and Cys85) migrated faster than wild type and the SH mutant (the mutant having reduced Cys75 and Cys85) myoglobins. We also measured whole molecular weight of the S–S mutant by FAB-mass spectroscopy. The molecular weight of the apo S–S mutant was 16985 ± 0.2 Da (data not shown). This value is exactly 2 Da smaller than the calculated value of the apo SH mutant, indicating that the two cysteine residues lost two hydrogen atoms by forming the disulfide bond.

Laser Photolysis of Carbonmonoxy Mutants. A set of time courses for CO recombination to the S–S and SH mutant myoglobins at 10-deg intervals (283, 293 and 303 K) are shown in Figure 3. The time axis is plotted on a logarithmic scale. As clearly shown in Figure 3, the time course consists of the two distinct phases. The fast phase which is

independent of the ligand concentration is the geminate rebinding process, and the second one being dependent on it is the bimolecular rebinding process.

The bimolecular rebinding rate constants (k_{on}) were obtained by millisecond kinetic set up, and the results are listed in Table I. As shown in Table I, the k_{on} value for the SH mutant is almost the same as that for wild type myoglobin, indicating that the effects of replacement of Ile75 and Glu85 by cysteine on k_{on} are rather small. However, the rate of CO binding to the S–S mutant (1.8 $\mu M^{-1}s^{-1}$) was significantly larger than that of the SH mutant (0.98 $\mu M^{-1}s^{-1}$). Temperature dependence of CO bimolecular rebinding for the mutants was measured from 275 K to 315 K. The activation energy, E_a, for the bimolecular CO rebinding was estimated by the equation 3 as described in EXPERIMENTAL PROCEDURE. The activation energy was not affected by the introduction of the disulfide bond. To gain further insight into this acceleration of bimolecular rebinding rate, we analyzed the rebinding process in more detail. In this work, we adopted the three-state sequential scheme (Alberding et al., 1976; Henry et al., 1983) to the time course of carbon monoxide rebinding (equation 5) and obtained the rate constants for each elementary step. Since the geminate process could be fitted with a single exponential within our experimental error, the model is adequate to our experiments under the present conditions[3]. The parameters for the geminate kinetics are estimated from the data of Figure 3, and the results are summarized in Tables I and II. The rate constant (k_g) for the S–S mutant was virtually the same as that for the SH mutant. On the other hand, the geminate yield for the S–S mutant (0.092±0.001) is significantly larger than that for the SH mutant (0.072±0.001). In the rate constants for the elementary steps, the introduction of the disulfide bond into myoglobin accelerated k_{BA}, the rate for the bond formation from the heme environment to the heme iron (0.27 s^{-1} to 0.35 s^{-1}), and k_{SB}, the rate for the migration from solvent to the heme environment (14 s^{-1} to 19 s^{-1}).

Measurement of Dissociation Rate. The time courses of CO dissociation reaction for the S–S and SH mutants were measured by conventional NO replacement method (Lambright et al., 1989; Rohlfs et al., 1990) and the values of k_{off} are also summarized in Table I. Although the k_{off} value for the wild type myoglobin (0.018 s^{-1}) was a little smaller than that obtained by Dou et al. (0.022 s^{-1}) (1995), the rate constant for the SH mutant (0.016 s^{-1}) was almost identical to that for wild type myoglobin. As listed in Table I, the formation of the disulfide bond decelerated the

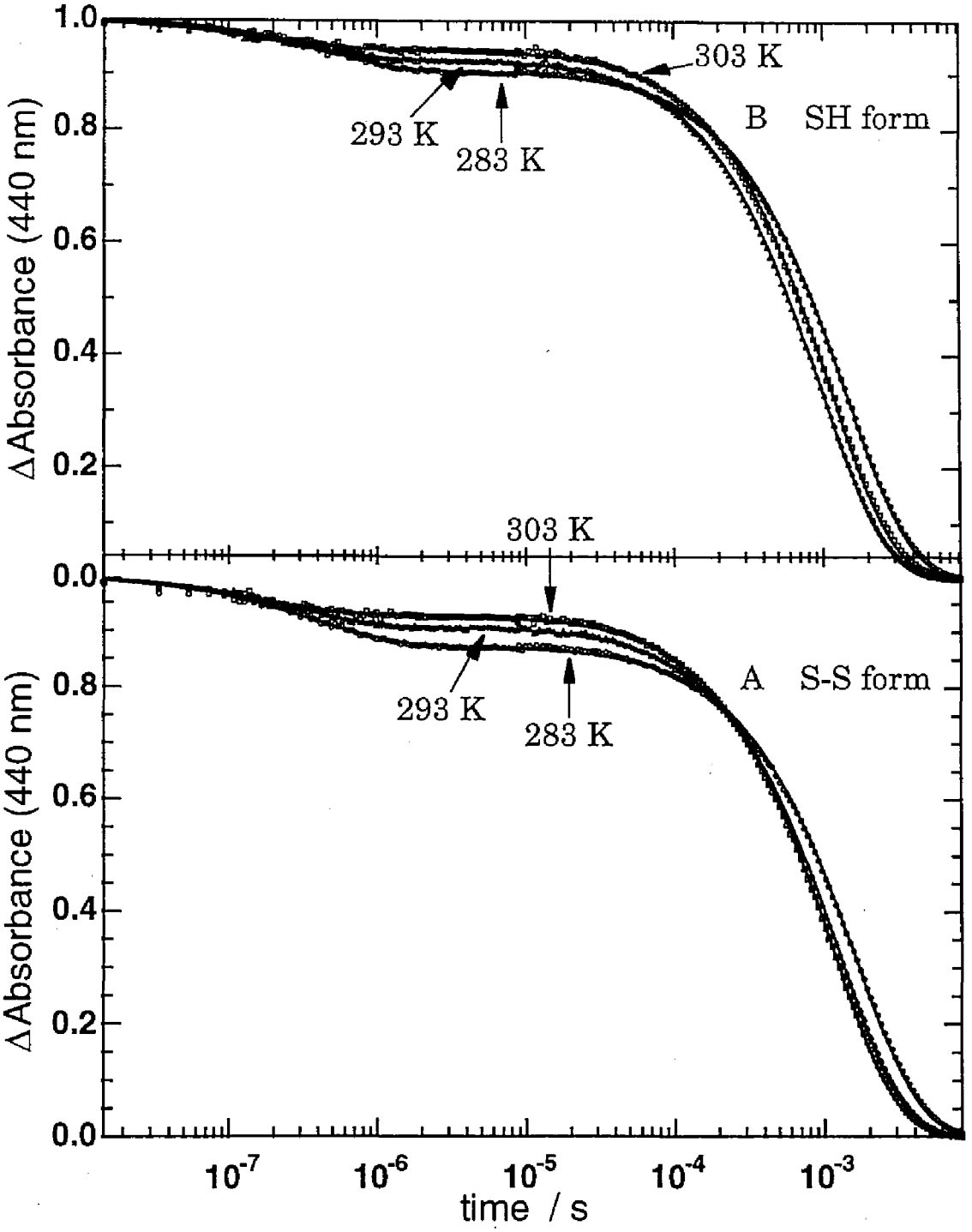

Figure 3. Time courses for CO rebinding to the S–S (A) and SH (B) mutants. The dots are the experimental data and the solid lines are fitting curves simulated by the equation 3. The solid lines are the data, and the dashed lines are fits to a Gaussian functions.

dissociation rate from 0.016 s^{-1} to 0.012 s^{-1}. From the bimolecular rebinding (k_{on}) and dissociation rate (k_{off}) constants, apparent CO affinity, $K_{CO} = k_{on}/k_{off}$, was estimated as given in Table I. The S–S mutant shows higher affinity to carbon monoxide (147 μM^{-1}) than the SH mutant (61 μM^{-1}) and wild type myoglobin (61 μM^{-1}).

TABLE I: Kinetic Parameters for CO Rebinding to Human Myoglobins in 0.1 M Sodium Phosphate Buffer, pH 7.0 at 20 °C

	k_{on}	k_{off}	K_{CO}	k_g	ϕ_g
	$\mu M^{-1}s^{-1}$	s^{-1}	μM^{-1}	μs^{-1}	
S–S	1.8 ± 0.0*	0.012 ± 0.001	147 ± 14	3.8 ± 0.1	0.092 ± 0.001
SH SH	0.98 ± 0.01	0.016 ± 0.001	61 ± 4	3.8 ± 0.1	0.072 ± 0.001
Wild Type	1.1 ± 0.0[a]	0.018 ± 0.001	61 ± 5	3.3 ± 0.1	0.068 ± 0.001

[a] Error is less than 0.03

TABLE II: Kinetic Parameters for CO Rebinding to Human Myoglobins in 0.1 M Sodium Phosphate Buffer, pH 7.0 at 20 °C

	kAB	kBA	kBS	kSB
	s^{-1}	μs^{-1}	μs^{-1}	$\mu M^{-1}s^{-1}$
S–S	0.013 ± 0.001	0.35 ± 0.01	3.4 ± 0.1	19 ± 0*
SH SH	0.017 ± 0.001	0.27 ± 0.01	3.5 ± 0.1	14 ± 0[a]
Wild Type	0.019 ± 0.001	0.22 ± 0.01	3.1 ± 0.1	16 ± 1

[a] Error is less than 0.5

Pressure Effect on Bimolecular Ligand Binding. Pressure dependence of the CO bimolecular rebinding kinetics of the S–S and SH mutants is given in Figure 4 and their activation volumes, $\Delta V^{\neq}$, are listed in Table III. The time courses at the elevated pressure we applied here were fitted by a simple single exponential within experimental error (results not shown). The rates of CO rebinding for both mutant myoglobins were accelerated and apparent quantum yields were decreased by pressurization as found for native myoglobin (Adachi & Morishima, 1989). The activation volume of CO rebinding in the S–S mutant was identical to that in the SH mutant. In the pressure

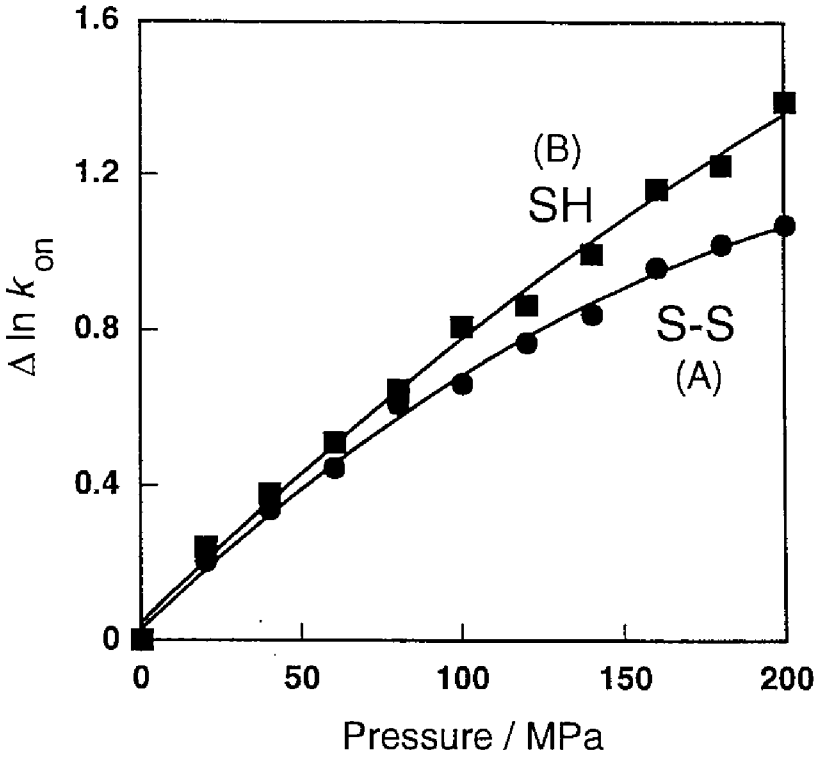

Figure 4. Logarithmic plots of the rate constants for the bimolecular CO rebinding reaction vs hydrostatic pressure for the S–S (A) and SH (B) mutants.

dependence of the rebinding rate for the S–S mutants, however, some deviations from that for the SH mutant were observed at the elevated pressure.

TABLE III: Activated parameters for CO rebinding to human myoglobins in 0.1 M sodium phosphate, pH 7.0 at 20 °C

Myoglobin	E_a	$\Delta V^{\neq}$
	kJ mol^{-1}	cm^3mol^{-1}
S–S	32 ± 1	–19 ± 0.9
SH SH	33 ± 1	–20 ± 1.2
Wild Type	36 ± 1	–20 ± 0.4

Infrared Spectra of Carbonmonoxy Mutant and Wild Type Myoglobins. The infrared spectra for carbonmonoxy S–S and SH mutant myoglobins in the region from 2000 to 1900 cm^{-1} at pH 7.0 are shown in Figure 5. All spectra could be decomposed by sum of three Gaussian

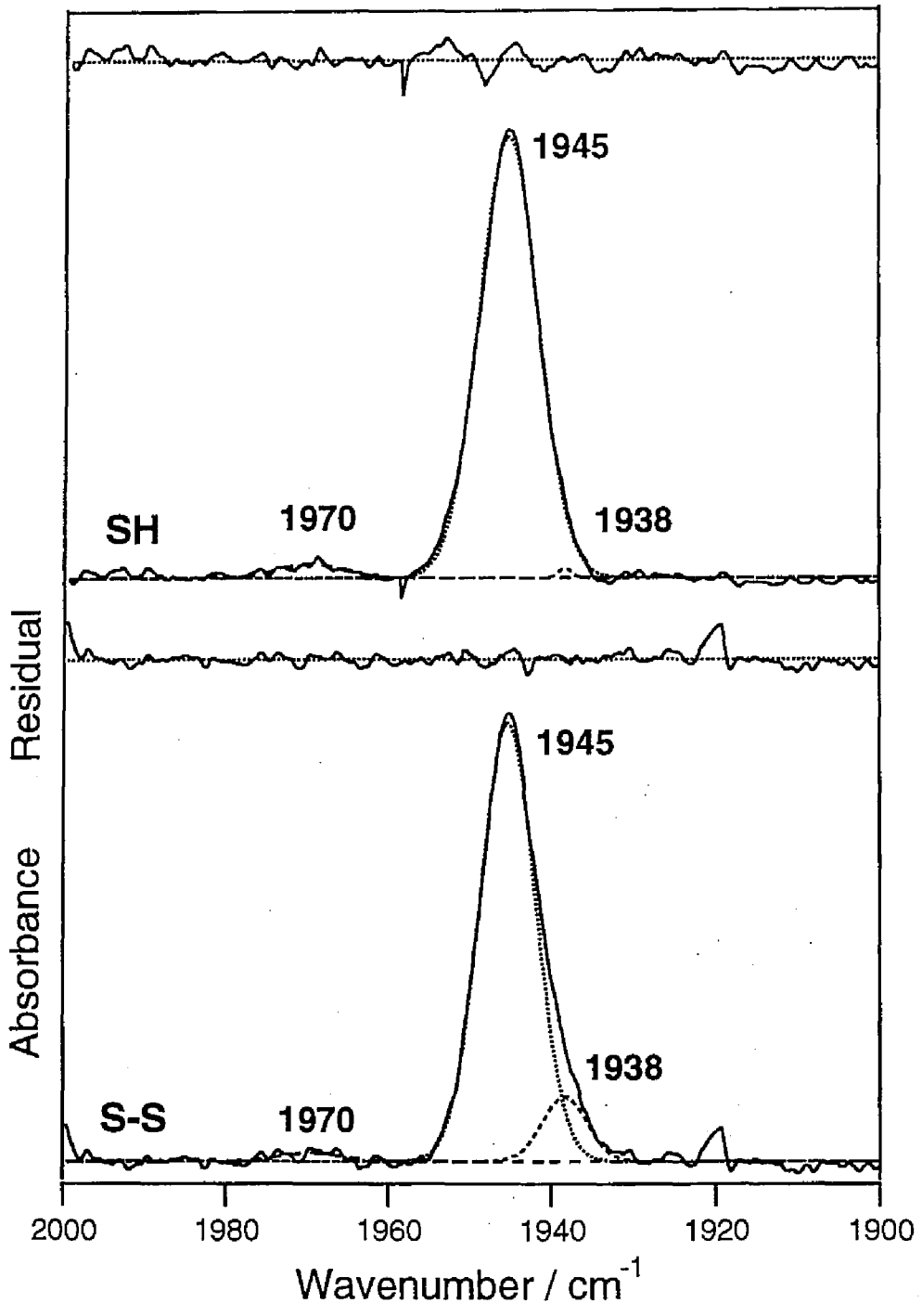

Figure 5. FT-IR spectra of C-O stretching region of the S–S and SH mutant myoglobins. Samples contain 1 mM protein in 0.1 M sodium phosphate buffer at pH 7.0.

functions. The positions of IR stretching band and population of conformers for wild type and mutant myoglobins are summarized in the Table IV. In myoglobin, at least three different CO conformers can be identified in IR spectra under various conditions and designated as listed in Table IV (Caughey et al., 1969; Makinen et al., 1979; Caughey et al., 1981; Ansari et al., 1987; Frauenfelder et al., 1988). For human wild type myoglobin, the main C-O stretch mode (A_1) was observed at 1945 cm^{-1}, and one minor band appeared at 1967 (A_0) cm^{-1} at room temperature. On the other hand, both of the mutants exhibited three C-O stretching bands; One major band at 1945 (A_1) cm^{-1} and two minor bands at 1970 (A_0) and 1938 (A_3) cm^{-1}. Although the peak positions of both mutants were identical, the population of A_3 conformer increased from 2 to 12% by the disulfide bond formation. The band width of main conformer for the S–S mutant was 8.5 cm^{-1}, which is also almost identical to that for the SH mutant (8.8 cm^{-1}) and wild type myoglobin (9.0 cm^{-1}).

TABLE IV: IR stretching band, population of conformers for wild type and mutant myoglobins.

Myoglobin	A_0	A_1	A_3
		cm^{-1} (%)	
Wild Type	1967 (3)	1945 (97)	ND[a]
S–S	1970 (2)	1945 (86)	1938 (12)
SH	1970 (3)	1945 (95)	1938 (2)

[a] not detected.

NMR Spectra of Mutant and Wild Type Myoglobins. In Figure 6, the ^{1}H-NMR spectra of carbonmonoxy mutant myoglobins are illustrated. The ring-current-shifted proton peak at –2.5 ppm (**f**) in Figure 6A, which has been assigned to a methyl group of Val68, serves as a marker for the structure of the heme vicinity in carbonmonoxy myoglobin (Shulman et al., 1970). The resonance position of this methyl group in the mutants was identical with that of wild type myoglobin. The signals observed in the upfield region (**a–e**), which are assignable to a methyl group of Val17, Leu29, and Val68 (Shulman et al., 1970; Dalvit & Wright, 1987) as listed in Table V, were also insensitive to the formation of the disulfide bond, although slight shifts were detected in their signal positions.

Table V: Proton NMR chemical shifts of mutant carbomonoxy myoglobins in sodium phosphate, pD 7.0 at 23 °C (ppm from TMS)

	Val17	Leu29	Val17	Val68	Leu29	Val68
	$C_\gamma H_3$	$C_\delta H_3$	$C_\gamma H_3$	$C_\gamma H_3$	$C_\delta H_3$	$C_\gamma H_3$
	a	**b**	**c**	**d**	**e**	**f**
S–S	–0.36	–0.46	–0.56	–0.68	–0.78	–2.5
SH SH	–0.35	–0.43	–0.53	–0.68	–0.77	–2.5
Wild Type	–0.35	–0.43	–0.56	–0.60	–0.79	–2.5

The NMR spectra of the deoxygenated form of the S–S and SH mutants are shown in Figure 6B. In a far downfield region (A), one exchangeable proton peak was observed (**g**). This resonance was assigned to the $N_\delta H$ proton of the proximal histidine (Goff & La Mar, 1977; La Mar et al., 1977; La Mar et al., 1993). The signal for wild type myoglobin is observed at 78.5 ppm from TMS, whereas the S–S mutant bears the signal at 83.2 ppm, which is identical to that for the SH mutant. The resonance of the 5-methyl group at the heme (**h**) appeared at 15.1 ppm for the S–S mutant and 14.9 ppm for the SH mutant as shown in (B). The peak at 11.2 ppm in the S–S mutant (**k**) is assignable to the 3-methyl group, which was also observed at the same position for the SH mutant. However, in the region (B), the resonances (**i**) and (**j**), which were assigned to 6-H_α, 4-H_α of the heme, respectively, shifted to downfield and significant spectral changes in the upfield (C) were detected. The SH mutant exhibited the resonances from γ-methyl groups of Val68 at –4.7 (**m**) and –6.0 ppm (**n**), whereas the corresponding signals for the S–S mutant were –5.3 (**m**) and –6.4 ppm (**n**). These NMR spectral changes indicate that some conformational changes are induced by the formation of the disulfide bond at the EF corner in the unliganded form. The prominent NMR resonances are listed in Tables VI.

Near-Infrared Absorption Spectra of Deoxy Myoglobins. The near-infrared absorption spectra (band III) for the S–S and SH mutant myoglobins in the deoxy form are illustrated in Figure 7. These spectra can be well described by a Gaussian function on top of a cubic polynomial background and the center frequency for the SH mutant was 762.4 nm, corresponding to that for wild type myoglobin. The wavelength of the S–S mutant was 763.8 nm, which showed 1.4 nm red-shifted from that of the SH mutant. Since this band arises from electron transfer from the a_{2u}

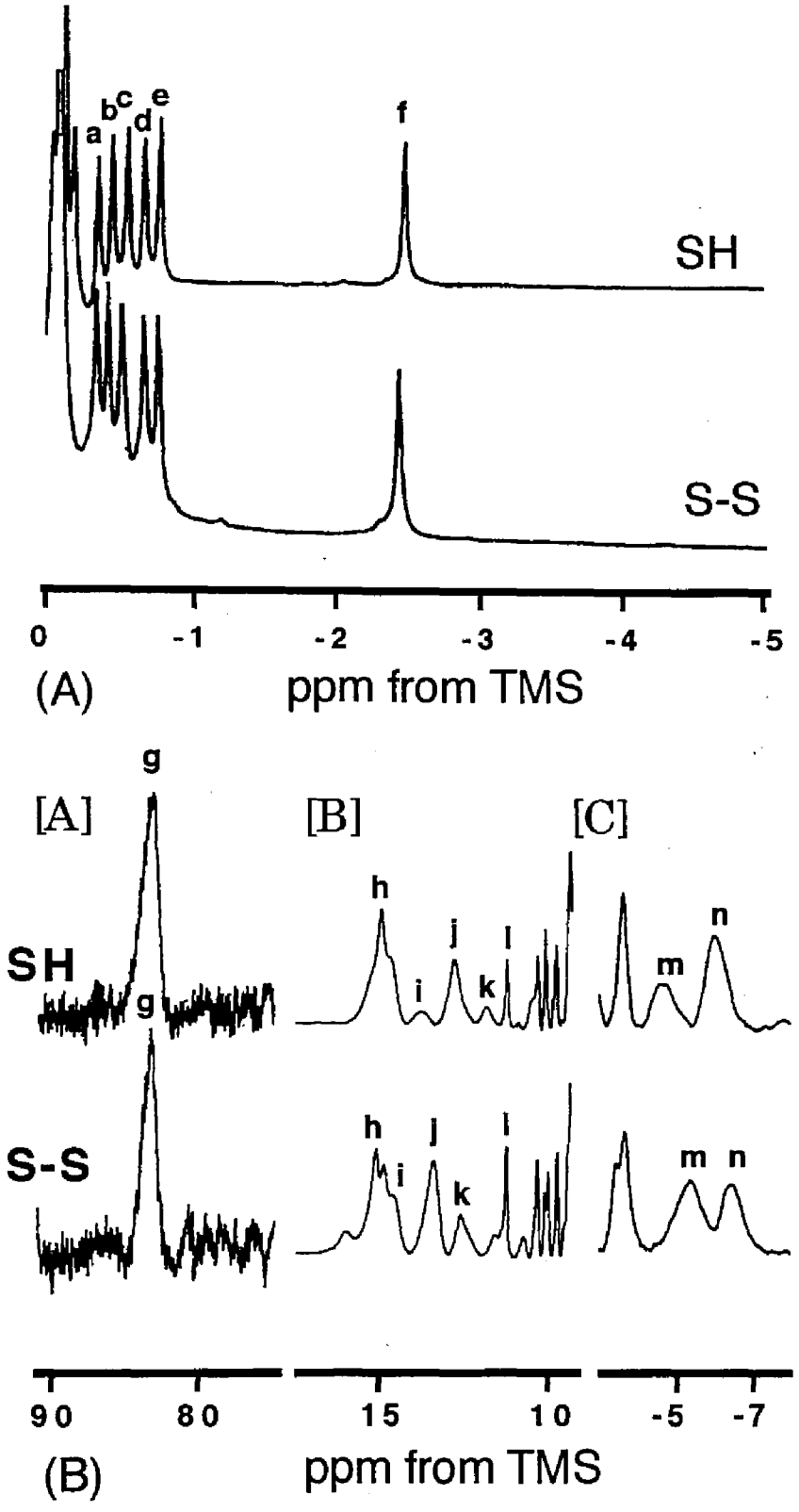

Figure 6. ^{1}H-NMR spectra of the S–S and SH mutants. The samples contain 1 mM protein in 0.1 M sodium phosphate buffer at pD 7.0: (A) carbonmonoxy form; (B) deoxy form.

orbital of the porphyrin to the d_{yz} orbital of heme iron (Eaton & Hofrichter, 1981), the red-shift in the S–S mutant is interpreted as a decrease in the transition energy between the two orbitals (Sassaroli & Rousseau, 1987; Campbell et al., 1987) and it can be concluded that displacement of the heme iron from the heme plane in the S–S mutant was smaller than that of the SH mutant.

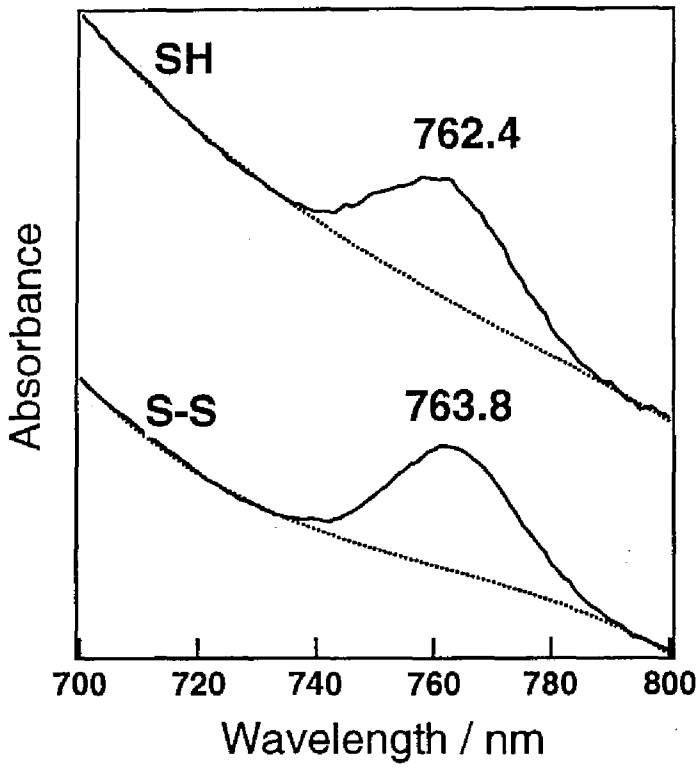

Figure 7. Near-Infrared absorption spectra of deoxy mutant myoglobins. The data were modeled with a Gaussian function plus a cubic polynomial function. The dashed lines represent the background. Samples contain 1 mM protein in 0.1 M sodium phosphate buffer at pH 7.0.

DISCUSSION

The Effects of the Disulfide Bond on the Heme Environmental Structure. The IR spectra of carbonmonoxy complexes of heme proteins have provided unique information on the local environment of the distal side of the heme pocket (Balasubramanian et al., 1993; Li et al., 1994; Decature & Boxer, 1995). Recently, the electrostatic potential around the iron-bound carbon monoxide is considered to be one of the major factors for the C-O stretching frequencies (Li & Spiro, 1988; Park et al., 1991; Ray et

al., 1994; Li et al., 1994). It has been revealed that the downshift of the C-O stretching mode is induced by the presence of positive charges, whereas the presence of negative charges causes the upshift of the mode (Li & Spiro, 1988; Oldfield et al., 1991; Park et al., 1991; Ray et al., 1994; Li et al., 1994). As shown in Figure 5 and Table IV, the peak positions for the S–S mutant are identical to those for the SH mutant. With forming the disulfide bond, however, the A_3 conformer increased from 2 to 12%. The A_3 conformer was observed for sperm whale myoglobin with 30% content, while this conformer was not detected for the human wild type myoglobin (Adachi et al., 1992; Balasubramanian et al., 1993), even though the two myoglobins have similar heme environmental structures. Increase in A_3 conformer by the disulfide bond formation may suggest to induce some structural changes of heme pocket residues. However, since the IR-detected population change is very sensitive to the environment around ligated carbon monoxide, this disulfide bond-induced change would be much smaller than those observed for the distal pocket mutants (Adachi et al., 1992; Balasubramanian et al., 1993; Li et al., 1994).

In ^{1}H-NMR spectra of the carbonmonoxy form of the mutants, the peaks of γ-methyl groups of Val68 in the S–S form appeared at –0.68 (**d**) and –2.5 ppm (f) from TMS, which are almost identical with those of the SH form. The peak positions of δ-methyl groups of Leu29 and γ-methyl groups of Val17 in the S–S form were also in good agreement with those of the SH form. Since the ring current shifts are sensitive to conformational alteration near porphyrin ring (Shulman et al., 1970), the structural changes induced by the S–S bond formation would be small in the heme environment of the carbonmonoxy form.

In the deoxygenated state, however, some significant structural differences between the S–S and SH mutants were observed. In Figure 6B, the signal patterns in (B) and (C) for the S–S mutant are significantly different from those of the SH mutant, although the signal position of $N_\delta H$ in the proximal histidine (**g**) is identical. Since the resonances (**m**) and (**n**) have been assigned to γ-methyl groups of Val68, which is located in the distal side, formation of the disulfide bond induced some structural changes in the distal side. The peak position of the charge transfer band (band III) in the near IR region (Figure 7) also shows the red-shift for the S–S mutant. The red shift suggests that displacement of the heme iron is decreased in the deoxygenated S–S mutant.

These preferential structural changes in the deoxygenated form of the S–S mutant can be deduced from the structural differences around the

EF corner between the deoxy and carbonmonoxy forms. The crystallographic structure of native myoglobin has revealed that distance from the γ-methylene carbon of Ile75 to the γ-carbonyl carbon of Glu85 is 4.05 Å in the carbonmonoxy form (Cheng & Schoenborn, 1991), whereas, in the deoxygenated form, the distance becomes longer (4.78 Å) (Takano, 1977). Since the typical bond length of a disulfide bond is about 2 Å, the conformational strains in the EF corner should be enhanced in the deoxygenated S–S mutant than those in the carbonmonoxy form.

Ligand Binding Properties. On the basis of the present kinetic results, the free energy diagrams for the binding of CO to the S–S and SH mutants are schematically shown in Figure 8, where the free energy of the system is depicted as a function of the reaction coordinate. The increased affinity of carbon monoxide (K_{CO}) for the S–S mutant corresponds to the increased free energy difference between the states "MbCO" and "Mb + CO" in Figure 8. More prominent conformational changes in the deoxygenated form imply that the difference of the free energy can be localized in the deoxygenated form, which is represented as "Mb + CO" in the figure. The energy level of the state "MbCO" for the S–S

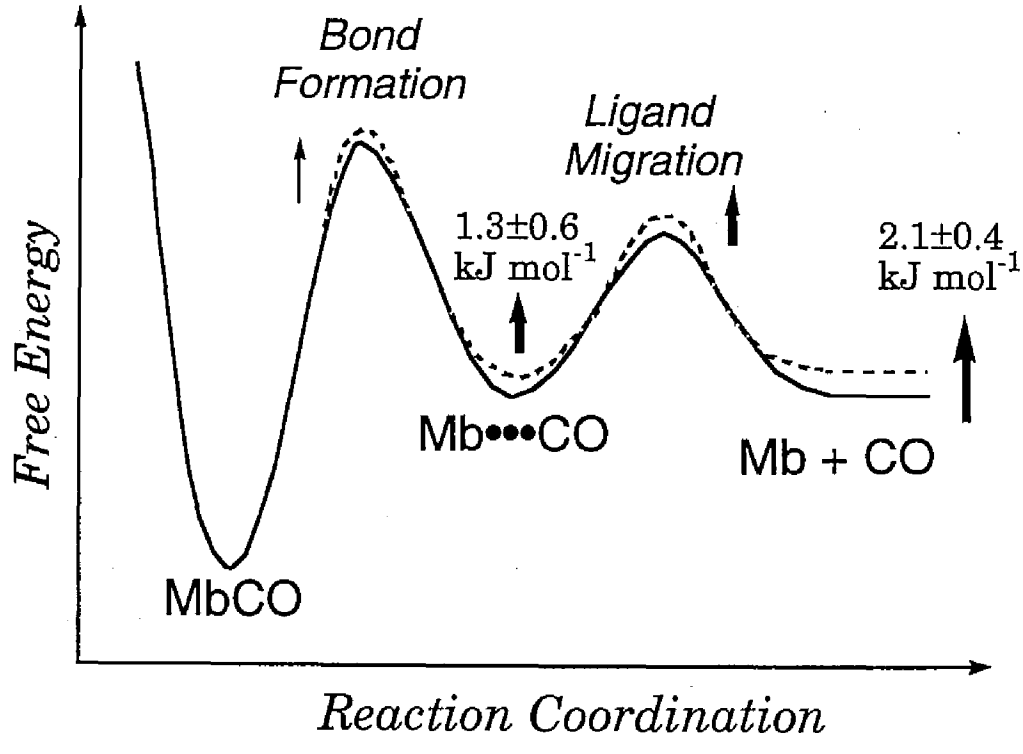

Figure 8. Relative free energy schematically plotted vs the reaction coordinate. The solid and dashed curves represent the free energies for the SH and S–S myoglobins, respectively.

mutant would be the same as that for the SH mutant. Taking into account that the dissociation rate (k_{AB}) was slowed down and the bond formation (k_{BA}) was accelerated, the energy level of the state "Mb···CO" and the energy barrier for the bond formation would be raised as shown in the figure. Since previous studies (Carver et al., 1990; Gibson et al., 1992) reported that the bond formation process is affected by the local fluctuations immediate near the ligand of the heme, which would be determined by the motions of the side chains of the amino acid residues in the distal side, the elevated energy barrier for the bond formation process can be induced by the restricted motion at the EF corner.

On the other hand, the ligand migration rate was accelerated (k_{SB}), while the rate of ligand diffusion from the interior of protein to solvent (k_{BS}) was not changed. These alterations in the migration process indicate that the energy barrier for the ligand migration becomes higher by formation of the disulfide bond. Since the protein fluctuations play key roles in forming the "ligand entry channel" to pass through the interior of the protein (Takano, 1977; Phillips, 1980; Kuriyan et al., 1986; Elber & Karplus, 1990), it can be considered that the perturbation in the motion of the EF corner is one of the factors for the enhancement of the energy barrier in the ligand migration process.

The free energy changes for the ligand binding were also encountered in the distal histidine and leucine-29 mutant myoglobins (Springer et al., 1994). By the substitution of these residues, drastic changes were induced in heme environmental structure (Quillin et al., 1993). The hydrogen bond of the distal histidine was disrupted in the mutant myoglobin having the mutation at the distal histidine, which leads to an increase in the ligand association rates (Carver et al., 1990; Quillin et al., 1993). The mutation at leucine-29 (B10) remarkably reduced the ligand binding rate probably due to introducing extra water molecules into heme pocket (Rohlfs et al., 1990; Carver et al., 1990; Adachi et al., 1992). Most of the distal histidine mutants exhibited 10-15-fold larger binding rates (k_{on}). In other words, the energy change between the deoxy and carbonmonoxy forms was up to 7 kJ/mol. Present results showed that formation of the disulfide bond at the EF corner only affected about 2 kJ/mol in the free energy difference between the two states. The effects of the disulfide bond formation on the binding rate and free energy for the ligand binding were rather smaller than those of the substitution of the distal amino acid residues.

The Effects of the Disulfide Bond Formation on Fluctuation. In spite of the EF corner being near the active site for the ligand binding, functional and structural deviations of the S–S mutant from the SH mutant were smaller than we expected. It is rather likely that the effects of the disulfide bond on protein fluctuation are localized at the mutated site as found for lysozyme C77A/C95A mutant (Kidera et al., 1994). In the lysozyme mutant, although the effects of the mutation on the internal fluctuations were detected in the long flexible loop region containing residue 77, the other mutation site 95 in the α-helix did not exhibit any changes in the dynamic structure. They concluded that the cleavage of the disulfide linkage in the mutant lysozyme caused no significant changes in the protein fluctuations except for the mutated site. Schulman and Kim (1994) also reported that amide proton exchange rates in BPTI (bovine pancreatic trypsin inhibitor) mutants, in which disulfide bonds are removed, were very similar to that of wild type BPTI and the structural changes were localized at the mutated amino acid residues.

In summary, the present results indicate that the restriction effects by formation of the disulfide bond at the EF corner on protein fluctuation may be localized in the mutation site and the disulfide linkage cannot seriously affect the dynamic properties of the E-, and F-helices nor the ligand binding process. Our preliminary results from the SDS denaturation studies also showed that the free energy for the denaturation was almost insensitive to the disulfide bond formation. The other regions and motions would be crucial for regulating the fluctuation in the ligand binding. Some mutants having other disulfide bonds or cross linkages at the various positions are now being investigated in our group.

FOOTNOTES

[1] The abbreviations used are: DTT, dithiothreitol; SDS-PAGE, sodium dodesyl sulfate polyacrylamide gel electrophoresis; FT-IR, Fourier transform infrared; TMS, tetramethylsilane; ppm, parts per million; EDTA, ethylenediaminetetraacetate; WEFT, water-eliminated Fourier transform; FAB, fast-atom-bombardment.

[2] Varadarajan et al. replaced cysteine 110 of human myoglobin by alanine to prevent difficulties in protein purification (Varadarajan et al, 1989). In this study, we denote this mutant (Cys110→Ala) of human myoglobin as "wild type".

[3] The geminate rebinding for MbCO is distinctly non-exponential and can be fitted more adequately with either a stretched exponential or with a biexponential form (Tian et al., 1992). Steinbach (1991) also described this reaction by time dependent barrier model, which postured that the barrier to rebinding increases a function of a time as the protein relaxes towards the equilibrium. However, the CO geminate process of human wild type myoglobin and most mutants under aqueous solution at room temperature can be simulated by a single exponential well (Lambright et al., 1994).

REFERENCES

Adachi, S., & Morishima, I. (1989) *J. Biol. Chem. 264*, 18896-18901.

Adachi, S., Sunohara, N., Ishimori, K., & Morishima, I. (1992) *J. Biol. Chem. 267*, 12614-12621.

Alberding, N., Chan, S. S., Eisenstein, L., Frauenfelder, H., Good, D., Gunsalus, I. C., Nordlung, T. M., Perutz, M. F., Reynolds, A. H., & Sorensen, L. B. (1978) *Biochemistry 17*, 43-51.

Ansari, A., Berendzen, J., Braunstein, D., Cowen, B. R., Frauenfelder, H., Hong, M. K., Iben, I. E. T., Johnson, E. T., Ormos, P., Sauke, T. B., Scholl, R., Schulte, A., Steinbach, P. J., Vittitow, P. J., & Young, R. D. (1987) *Biophys. Chem. 26*, 337-355.

Antonini, E., & Brunori, M. (1971) *Hemoglobin and Myoglobin in Their Reactions with Ligands*, North-Holland, Amsterdam.

Austin, R. H., Beeson, K. W., Eisenstein, L., Frauenfelder, H., & Gunsalus, I. C. (1975) *Biochemistry 14*, 5355-5373.

Balasubramanian, S., Lambright, D. G., Marden, M. C., & Boxer, S. G. (1993) *Biochemistry 32*, 2202-2212.

Campbell, B. F., Chance, M. R., & Friedman, J. M. (1987) *Science 238*, 373-376.

Careaga, C. L., & Falke, J. J. (1992) *Biophys. J. 62*, 209-219.

Carver, T. E., Rohlfs, R. J., Olson, J. S., Gibson, Q. H., Blackmore, R. S., Springer, B. A., & Sligar, S. G. (1990) *J. Biol. Chem. 265*, 20007-20020.

Caughey, W. S., Alben, J. O., McCoy, S., Boyer, S. H., Carache, S., & Hathaway, P. (1969) *Biochemistry 8*, 59-62.

Caughey, W. S., Shimada, H., Choc, M. G., & Tucker, M. P. (1981) *Proc. Natl. Acad. Sci. U.S.A. 75*, 2903-2907.

Chatfield, M. D., Walda, K. N., & Madge, D. (1990) *J. Am. Chem. Soc. 112*, 4680-4687.

Cheng, X., & Schoenborn, B. P. (1991) *J. Mol. Biol. 220*, 381-399.

Daggett, V., & Levitt, M. (1993) *J. Mol. Biol. 232*, 600-619.

Dalvit, C., & Wright, P. E. (1987) *J. Mol. Biol. 194*, 313-327.

Decatur, S. M., & Boxer, S. G. (1995) *Biochem. Biophys. Res. Commun. 212*, 159-164.

Dou, Y., Admiraal, S. J., Ikeda-Saito, M., Krzywda, S., Wilkinson, A. J., Li, T. S., Olson, J. S., Prince, R. C., Pickering, I. J., & George, G. N. (1995) *J. Biol. Chem. 270*, 15993-16001.

Eaton, W. A., & Hofrichter, J. (1981) *Methods Enzymol. 76*, 175-261.

Elber, R., & Karplus, M. (1990) *J. Am. Chem. Soc. 112*, 9161-9175.

Frauenfelder, H., Petsko, G. A., & Tsernoglou, D. (1979) *Nature 280*, 558-563.

Frauenfelder, H., Park, K. D., & Young, R. D. (1988) *Annu. Rev. Biophys. Chem 17*, 451-479.

Frauenfelder, H., Sligar, S. G., & Wolynes, P. G. (1991) *Science 254*, 1598-1603.

Gibson, Q. H., Olson, J. S., McKinnie, R. E., & Rohlfs, R. J. (1986) *J. Biol. Chem. 261*, 10228-10239.

Gibson, Q. H., Regan, R. R., Elber, R., Olson, J. S., & Carver, T. E. (1992) *J. Biol. Chem. 267*, 22022-22034.

Goff, H. M., & La Mar, G. N. (1977) *J. Am. Chem. Soc. 99*, 6599-6606.

Gurd, F. R. N., & Rothgeb, T. M. (1979) *Adv. Prot. Chem. 33*, 73-165.

Gusev, N. B., Grabarek, Z., & Gergely, J. (1991) *J. Biol. Chem. 266*, 16622-16626.

Henry, E. R., Sommer, J. H., Hofrichter, J., & Eaton, W. A. (1983) *J. Mol. Biol. 166*, 443-451.

Jeng, M.-F., & Dyson, H. J. (1995) *Biochemistry 34*, 611-619.

Kanaya, S., Katsuda, C., Kimura, S., Nakai, T., Kitakuni, E., Nakamura, H., Katayanagi, K., Morikawa, K., & Ikehara, M. (1991) *J. Biol. Chem. 266*, 6038-6044.

Karplus, M., & McCammon, J. A. (1983) *Ann. Rev. Biochem. 52*, 263-300.

Kidera, A., Inaka, K., Matsushima, M., & Go, N. (1994) *Protein Sci. 3*, 92-102.

Kunkel, T. A. (1985) *Proc. Natl. Acad. Sci. U.S.A. 82*, 488-492.

Kuriyan, J., Wilz, S., Karplus, M., & Petsko, D. A. (1986) *J. Mol. Biol 192*, 133-154.

La Mar, G. N., Budd, D. L., & Goff, H. M. (1977) *Biochem. Biophys. Res. Commun. 77*, 104-110.

La Mar, G. N., Davis, N. L., Johnson, R. D., Smith, W. S., Hauksson, J. B., Budd, D. L., Dalichow, F., Langry, K. C., Morris, I. K., & Smith, K. M. (1993) *J. Am. Chem. Soc. 115*, 3869-3876.

Lambright, D. G., Balasubramanian, S., & Boxer, S. G. (1989) *J. Mol. Biol. 207*, 289-299.

Lambright, D. G., Balasubramanian, S., & Boxer, S. G. (1991) *Chem. Phys. 158*, 249-260.

Lambright, D. G., Balasubramanian, S., Decatur, S. M., & Boxer, S. G. (1994) *Biochemistry 33*, 5518-5525.

Li, X.-Y., & Spiro, T. G. (1988) *J. Am. Chem. Soc. 110*, 6024-2033.

Li, T., Quillin, M. L., Phillips Jr., G. N., & Olson, J. S. (1994) *Biochemistry 33*, 1433-1446.

Makinen, M. W., Houtchens, R. A., & Caughey, W. S. (1979) *Proc. Natl. Acad. Sci. U.S.A. 76*, 6042-6046.

Matsumura, M., Becktel, W. J., Levitt, M., & Matthews, B. W. (1989) *Proc. Natl. Acad. Sci. U.S.A. 86*, 6562-6566.

Newmann Jr., R. C., Kauzmann, W., & Zipp, A. (1973) *J. Phys. Chem. 77*, 2687-2691.

Oldfield, E., Guo, K., Augspurger, J. D., & Dykstra, C. E. (1991) *J. Am. Chem. Soc. 113*, 7537-7541.

Olson, J. S., Mathews, A. J., Rohlfs, R. J., Springer, B. A., Egeberg, K. D., Sligar, S. G., Tame, J., Renaud, J.-P., & Nagai, K. (1988) *Nature 336*, 265-266.

Pantoliano, M. W., Landner, R. C., Bryan, P. N., Rollence, M. L., Wood, J. F., & Poulos, T. L. (1987) *Biochemistry 26*, 2077-2082.

Park, K. D., Guo, K., Adeboun, F., Chiu, M. L., Sligar, S. G., & Oldfield, E. (1991) *Biochemistry 30*, 2333-2347.

Perry, L. J., & Wetzel, R. (1984) *Science 226*, 555-557.

Perutz M. F. (1965) *J. Mol. Biol. 13*, 646-668

Phillips, D. C. (1966) *Sci. Am. 215*, 75-80.

Phillips, S. E. V. (1980) *J. Mol. Biol. 142*, 531-554.

Pollitt, S., & Zalkin, H. (1983) *J. Bacteriol. 153*, 27-32.

Powers, L., Chance, B., Campbell, B., Friedman, J., Khalid, S., Kumar, C., Naqui, A., Reddy, K. S., & Zhou, Y. (1987) *Biochemistry 26*, 4785-4796.

Quillin, M. L., Arduini, R. M., Olson, J. S., & PhillipsJr., G. N. (1993) *J. Mol. Biol. 234*, 140-155.

Ray, G. B., Li, X.-Y., Ibers, J. A., Sessler, J. L., & Spiro, T. G. (1994) *J. Am. Chem. Soc. 116*, 162-176.

Rohlfs, R. J., Mathews, A. J., Carver, T. E., Olson, J. S., Springer, B. A., Egeberg, K. D., & Sligar, S. G. (1990) *J. Biol. Chem. 265*, 3168-3176.

Sassaroli, M., & Rousseau, D. L. (1987) *Biochemistry 26*, 3092-3098.

Shulman, R. G., Wüthrich, K., Yamane, T., Patel, D. J., & Blumberg, W. E. (1970) *J. Mol. Biol. 53*, 143-157.

Schulman, B. A., & Kim, P. S. (1994) *Protein Sci. 3*, 2226-2232.

Springer, B. A., Sligar, S. G., Olson, J. S., & Phillips Jr., G. N. (1994) *Chem. Rev. 94*, 699-714.

Steinbach, P. J., Ansari, A., Berendzen, J., Braunstein, D., Chu, K., Cowen, B. R., Ehrenstein, D., Frauenfelder, H., Johnson, J. B., Lamb, D. C., Luck, S., Mourant, J. R., Nienhaus, G. U., Ormos, P., Philipp, R., Xie, A., & Young, R. D. (1991) *Biochemistry 30*, 3988-4001.

Takano, T. (1977) *J. Mol. Biol. 110*, 537-584.

Tian, W. D., Sage, J. T., Srajer, V., & Champion, P. M. (1992) *Phys. Rev. Lett. 68*, 408-411.

Tian, W. D., Sage, J. T., Champion, P. M., Chien, E., & Sligar, S. G. (1996) *Biochemistry 35*, 3487-3502.

Unno, M., Ishimori, K., & Morishima, I. (1990) *Biochemistry 29*, 10199-10205.

Unno, M., Ishimori, K., Morishima, I., Nakayama, T., & Hamanoue, K. (1991) *Biochemistry 30*, 10679-10685.

Unno, M., Ishimori, K., Ishimura, Y., & Morishima, I. (1994) *Biochemistry 33*, 9762-9768.

Varadarajan, R., Szabo, A., & Boxer, S. G. (1985) *Proc. Natl. Acad. Sci. U.S.A. 82*, 5681-5684.

Varadarajan, R., Lambright, D. G., & Boxer, S. G. (1989) *Biochemistry 28*, 3771-3781.

CHAPTER 2.

Unusual Pressure Effects on Carbon Monoxide Rebinding to the Human Myoglobin Leucine29 Mutants

ABSTRACT

By using a laser flash photolysis under high pressure, we examined carbon monoxide rebinding reaction in some mutant myoglobins to access effects of hydrophobicity in the heme pocket on the ligand binding. The human myoglobin mutants bearing a less hydrophobic amino acid residue (Ala, Gly, Ser) at the leucine-29 position showed quite slow CO association rates at ambient pressure and their activation volumes ($\Delta V^{\neq}$) were positive (10–15 cm^3mol^{-1}), which is in sharp contrast to those of wild type myoglobin and other hemoproteins. The positive activation volume has been obtained for the ligand rebinding reactions in which the ligand diffusion process is the rate-determining step, for example, oxygen rebinding, suggesting that the rate-determining step was switched from the bond formation to the ligand migration process by the mutation. However, the small geminate yield in the Leu29 mutants ruled out the possibility of the ligand diffusion process as the rate-determining step. On the basis of the three-state model, the apparent activation volume ($\Delta V^{\neq}$) of the CO rebinding can be decomposed into the negative activation volume for the bond formation process ($\Delta V^{\neq}_{21}$) and the positive reaction volume change from the deoxy state to the geminate state (ΔV_{32}), which allows us to speculate that the positive apparent activation volume was originated from the enhancement of the reaction volume change, ΔV_{32}, instead of the switch of the rate-determining step. Since the reaction volume change depends on the hydration of the heme cavity, the increase of the water contents in the heme pocket of the less hydrophobic mutants would enhance the reaction volume change from the deoxy state to the geminate state, resulting in the positive apparent activation volume for the CO rebinding reaction in the Leu29 myoglobin mutants.

INTRODUCTION

In biophysical chemistry, hydrostatic pressure has long been used to affect dynamics, conformational equilibrium, and other properties of the native state of proteins (Heremans, 1982; van Eldik, 1986; van Eldik et al., 1989; Frauenfelder et al., 1990). One of the elegant applications of hydrostatic pressure on protein dynamics is pressure effects on the ligand binding to hemoproteins. Although various gaseous ligands can bind to the heme iron located inside the protein matrix, the X-ray structures of hemoproteins show no explicit pathways for entry and escape of the ligands, implying that the large protein fluctuation would be required for the ligand binding reactions, which would be perturbed by the hydrostatic pressure. The influence of pressure on gaseous ligand binding to ferrous hemoproteins has been extensively studied by our group (Adachi & Morishima, 1989; Adachi et al., 1992; Unno et al., 1990, 1991, 1994) and by others (Hasinoff, 1974; Balny & Travers, 1989; Projahn et al., 1990; Taube et al., 1990; Frauenfelder et al., 1990; Projahn & van Eldik, 1991). By measurements of the pressure dependence of ligand binding kinetics, we can determine the activation volume of the ligand binding reaction (that is, the volume change of the transition state with respect to the ground state) according to,

$$\frac{\partial \ln k}{\partial p} = - \frac{\Delta V^{*}}{RT} \tag{1}$$

Since the magnitude of the activation volume ($\Delta V^{\neq}$) results from conformational changes accompanied with the reaction of the protein and also reflects the specific interactions of the transition state with ligands, the volume profile can provide a wealth of information on dynamics of the ligand binding process.

For the carbon monoxide rebinding reactions for hemoproteins, negative activation volumes ranging between –42 and –9 cm^3mol^{-1} has been obtained (Hasinoff, 1974; Adachi & Morishima, 1989; Balny & Travers, 1989; Taube et al., 1990; Unno et al., 1991; Adachi et al., 1992; Lange et al., 1994), whereas the oxygen rebinding reaction exhibited small positive activation volumes (0–8 cm^3mol^{-1}) (Hasinoff, 1974; Adachi & Morishima, 1989; Taube et al., 1990; Projahn et al., 1990; Projahn & van Eldik., 1991; Adachi et al., 1992). As investigated by using small compounds and model systems (Taube et al., 1990; Projahn et al., 1990), these differences in the activation volume have been attributed to the different rate-

determining step for the ligand binding process. The negative activation volume for the CO binding to the heme corresponds to a bond formation process as the rate-determining step and the positive activation volume for the O_2 binding implies that a ligand diffusion process is the rate-determining step.

In our previous studies (Adachi et al., 1992; Unno et al., 1994), we found an anomalous pressure dependence of the CO rebinding rates for the myoglobin Leu29 → Ala (L29A[1]) mutant and cytochrome P450 in the absence of camphor. Both of them exhibited positive activation volumes, which could be interpreted in the sense that the rate-determining step was switched from the bond formation to the ligand diffusion process. Without the substrate, the CO rebinding rate for cytochrome P450 was extremely fast, characteristic of the ligand diffusion process as the rate-determining step (Unno et al., 1994). However, the CO rebinding rate for the myoglobin L29A mutant was substantially slow as compared with wild type myoglobin (Adachi et al., 1992), suggesting that the some other factors can affects activation volume for the ligand binding process in addition to the switch of the rate-determining step.

As we have shown in our latest paper for the Leu29 mutants (Uchida et al., 1997), the mutation-induced changes of the hydrophobicity in the heme cavity as well as the volume changes of the side chain at the 29 position are the possible key factors for the highly decelerated ligand binding rate (Figure 1). We speculated that the replacement of the highly hydrophobic residue, Leu29, by other less hydrophobic residue reduces the hydrophobicity in the heme cavity and allows a flux of some water molecules inside or near the heme cavity, which enhances the barrier of the CO binding to the heme iron. Such an essential role of the hydrophobicity in the heme cavity on the ligand binding kinetics prompted us to examine whether the activation volume for the CO rebinding reaction is also sensible to hydrophobicity in the heme cavity. Jung and co-workers have found that pressure has significant effects on the CO vibrational frequency and population distribution among sub-conformers (Jung et al., 1992; Schultz et al., 1994) and suggested that these changes are caused by substrate mobility and a flux of water molecules into the heme pocket. To gain further insights into the positive activation volume in the CO recombination reaction of the L29A mutant, we have examined here the pressure dependence of the CO recombination rates for the Leu29 mutants which bear various hydrophobicity inside the heme pocket and

discussed in relation to the volume profile during CO rebinding and to hydrophobicity in the heme pocket.

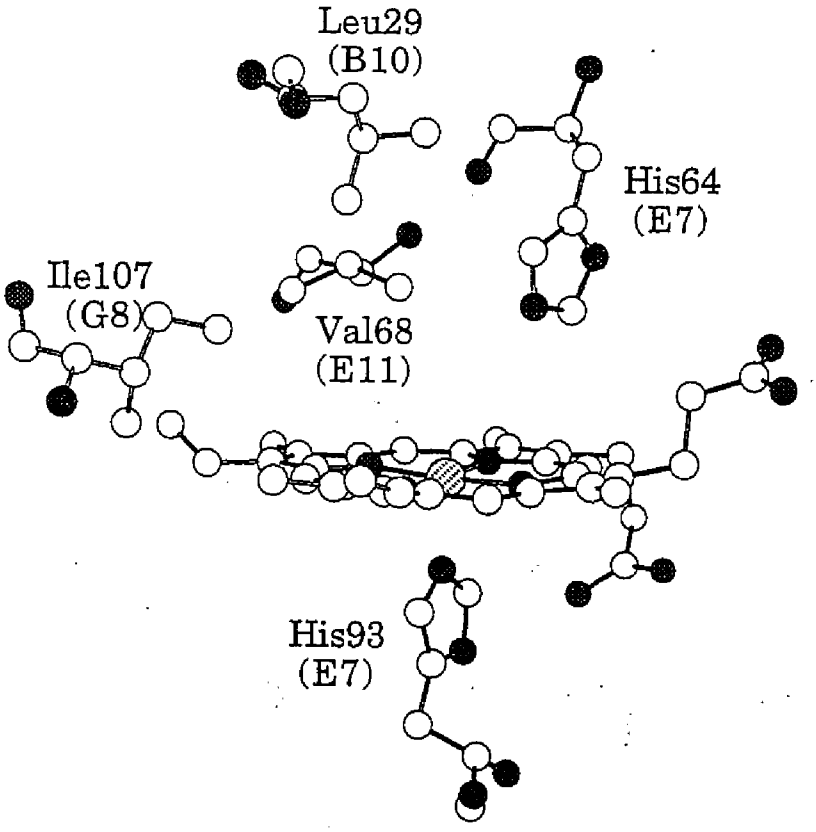

Figure 1. Heme environmental structure of human myoglobin (Hubbard et al., 1990). The heme and some selected amino acid residues constituting the heme pocket are shown.

EXPERIMENTAL PROCEDURE

Preparation of Mutant Myoglobins. The original expression vector of human myoglobin[2], pMb3 (pLcIIFXMb), is a gift from Varadarajan and Boxer (Varadarajan et al., 1985). The procedures for the site-directed mutagenesis are described in the previous papers (Kunkel, 1985; Varadarajan et al., 1989; Adachi et al., 1992). Preparation and purification of wild type and mutant myoglobins were followed by the method described previously (Varadarajan et al., 1989; Adachi et al., 1992; Uchida et al., 1997).

Laser Photolysis Measurements under Various Pressure. The CO association rate constants under high pressure were obtained by a laser

Morishima, 1889; Unno et al., 1990, 1991, 1994; Adachi et al., 1992). The absorption changes were monitored at 440 nm. Signals were detected in transmission using a photomultiplier (Hamamatsu Photonics, R2949) and the transient signals were digitized using a Tektronix TDS-320 oscilloscope. Ligand rebinding to wild type and mutant myoglobins except for the L29S mutant (80–140 MPa) were analyzed by fitting the time courses of the absorbance change to the equation,

$$\Delta A_t = \Delta A_0 \exp(-k_{app}\, t) \tag{2}$$

Two exponentials were required to fit the time courses of the L29S mutant at 80–140 MPa,

$$\Delta A_t = \Delta A_1 \exp(-k_{app1}\, t) + \Delta A_2 \exp(-k_{app2}\, t) \tag{3}$$

where ΔA_t is the absorbance change at any time t, ΔA_0 is the total absorbance change (absorbance at $t = 0$ minus absorbance at $t = \infty$). k_{app} is the observed first-order rate constant and satisfies the following equation (Antonini & Brunori, 1971),

$$k_{app} = k_{on}[CO] \tag{4}$$

where k_{on} is the bimolecular ligand binding rate constant. All the experiments under high pressure were performed in 100 mM Tris-HCl buffer pH 7.8. The pH of Tris buffer has been shown to be independent of pressure up to 200 MPa (Newmann et al., 1973).

The activation volume is given by the equation,

$$\Delta V^{\ddagger} = -RT\left(\frac{\partial(\ln k_p / k_1)}{\partial P}\right)_T \tag{5}$$

where R is the gas constant (= 8.314 J K^{-1} mol^{-1}), T is absolute temperature and k_1 and k_p are the observed first-order rate constants at 0.1 and P MPa, respectively. The slopes of the plot of ln k_p/k_1 versus pressure for the mutant myoglobins at atmospheric pressure were calculated by the optimized second order polynomial function (van Eldik et al., 1989). Since the sample was placed in a sealed quartz capsule with no gas phase CO in contact with the ligand sample, the pressure dependence of [CO] is negligible over the range of applied pressure.

Electronic Absorption Spectra under Various Pressure. The measurements of electronic absorption spectra under high pressure were performed by using a high pressure cell and its inner capsule made of quartz. The inner sample capsule consists of the upper cylindrical part and the lower square-shaped part. The lower optical square-shaped part has the path length of 5.0 mm. The high pressure cell and its inner capsule have been described in our previous paper in detail (Hara & Morishima, 1988; Adachi & Morishima, 1989). The pressure was transmitted from an intensifier (Hikari High-Pressure Co., Ltd. KP-5-B) and was measured by using a Bourdon tube gauge. A background spectrum was taken using a buffer containing inner sample capsule. Electronic absorption spectra were recorded on a SHIMADZU UV 2200 UV/visible spectrophotometer. The buffer condition was 100 mM Tris-HCl buffer pH 7.8. Pressure-induced spectral changes were fully reversible.

RESULTS

Laser Photolysis Measurements under Various Pressure. In order to evaluate the pressure effect on the CO binding reaction, CO bimolecular rebinding kinetics for the Leu29 mutants were measured under various hydrostatic pressures. The effects of pressure on the time courses of the absorbance at 440 nm for CO rebinding to the Leu29 mutants at 0.1 and 100 MPa are exemplified for the L29S mutant in Figure 2A. The recombination rate for the L29S mutant was decreased by pressurization. The time courses of CO rebinding for wild type and mutant myoglobins except for the L29S mutant at 80–140 MPa can be fitted by equation 2 and the association rate constants at ambient pressure are compiled in Table I. As shown in Table I, all the mutants examined here showed highly reduced CO rebinding rate constants at ambient pressure. Particularly, the rebinding rate for the L29S mutant was extremely slow. Figure 3 illustrates the pressure dependence of the CO rebinding rate constants for wild type and mutant myoglobins. Pressurization accelerated the CO association rate for wild type myoglobin and its activation volume was estimated as $-21\ cm^3mol^{-1}$ by equation 5 (Table I), which is virtually the same as that reported by our previous work (Adachi et al., 1992). The pressure dependent features for the Leu29 mutants in Figure 3 can be clearly classified into two groups. One group consists of the L29F and L29I mutants, both of which have a hydrophobic residue at the position of leucine-29 and their rebinding rates were accelerated monotonously by

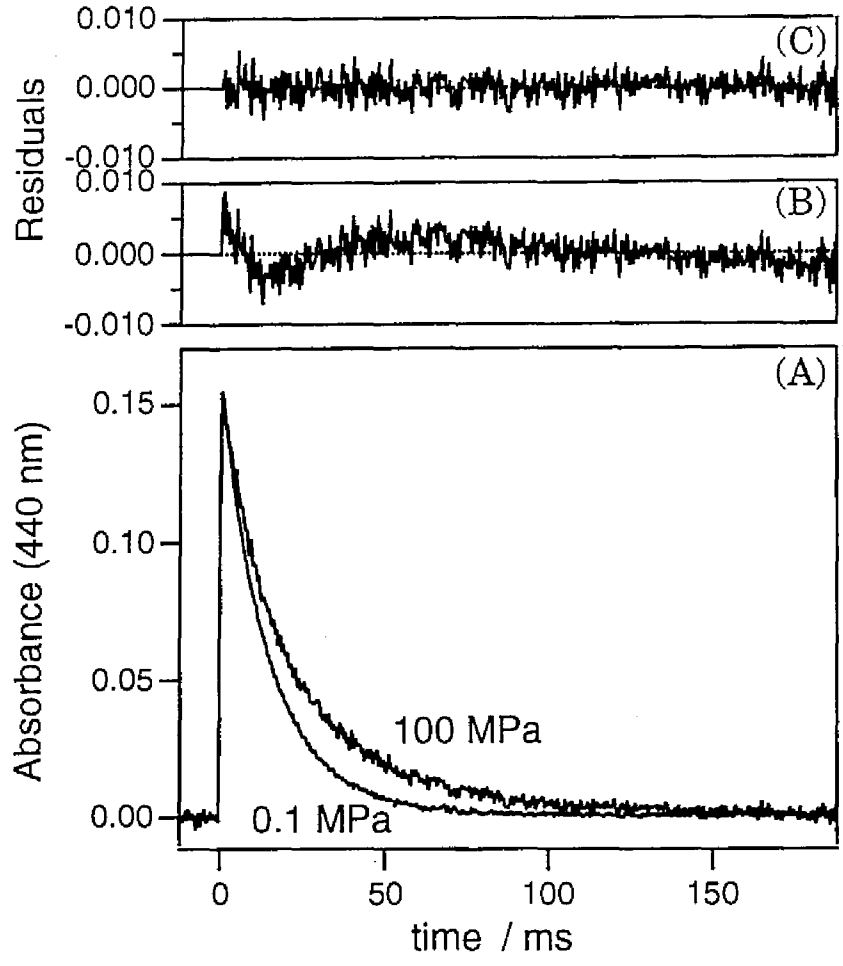

Figure 2. (A) Time courses for millisecond rebinding of CO to the L29S mutant myoglobin at 0.1 and 100 MPa. The absorbance at 0.1 MPa is normalized with that at 100 MPa. The middle panel (B) is the residuals from a single exponential fit and the upper panel (C) is the residuals from the best sum of two exponential fit. Reactions were monitored at 440 nm.

pressurization as observed for wild type myoglobin. The apparent activation volumes, $\Delta V^{\neq}$, at atmospheric pressure for the CO rebinding reaction in the L29F and L29I mutants are consequently negative (–10 and –3.7 cm^3mol^{-1}, respectively). On the other hand, the other group which includes the L29A, L29S and L29G mutants, exhibited quite different pressure dependence from those for wild type, L29I, and L29F myoglobins. As reported by our previous study (Adachi et al., 1992), pressurization decelerated the CO rebinding rate for the L29A mutant and its activation volume was positive (10 cm^3mol^{-1}). In the present work, the two mutants, L29G and L29S, which have less hydrophobic residue at the 29 position (Table I), also showed deceleration in the CO rebinding rates by

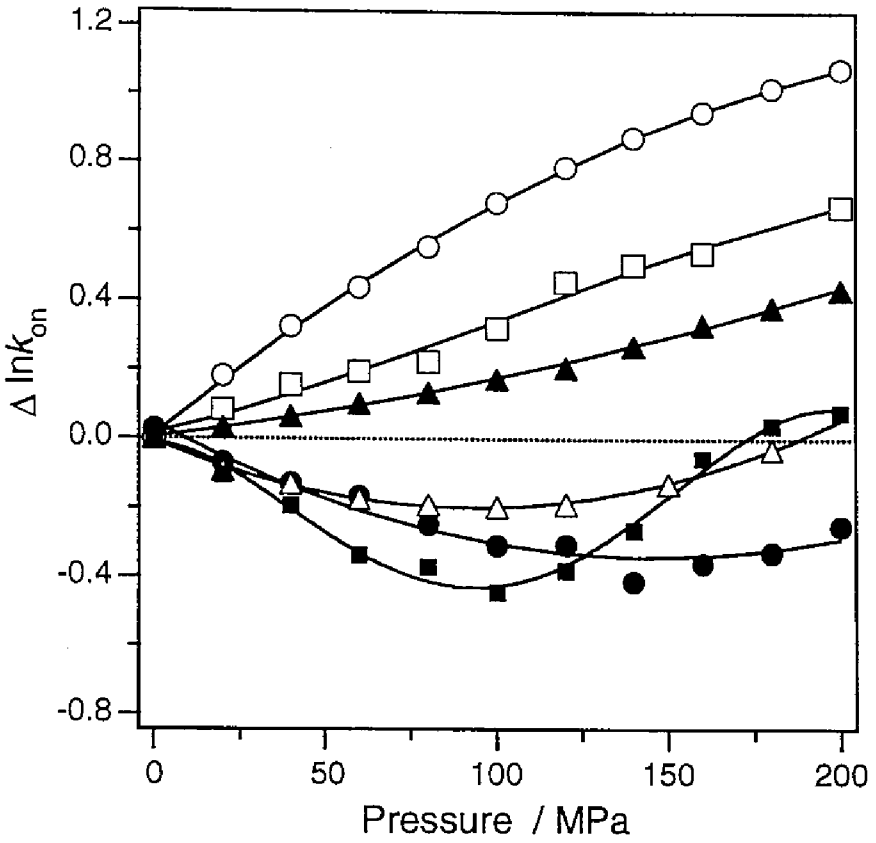

Figure 3. Logarithmic plot of the rate constants for the bimolecular CO association reaction *vs* hydrostatic pressure for (O), wild type; (■), L29S; (●), L29G; (Δ), L29A; (▲), L29I; (□), L29F at 20 °C.

TABLE I: Kinetic Rate Constants and Activation Volumes for CO Binding to Wild Type and Mutant Myoglobins and Hydrophobic Index of Residue at Position of Leu29.

Myoglobin	k_{on}^{CO} $\mu M^{-1}s^{-1}$	$\Delta V^{\neq}_{CO}$ cm^3mol^{-1}	hydrophobicity[a] kcal mol^{-1}
Wild type	1.1	-21	+2.31
L29I	0.19	-3.7	+2.45
L29A	0.15	10	+0.42
L29G	0.11	13	0.0
L29S	0.069	15	-0.05
L29F	0.081	-10	+2.43

[a]Fauchère & Pliska (1983).

pressurization. Their activation volumes are positive and estimated as 13 and 15 cm^3mol^{-1} at normal pressure, respectively. Another characteristic

feature of this group is a large deviation from the linear relation in the pressure dependence of the rate constants, implying that the activation volume depends on pressure. Their rate constants decreased as hydrostatic pressure was elevated up to 100–150 MPa, whereas in the higher pressure region, the rate constants were increased by pressurization.

Under high pressure above 80 MPa, the time courses for the L29S mutant cannot be simulated by equation 2 as shown in Figure 2B. The residuals from the two exponentials (equation 3) exhibit a random distribution (Figure 2C), indicating that multi-exponentials are required to fit the time courses at 80–140 MPa. We fitted the time courses for CO rebinding to the L29S mutant from 80 to 140 MPa with a sum of two exponentials. The fraction and rate constants of each component under various pressure are illustrated in Figures 4A and 4B, respectively. Although the pressure dependence of CO association rates for the L29G and L29A mutants are similar to that for the L29S mutant, we can fit the time courses of CO rebinding for the L29G and L29A mutants by a single exponential.

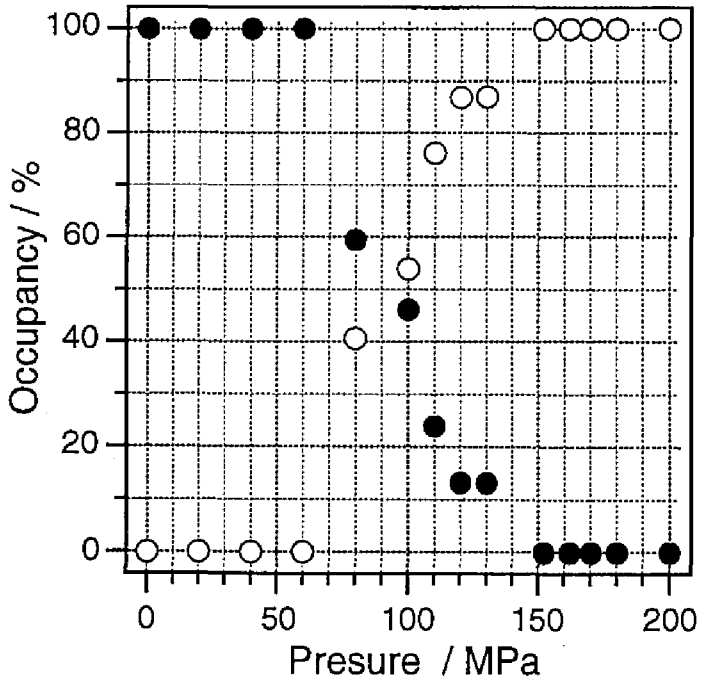

Figure 4. (A) Dependence of the population of two components on the hydrostatic pressure. We fitted the time course of CO rebinding by two exponentials (equation 3) at 80–140 MPa and by one exponential other region (equation 2); (●), ΔA_1; (○), ΔA_2.

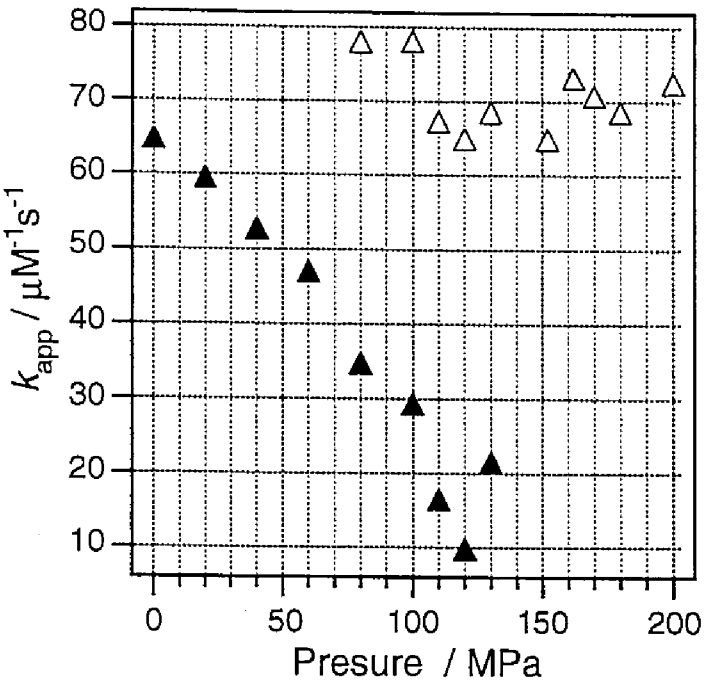

Figure 4. (B) Dependence of the CO bimolecular rebinding rate constants on the hydrophobic pressure. We fitted the time course of CO rebinding by two exponentials (equation 3) at 80–140 MPa and by one exponential other region (equation 2); (▲), k_{app1} ; (△), k_{app2}.

Geminate Rebinding. Since the previous studies showed that the activation volume depends on the rate-determining step for the CO binding to hemoglobin (Unno et al., 1991) and cytochrome $P450_{cam}$ (Unno et al., 1994), we measured geminate rebinding process at atmospheric pressure to examine the effects of the mutation on the rate-determining step. Time courses for nanosecond rebinding of carbon monoxide to wild type and the L29S mutant myoglobins are illustrated in Figure 5. Wild type myoglobin showed about 2% geminate yield, while the geminate yield for the L29S mutant was about the half (1%) under this condition. Although we cannot estimate the rate constants for each elementary reaction process due to the low geminate yield, it can be safely said that almost all the photolyzed CO molecules do not bind to the heme iron in the geminate process, but diffuse to solvent, resulting in the slow bimolecular rate with the bond formation process (k_{21}) being the rate-determining step. Both of the L29G and L29A mutants with the positive activation volumes also exhibited quite small geminate rebinding as observed for the L29S

mutant[3]. These results indicate that the bond formation process is the rate-determining step for the L29S, L29G and L29A mutants.

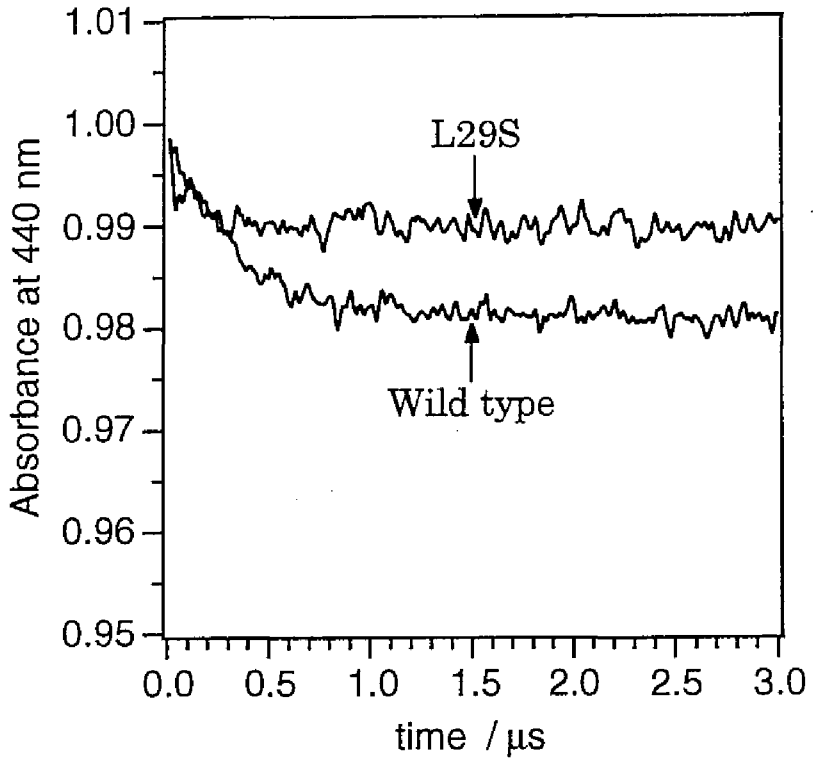

Figure 5. Time courses for geminate rebinding of CO to wild type and L29S mutant myoglobins at 0.1 M Tris pH 7.8, 20 °C. The absorbance changes were monitored at 440 nm.

Electronic Absorption Spectra under Various Pressure. The absorption spectra have been used to evaluate the alteration in conformational equilibrium and protein dynamics induced by hydrostatic pressure (Hui Bon Hoa et al., 1982, 1989; Gross & Jaenicke, 1994). The peak position of the Soret band for carbonmonoxy P450 has been considered to be one of the markers for hydrophobicity in the heme pocket (Jung et al., 1995, 1996). Jung et al. proposed that the polar heme environment induces a red-shift in the Soret band (Jung et al., 1996). The Soret bands of wild type and L29S mutant myoglobins in the CO-form at 0.1, 80, 160, and 200 MPa are illustrated in Figure 6. The peak positions of the Soret band for both myoglobins are slightly but significantly red-shifted. In Figure 7A, the peak positions are plotted versus pressure. For wild type and all the mutant myoglobins, pressurization caused a pressure-induced red-shift for the Soret band, suggesting that the polarity of the heme cavity is increased under high pressure. Such a pressure-

induced red-shift was also encountered for P450 and hemoglobin (Gibson & Carey, 1977; Alden et al., 1989; Jung et al., 1995).

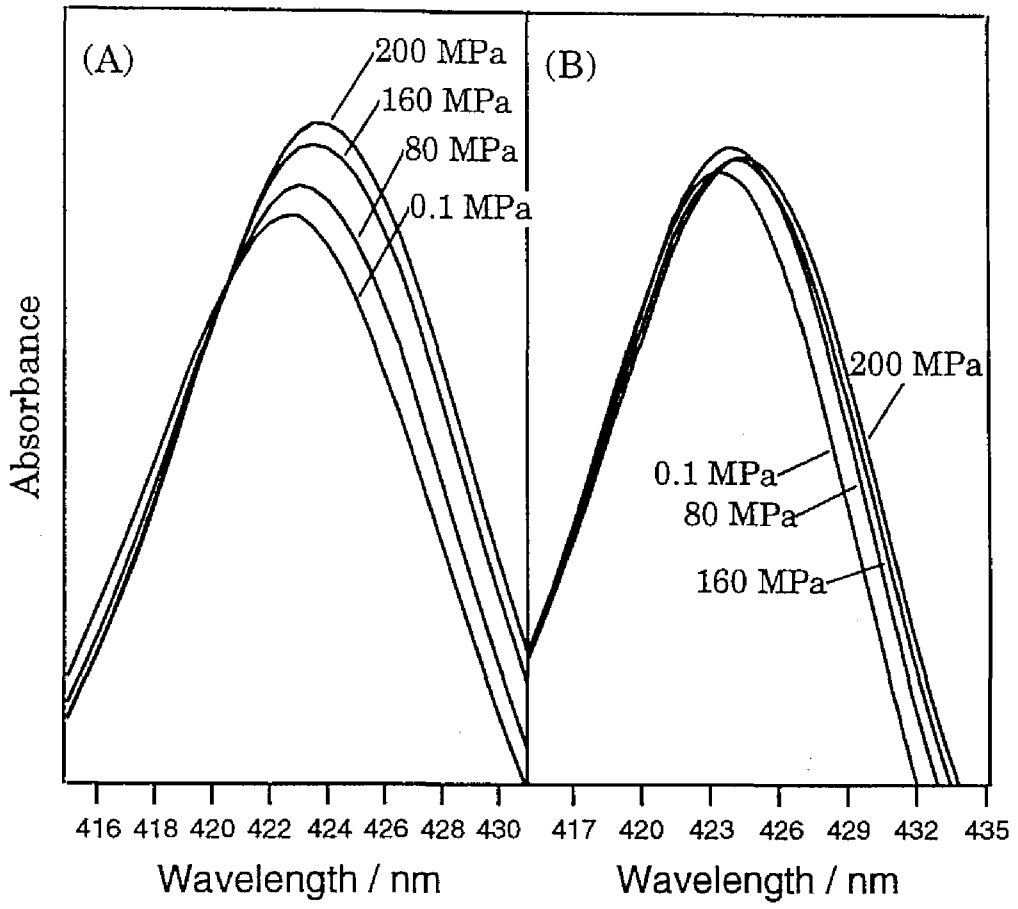

Figure 6. Absorption spectra for carbomonoxy wild type (A) and L29S mutant (B) myoglobins in the Soret region under various pressure. Spectra measured at 0.1, 80, 160 and 200 MPa are shown. The spectra were obtained in 100 mM Tris buffer at pH 7.8.

In Figure 7A, the pressure dependence of the Soret peak position for the L29S mutant shows an S-shape, suggestive of some pressure-induced conformational transition for this mutant. Pressure-induced broadening of the Soret band for the L29S mutant also appears to support this conformational transition (Figure 7B). Half-width of the Soret band (HWFM) for the other mutants and wild type myoglobins was almost insensitive to pressure or linearly increased as pressure is elevated. These pressure-induced changes of the Soret band in wild type and mutant myoglobins were reversible and protein was not denatured under high pressure. At neutral pH, the application of hydrostatic pressure

below 400 MPa does not produce any protein unfolding (Ogunmola et al., 1977; Heremans, 1982).

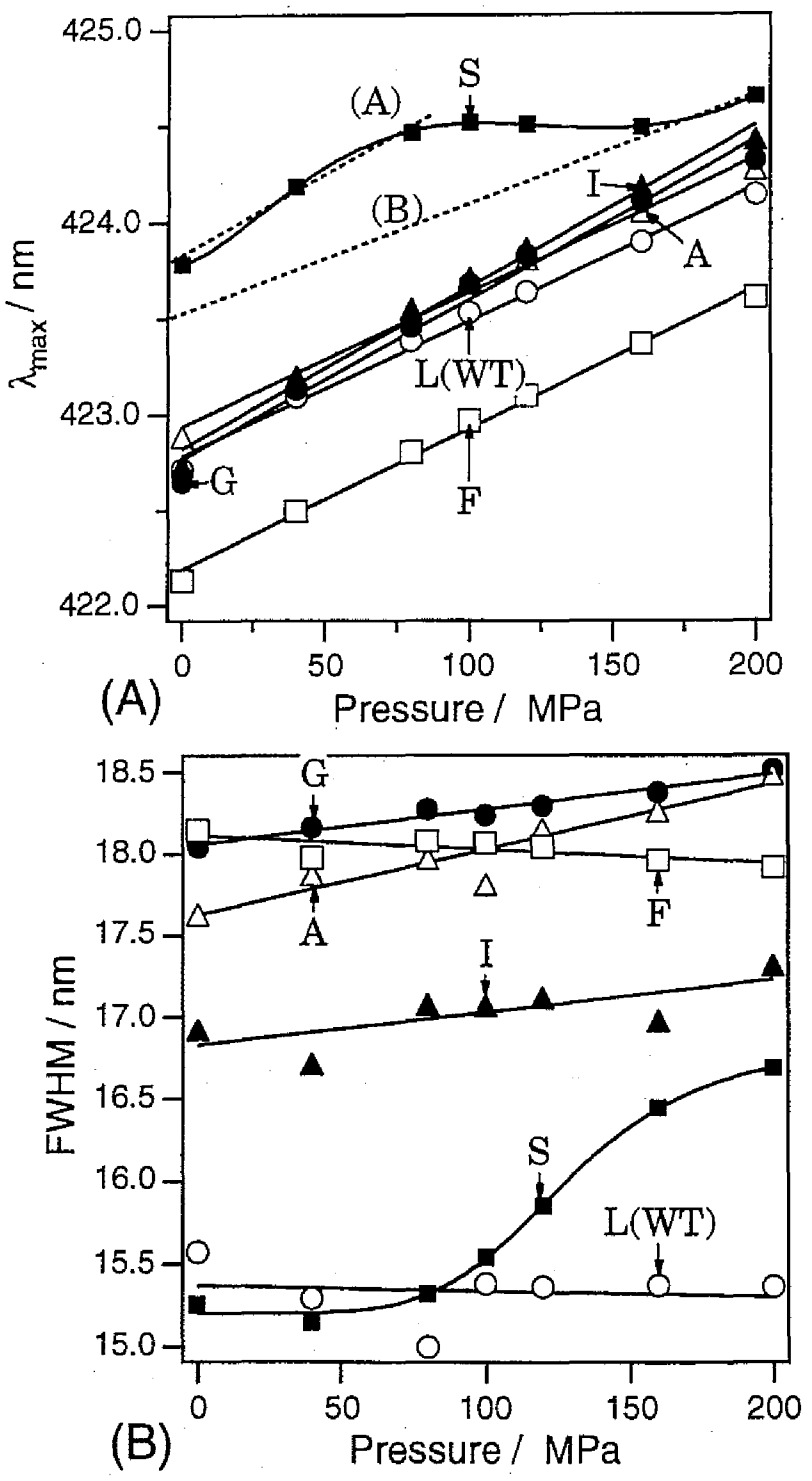

Figure 7. Pressure dependence on the center position (A) and the half-width (FWHM) (B) of the Soret band for the carbomonoxy myoglobins; (○), wild type; (■), L29S; (●), L29G; (△), L29A; (▲), L29I; (□), L29F.

DISCUSSION

Unusual Positive Activation Volume for Carbon Monoxide Binding to the Leu29 Mutants. The activation volumes, $\Delta V^{\neq}$, of small neutral exogenous ligand binding reaction to ferrous hemoproteins lie in between about +10 and –25 cm^3mol^{-1} (Hasinoff, 1971; Adachi & Morishima, 1989; Balny & Travers, 1989; Projahn et al., 1990; Taube et al., 1990; Unno et al., 1990, 1991, 1994). O_2, isocyanide, and imidazole binding experiences a positive $\Delta V^{\neq}$, while CO binding gives a negative $\Delta V^{\neq}$. This difference has been explained in terms of the different rate-determining step of the ligand binding process (Projahn et al., 1990; Taube et al., 1990; Traylor et al., 1992). It has been generally accepted that the ligand binding process in aqueous solution is described by a three-state model (Henry et al., 1983) as indicated by the following scheme.

$$\underset{1}{\mathrm{MbL}} \underset{k_{21}}{\overset{h\nu}{\rightleftharpoons}} \underset{2}{\mathrm{Mb:L}} \underset{k_{32}}{\overset{k_{23}}{\rightleftharpoons}} \underset{3}{\mathrm{Mb+L}} \qquad (6)$$

where L represents ligands and Mb is myoglobin. The states 1 and 3 are referred to as the ligand bound and the deoxy states, respectively. The state 2 is the geminate state in which the iron-ligand bond has been photolyzed but the ligand is still trapped within the protein matrix (Henry et al., 1983). In the case of CO rebinding, Fe-CO bond formation process is the rate-determining step, which gives a negative activation volume. In contrast, the diffusion process (3 → 2) is the rate-determining step for the binding of O_2, resulting in the positive activation volume.

In contrast to the apparent negative activation volumes of CO rebinding for wild type myoglobin (Hasinoff, 1974; Adachi et al., 1989; Taube et al., 1990), hemoglobin (Unno et al., 1991), and horseradish peroxidase (Balny & Travers, 1988), the L29S, L29G, and L29A mutants have large positive activation volumes at 0.1 MPa as listed in Table I. One of the reasons for such a difference in the sign of the activation volumes would be the change of the rate-determining step from the bond formation process to the ligand diffusion process between these two systems. However, the present finding of the very small geminate yield (see Results and the footnote 4) clearly shows that the bond formation process is still the rate-determining step for the mutants. For O_2 binding to myoglobin, the geminate yield is more than 50%, which is characteristic of the diffusion control reaction (Jongeward et al., 1988). In the present study,

the geminate yield for the reaction of the L29S mutant with CO was quite low (only 1% of total photolyzed products). The geminate yields for the L29G and L29A mutants was also low as the case for the L29S mutant. These results imply that the switch of the rate-determining step is not responsible for the positive activation volume for the mutants having a less hydrophobic amino acid residue at the 29 position.

As reported for many other systems (Heremans, 1982), various determinants have been proposed to contribute to the observed value of $\Delta V^{\neq}$ for small ligand binding reaction to the hemeproteins. However, most of the factors contribute to a negative $\Delta V^{\neq}$, such as covalent bond formation (van Eldik et al., 1989), high-spin to low-spin transition (van Eldik, 1986), the motion of heme iron from "out-plane" to "in-plane" (Hasinoff, 1974; Projahn et al., 1990), solvation of hydrophobic residues (van Eldik et al., 1989), and formation of a hydrogen bonding (van Eldik et al., 1989). Desolvation was proposed to be an only factor for the positive activation volume (Taube et al., 1990). The loss of solvating molecules from the ligand upon entry into the hydrophobic heme pocket would result in a volume increase. However, the volume changes accompanied with the desolvation of the hydrated ligand for the mutants would be almost the same as that for wild type myoglobin, since the hydration of the ligand is expected to mainly depend on ligand itself, not on the protein. It is, therefore, unlikely that desolvation is the major factor to differentiate the activation volumes of the L29S, L29A, and L29G mutants from that of wild type myoglobin.

To qualitatively interpret the positive activation volumes for the L29S, L29A, and L29G mutants, we start from the three-state model (equation 6). In this model, the overall rate constants correlates with the rate constants of the elementary steps by equation 7 (Henry, 1983),

$$k_{on} = \frac{k_{21}}{k_{21} + k_{23}} k_{32} \tag{7}$$

If [CO] is assumed to be constant during the high pressure experiments, the apparent activation volume ($\Delta V^{\neq}$), which is defined by equation 5, is formulated as follows by using equations 5 and 7,

$$\Delta V^{*} = -RT\left\{\left(\frac{\partial \ln k_{21}}{\partial P}\right)_T + \left(\frac{\partial \ln k_{32}}{\partial P}\right)_T - \left(\frac{\partial \ln\left(k_{21} + k_{23}\right)}{\partial P}\right)_T\right\} \tag{8}$$

$$= \Delta V_{21}^{\neq} + \Delta V_{32}^{\neq} + RT\left(\frac{\partial \ln(k_{21}+k_{23})}{\partial P}\right)_T \quad (9)$$

Since the rate-determining step of the CO association reaction for the L29S mutant is the bond formation step as mentioned above, k_{23} is supposed to be much larger than k_{21} and equation 9 can be simplified as equation 10 or 11,

$$\Delta V^{\neq} \cong \Delta V_{21}^{\neq} + \Delta V_{32}^{\neq} + RT\left(\frac{\partial \ln(k_{23})}{\partial P}\right)_T \quad (10)$$

$$= \Delta V_{21}^{\neq} + \Delta V_{32}^{\neq} - \Delta V_{23}^{\neq} \quad (11)$$

If the partial volume of the transition state of the process $3 \rightarrow 2$ ($V_{32}^{\neq}$) is the same as that of the $2 \rightarrow 3$ process ($V_{23}^{\neq}$), we obtain the equation 12,

$$\Delta V_{32}^{\neq} - \Delta V_{23}^{\neq} = \left(V_{32}^{\neq} - V_3\right) - \left(V_{23}^{\neq} - V_2\right) = \Delta V_{32} \quad (12)$$

where V_2 and V_3 correspond to the partial volumes of the geminate and unliganded states, respectively. Finally we can get the following equation (equation 13),

$$\Delta V^{\neq} = \Delta V_{21}^{\neq} + \Delta V_{32} \quad (13)$$

The activation volume for the Fe-CO bond formation process of the mutants, $\Delta V_{21}^{\neq}$, is supposed to be negative[4], since the formation of covalent bonds has a $\Delta V^{\neq}$ of ≈ -10 cm^3 mol^{-1} (van Eldik et al., 1989; Traylor et al., 1992). It is most likely, therefore, that the positive values of $\Delta V^{\neq}$ for the L29S, L29G and L29A mutants are attributable to the positive reaction volume change, ΔV_{32}, which corresponds to the differences in the partial volume between the geminate and deoxy states. The positive value of ΔV_{32} for the mutants means that the partial volume of the geminate state (V_2) is larger than that of the unliganded state (V_3).

Although it is difficult to directly decide the determinant of the reaction volume changes (ΔV_{32}), some factors which can affect the reaction volume have been proposed (van Eldik et al., 1989; Gross & Jaenicke, 1994; Mozhaev et al., 1996). One of such factors for heme proteins is the hydration in the heme cavity. In the pressure-induced interconversion process from P450 to P420, the volume changes were

correlated to the hydration in the heme pocket (Di Primo et al., 1990, 1992). The volume change from P450 to P420 is –197 cm^3mol^{-1} in the presence of camphor, whereas, without camphor, the volume change is reduced to –73 cm^3mol^{-1}. On the basis of the x-ray crystal structures (Poulos et al., 1985, 1986), camphor binding perturbs the hydration of the heme cavity: the coordinated water molecule (or hydroxide ion) and water molecules located near the heme iron are kicked out from the heme cavity in the presence of the bound camphor, which renders the heme pocket more hydrophobic in camphor-bound P450. The difference in the volume changes upon the conversion from P450 to P420 between the camphor-bound (–197 cm^3mol^{-1}) and camphor-free (–73 cm^3mol^{-1}) forms comes from the alternation of the degree of hydration in the heme pocket, since the displacement of camphor in the heme pocket accompanied with the conversion from P450 to P420 in the camphor-bound form allows the entrance of the water molecules into the heme cavity, resulting in an increase in the volume change between P450 and P420.

As we reported previously (Uchida et al., 1997), the increase in the water contents in the heme pocket was proposed for the L29S, L29G and L29A mutants due to the less hydrophobic heme pocket, which also suggests the hydration of the heme pocket is perturbed in these mutants. Although it would be difficult and not so simple to compare the ligand binding process of myoglobin with the protein interconversion process of P450, it appears plausible that the different degree of hydration in the heme pocket affects the reaction volume (ΔV_{32}) for the ligand binding process of the mutant, eventually affording the positive activation volume, $\Delta V^{\neq}$. However, it is, so far, unclear why the increased water contents in the heme cavity enhance, not reduce, the reaction volume change, ΔV_{32}. On the basis of the x-ray structure, water molecules located in the heme cavity of wild type deoxy myoglobin has been suggested to be expelled out to allow the entry of the ligand (Quillin et al., 1993). In the less hydrophobic environment of the heme cavity in the Leu29 mutants, the entry of the ligand would not accompany the escape of the water molecules from the heme cavity, resulting in the larger expansion for the heme cavity in the geminate state.

Conformational Changes in the L29S Mutant under High Pressure. As shown in Figure 4, two components were detected in the time courses of the CO rebinding to the L29S mutant and the pressure-induced transition between the conformers were observed. The transition was also manifested as the shift of the Soret peak of absorption spectra upon

pressurization (Figures 6 and 7). The Soret peak for the L29S mutant exhibited a red-shift in proportion to pressure up to 80 MPa. In the region between 80–160 MPa, the peak position was almost insensitive to pressure and linearly red-shifted again above 160 MPa. This pressure dependence of the Soret maximum position for the L29S mutant is simulated by two lines, A and B, as depicted in Figure 7A. The conformer A is dominant at atmospheric pressure and the conformer B, which is supposed to have the Soret peak at 423.5 nm at ambient pressure, is the major conformer above 150 MPa.

It is quite interesting that the position of the Soret peak for the component B is placed between the positions of the conformer A for the L29S mutant (423.8 nm) and wild type myoglobin (422.7 nm) and the transition from the conformer A to B was promoted by pressure. Since the peak position of the Soret band is determined by the heme π–π^* transition energy which is lowered in the polar environments (Slichter & Drickamer, 1980; Laird & Skinner, 1989), the polarity of the heme pocket in the conformer B does not appear so high as compared with that of the conformer A. Therefore, pressurization is likely to reduce the polarity of the heme pocket in the L29S mutant. As suggested in our previous study (Uchida et al., 1997), the substituted serine at the position of leucine-29 allows extra water molecules inside the heme cavity at ambient pressure (Uchida et al., 1997). The more hydrophobic feature of the heme cavity for the conformer B at high pressure may suggest that pressurization expels some of the extra water molecules from the heme cavity of the L29S mutant.

The escape of the water molecules from the heme cavity by pressure is also suggested by the kinetic properties of the two conformers. The conformer A, the main conformer in the L29S mutant at atmospheric pressure (ΔA_1 in Figure 4), showed slow CO association rates with a positive activation volume (k_{app1} in Figure 4). On the other hand, the CO binding properties for the conformer B (ΔA_2 in Figure 4) is similar to that of wild type myoglobin (k_{app2} in Figure 4): the CO rebinding rate is significantly larger than that of the conformer A and its pressure dependence is small (Figure 4B). The similarity of the kinetic properties between the conformer B of the L29S mutant and wild type myoglobin corresponds to the more hydrophobic heme cavity of the conformer B as found for wild type myoglobin, supporting the pressure-induced escape of water molecules from the heme cavity.

Although the L29G and L29A mutants also showed a bimodal curve in the pressure dependence of CO association rate with positive $\Delta V^{\neq}$ in the low pressure region and a negative $\Delta V^{\neq}$ in the high pressure region (Figure 3), only one conformer was detected. Although the L29G and L29A mutants would also have two conformers as the L29S mutants (Figure 2), the small difference of the CO association rate constants for the two conformers in the mutants may have prevented us from distinguishing the two conformers.

In summary, the pressure dependence of the CO rebinding rates has revealed that the activation volumes for CO binding to the L29S, L29G, and L29A mutants are unusually positive. Although the positive activation volume appears to indicate that the rate-determining step is the ligand diffusion process, the switch of the rate-determining step from the bond formation process to the ligand diffusion process was not observed. Although it is not so clear why the apparent activation volume is positive in these mutants, we propose the contribution of the water molecules in the heme cavity to the activation volume. The increased water contents in the heme pocket of the mutants perturb the hydration of the heme cavity, which may alter the reaction volume change between the geminate and ligand ligated states (ΔV_{32}), and results in the positive activation volume ($\Delta V^{\neq}$). The contribution of the water molecules in the heme cavity to the ligand binding was also suggested by the pressure-induced conformational transition in the L29S mutant detected in the absorption spectra under high pressure. Pressurization facilitates the escape of the water molecules from the heme cavity and, under high pressure, the CO association rate constants and its pressure dependence for the L29S mutant becomes close to those of wild type myoglobin.

FOOTNOTES

[1] The myoglobin mutants are listed in the text using the single amino acid Abbreviations (i.e. Leu29(B10) → Phe, Leu29(B10) → Ile, Leu29(B10) → Ala, Leu29(B10) → Gly, and Leu29(B10) → Ser substitutions are designated as the L29F, L29I, L29A, L29G, and L29S mutants, respectively).

[2] Varadarajan et al. (1989) replaced cysteine-110 of human myoglobin by alanine to avoid difficulties in protein purification. In this study, we denote this mutant (Cys110 → Ala) of human myoglobin as "wild type".

[3] To avoid complexity, we showed the time courses of the geminate reaction only for wild type and the L29S mutant myoglobins, since those of the L29S, L29G and L29A mutants were quite similar.

[4] Our preliminary measurements of the geminate reactions for the Leu29 mutants at 100 MPa showed larger geminate yields (ϕ_g) than at 0.1 MPa, whereas the geminate rate constants (k_g) were almost independent of pressure. Since the three-state model (Henry, 1983) defines the bond formation rate (k_{21}) by the equation; $k_{21} = \phi_g k_g$, k_{21} for the Leu29 mutants would be increased under high pressure, corresponding to the negative activation volume for the bond formation process ($\Delta V^{\ddagger}_{21}$) in the Leu29 mutants. Although we have tried to measure the rate constants for the elementary steps in the mutants and examined their pressure dependence, the quantitative analysis has not yet been successful due to the small geminate yields at the ambient and high pressures.

REFERENCES

Adachi, S., & Morishima, I. (1989) *J. Biol. Chem. 264*, 18896-18901.

Adachi, S., Sunohara, N., Ishimori, K., & Morishima, I. (1992) *J. Biol. Chem. 267*, 12614-12621.

Alden, R. G., Satterlee, J. D., Mintorovitch, J., Constantinidis, I., Ondrias, M. R., & Swanson, B. I. (1989) *J. Biol. Chem. 264*, 1933-1940.

Antonini, E., and Brunori, M. (1971) *Hemoglobin and Myoglobin in Their Reactons with Ligands*, pp. 193-199, North Holland, Amsterdam.

Balny, C., & Travers, F. (1989) *Biophys. Chem. 33*, 237-244.

Di Primo, C., Hui Bon Hoa, G., Douzou, P., & Sligar, S. G. (1990) *Eur. J. Biochem. 193*, 383-386.

Di Primo, C., Hui Bon Hoa, G., Douzou, P., & Sligar, S. G. (1992) *Eur. J. Biochem. 209*, 583-588.

Fauchère, J. L., & Pliska, V. (1983) *Eur. J. Med. Chem. 18*, 369-375.

Frauenfelder, H., Alberding, N. A., Ansari, A., Braunstein, D., Cowen, B. R., Hong, M. K., Iben, I. E. T., Johnson, J. B., Lack, S., Marden, M. C., Mourant, J. R., Olmos, P., Reinisch, L., Scholl, R., Schulte, A., Shyamsunder, E., Sorensen, L. B., Steinback, P. J., Young, R. D., Xie, A., & Yue, K. T. (1990) *J. Phys. Chem. 94*, 1024-1037.

Gibson, Q. H., & Carey, F. G. (1977) *J. Biol. Chem. 252*, 4098-4101.

Gross, M., & Jaenicke, R. (1994) *Eur. J. Biochem. 221*, 617-630.

Hara, K., & Morishima, I. (1988) *Rev. Sci. Instrum. 59*, 2397-2398.

Hasinoff, B. B. (1974) *Biochemistry 13*, 3111-3117.

Henry, E. R., Sommer, J. H., Hofrichter, J., & Eaton, W. A. (1983) *J. Mol. Biol. 166*, 443-451.

Heremans, K. (1982) *Annu. Rev. Biophys. Bioeng. 11*, 1-21.

Hubbard, S. R., Hendrickson, W. A., Lambright, D. G., & Boxer, S. G. (1990) *J. Mol. Biol. 213*, 215-218.

Hui Bon Hoa, G., & Marden, M. C. (1982) *Eur. J. Biochem. 124*, 311-315.

Hui Bon Hoa, G., Di Primo, C., Dondaine, I., Sligar, S. G., Gunsalus, I. C., & Douzou, P. (1989) *Biochemistry 28*, 651-656.

Jongeward, K. A., Magde, D., Taube, D. J., Marsters, J. C., Traylor, T. G., & Sharma, V. S. (1988) *J. Am. Chem. Soc. 110*, 380-387.

Jung, C., Hui Bon Hoa, G., & Frauenfelder, H. (1992) *Cytochrome P-450* (Archakov, A. I., & Bachmanova, G. I., eds) pp. 33-38, INCO-TNC, Joint Stock Company, Moscow.

Jung, C., Hui Bon Hoa, G., Davydov, D., Gill, E., & Heremans, K. (1995) *Eur. J. Biochem. 233*, 600-606.

Jung, C., Schulze, H., & Deprez, E. (1996) *Biochemistry 35*, 15088-15094.

Kunkel, T. A. (1985) *Proc. Natl. Acad. Sci. U.S.A. 82*, 488-492.

Laird, B. B., & Skinner, J. L. (1989) *J. Chem. Phys. 90*, 3274-3281.

Lange, R., Heiber-Langer, I., Bonfils, C., Fabre, I., Negishi, M., & Balny, C. (1994) *Biophys. J. 66*, 89-98.

Mozhaev, V. V., Heremans, K., Frank, J., Masson, P., & Balny, C. (1996) *Proteins 24*, 81-91.

Newmann Jr, R. C., Kauzmann, W., & Zipp, A. (1973) *J. Phys. Chem. 77*, 2687-2691.

Ogunmola, G., Zipp, A., Chen, F., & Kauzmann, W. (1977) *Proc. Natl. Acad. Sci. U.S.A. 74*, 1-4.

Poulos, T. L., Finzel, B. C., Gunsalus, I. C., Wagner, G. C., & Krayt, J. (1985) *J. Biol. Chem. 260*, 16122-16130.

Poulos, T. L., Finzel, B. C., & Howard, A. J. (1986) *Biochemistry 25*, 5314-5322.

Projahn, H.-D., Dreher, C., & van Eldik, R. (1990) *J. Am. Chem. Soc. 112*, 17-22.

Projahn, H.-D., & van Eldik, R. (1991) *Inorg. Chem. 30*, 3288-3293.

Quillin, M. L., Arduini, R. M., Olson, J. S., & Phillips Jr., G. N. (1993) *J. Mol. Biol. 234*, 140-155.

Schulze, H., Ristau, O., & Jung, C. (1994) *Eur. J. Biochem. 224*, 1047-1055.

Slichter, C. P., & Drickamer, H. G. (1980) *Phys. Rev. B. 22*, 4097-4108.

Taube, D. J., Projahn, H.-D., van Eldik, R., Magde, D., & Traylor, T. G. (1990) *J. Am. Chem. Soc. 112*, 6880-6886.

Traylor, T. G., Luo, J., Simon, J. A., & Ford, P. C. (1992) *J. Am. Chem. Soc. 114*, 4340-4345.

Uchida, T., Ishimori, K., & Morishima, I. (1997) *J. Biol. Chem.* in press.

Unno, M., Ishimori, K., & Morishima, I. (1990) *Biochemistry 29*, 10199-10205.

Unno, M., Ishimori, K., Morishima, I., Nakayama, T., & Hamanoue, K. (1991) *Biochemistry 30*, 10679-10685.

Unno, M., Ishimori, K., Ishimura, Y., & Morishima, I. (1994) *Biochemistry 33*, 9762-9768.

van Eldik, R. (1986) *Inorganic High Pressure Chemistry: Kinetics and Mechanisms*, Elsevier, Amsterdam.

van Eldik, R., Asano, T., & le Noble, W. J. (1989) *Chem. Rev. 89*, 549-668.

Varadarajan, R., Szabo, A., & Boxer, S. G. (1985) *Proc. Natl. Acad. Sci. U.S.A. 82*, 5681-5684.

Varadarajan, R., Lambright, D. G., & Boxer, S. G. (1989) *Biochemistry 28*, 3771-3781.

PART III.

THE EFFECTS OF HEME ENVIRONMENTAL PROPERTIES ON LIGAND BINDING KINETICS IN THE HEME PROTEIN

CHAPTER 1.

The Effects of Hydrophobicity of Heme Pocket on the Ligand Binding Dynamics in Myoglobin as Studied with Leucine29 Mutants

ABSTRACT

To examine the effects of heme pocket hydrophobicity on the ligand binding in myoglobin, some artificial mutants of human myoglobin have been prepared, in which less hydrophobic amino acid residue (Ala, Gly, Ser) is located at Leu29(B10) position. CO rebinding rates for the mutants were markedly decelerated, while the ^{1}H-, and ^{15}N NMR spectra of the mutants show that the structural changes around the heme iron for these mutants are rather small. The kinetic and structural properties of the mutants indicate that the ligand binding rate depends on the hydrophobicity inside the heme cavity for these mutants in addition to the volume of the side chain at the 29 position. On the basis of the IR stretching frequency of liganded CO, invasion of water molecules into the heme pocket in the mutants is suggested, which would be induced by the decrease in the hydrophobicity due to the amino acid substitution. A slight red-shift of the position of the Soret peak for serine mutant L29S also supports the reduced hydrophobicity inside the heme cavity. We can conclude that, together with the kinetic properties of the mutants, the hydrophobicity of the heme pocket is one of the key factors in regulating the ligand binding to the heme iron.

INTRODUCTION

Various elegant techniques to elucidate the molecular mechanism of ligand binding process in hemoproteins have provided us with abundant information about the structural and functional factors that regulate the ligand binding dynamics (Gibson et al., 1986; Rohlfs et al., 1990; Carver et al., 1990). Site-directed mutagenesis, which is one of the potent techniques recently developed, has been applied to investigate functional roles of key residues in the active site of myoglobin (Carver et al., 1990; Egeberg et al., 1990; Adachi et al., 1992; Lambright et al., 1994; Springer et al., 1994), since it is a small molecular-weight protein and has been used as a model for hemoproteins.

In myoglobin, some amino acid residues essential for the ligand binding have already been suggested (Case & Karplus, 1979; Elber & Karplus, 1990; Carver et al., 1990, 1991; Egeberg et al., 1990; Lambright et al., 1993, 1994; Huang & Boxer, 1994; Springer et al., 1994; Lai et al., 1995). Among these amino acid residues, Leu29 at B10[1] (Leu29) has been one of the crucial amino acid residues, that control the ligand binding process and geometry of ligand (Adachi et al., 1992; Carver et al., 1992; Gibson et al., 1992, 1993). The x-ray structure of myoglobin has shown that leucine 29 forms a hydrophobic cluster with other distal hydrophobic residues to restrict the movement of the distal side chains (Figure 1) (Phillips, 1980). A simulation study (Elber & Karplus, 1990) has revealed that most of CO molecules undergo many collisions with the residues forming walls of the heme pocket including the hydrophobic cluster. The number of collisions of Leu29 was second to that of Val68 in myoglobin (Elber & Karplus, 1990), which has been also supported by picosecond and nanosecond geminate recombination studies (Gibson et al., 1992). On the basis of a detailed analysis of kinetics, Gibson and co-workers (Gibson et al., 1992, 1993) concluded that the initial movements of ligand after dissociation are toward the back of the distal pocket with the side chain of Leu29 acting as a part of the physical barrier that restricts the ligand movement away from and back toward the heme iron atom.

In our previous study (Adachi et al., 1992), we prepared two mutants that replaced Leu29 with alanine (L29A[2]) or isoleucine (L29I). These substitutions caused a 3–5-fold decrease in the rate constants for CO and O_2 association. Based on the remarkable decrease in the association constants, we have concluded that the leucine residue is an important constituent of the hydrophobic cluster for maintaining myoglobin's ligand binding properties. Since, the mutation of the amino acids forming other

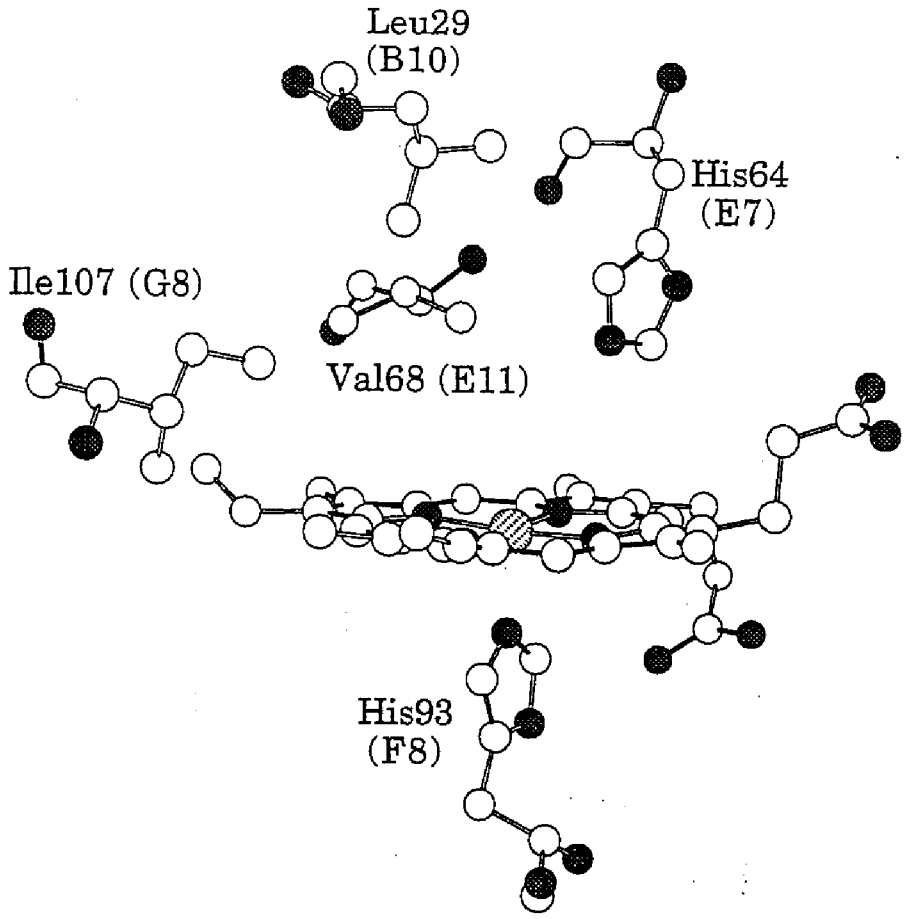

Figure 1. Heme environmental structure of human myoglobin. The heme and some selected myoglobin residues constituting the heme pocket are shown.

hydrophobic clusters in the distal pocket affects a slight alteration of the ligand binding process (Adachi et al., 1992), the hydrophobicity of the leucine residue seems to be essential for the large alteration of the ligand binding rates. To gain further insights into the functional and structural roles of the hydrophobicity at position 29 in the ligand binding dynamics, we prepared some more Leu29 mutants in which the hydrophobicity of the amino acid substituted for leucine is decreased.

One of the mutants we have prepared here has a glycine residue at position 29 (L29G). The hydrophobic index of glycine is 0, which is lower than that of leucine (+2.31) (Fauchère et al., 1983). The other amino acid we substituted for the leucine is serine (L29S). Serine is less hydrophobic due to its hydroxy group (hydrophobic index is –0.05), while its steric hindrance is similar to that of alanine. We also tried to introduce some other hydrophilic amino acid residue such as threonine and asparagine.

Unfortunately, however, the mutants having a hydrophilic amino acid residue at the 29 position are highly unstable and fail to keep the heme inside the heme pocket in the cyanomet form. To discriminate effects of the hydrophobicity on the ligand binding from those of the steric difference in the side chain of the substituted amino acid residue, we prepared an additional mutant in which a phenylalanine residue is introduced into position 29 (L29F). The hydrophobicity of phenylalanine (its hydrophobic index is +2.43) is similar to that of leucine, whereas the steric hindrance is quite different (Carver et al., 1992).

In this study, we utilized laser photolysis technique to characterize the ligand binding properties of the mutants. Also, we examined the structural changes around the active site by using ^{1}H, ^{15}N NMR, IR and electronic absorption spectroscopies to elucidate the relationship between ligand binding properties and the hydrophobicity of heme pocket.

EXPERIMENTAL PROCEDURE

Reagents. ^{15}N enriched $KC^{15}N$ was purchased from CIL, Ltd. (U.S.A.) and sodium dithionite were purchased from Wako Pure Chemical Industries, Ltd. (Japan) without further purification.

Preparation of Mutant Myoglobins. The original expression vector of human myoglobin[3], pMb3 (pLcIIFXMb), is a gift from Varadarajan and Boxer (1985). The procedures for site-directed mutagenesis are described in previous papers (Kunkel, 1985; Varadarajan et al., 1989; Adachi et al., 1992). DNA sequencing for all mutants was performed by the DyeDeoxy Terminator method using ABI 373S DNA sequencer and were analyzed by 373S DNA sequencing system. Protein preparation and purification were followed by the method described previously (Varadarajan et al., 1989; Adachi et al., 1992). Wild type myoglobin and the L29F mutant were purified as an aquomet form. Since L29G, L29A, and L29S mutants are unstable in the aquomet form, we purified them in the cyanomet form.

Electronic Absorption and IR Spectra. Electronic absorption spectra of purified proteins in 100 mM sodium phosphate buffer, pH 7.0, were recorded on a SHIMADZU UV 2200 UV/visible spectrophotometer. The sample concentration was 5 μM.

Infrared spectra were measured at 1 cm^{-1} resolution on a Bio-Rad FTS-30 spectrophotometer. The protein solution was loaded into a CaF_2 cell with 0.1 mm path length. The spectral ranges were 1900–2000 cm^{-1} for carbonmonoxy forms and 2000–2200 cm^{-1} for cyanomet forms. We used

the equimolar aquomet form of wild type myoglobin as a reference. In the measurements of the cyanomet forms, we used a D_2O buffer solution, since the signal to noise ratio was significantly higher in D_2O than in H_2O and no isotope effects have been observed (Yoshikawa et al., 1985). An average of 512 scans was used for each spectrum. The sample concentration was about 1 mM for the carbonmonoxy forms, pH 7.0 and 3 mM for cyanomet forms in 100 mM sodium phosphate, pD 7.0.

Kinetic Measurements of CO and O_2 Binding. The association rate constants of CO and O_2 were obtained by a laser photolysis apparatus, which has been previously described in detail (Adachi & Morishima, 1989; Adachi et al., 1992). For milli- to microsecond experiments, a flashlamp-pumped dye laser with a half-peak duration of 300 ns (UNISOKU LA-501) was used. Rhodamine 6G (Eastman Kodak Co.) in methanol was used to produce an excitation pulse at 590 nm, the wavelength of maximum intensity. The probe light at 440 nm was focused onto the slit of a monochromator (UNISOKU USP-501) and detected by a photomultiplier. A transient memory (GRAPHTEC TMR-80) was used to digitize the signal (50 ns/point, 4096 points), and data were transferred to a NEC PC-9801VX computer for further data analysis. The sample concentration was about 5 μM. The buffer conditions were 100 mM sodium phosphate, pH 7.0, at 20 °C.

Ligand rebinding to the mutant and wild type myoglobins were analyzed by fitting to the following equation[4],

$$\Delta A_t = \Delta A_0 \exp(-k_{app}\, t) \tag{1}$$

where ΔA_t is the absorbance change at any time t, ΔA_0 is the total absorbance change (absorbance at $t = 0$ minus absorbance at $t = \infty$). k_{app} is the observed first-order rate constant and satisfies the following equation (Antonini & Brunori, 1971),

$$k_{app} = k_{on}[L] \tag{2}$$

where k_{on} is the bimolecular ligand binding rate constant and [L] is ligand concentration.

The kinetics measurements of the CO dissociation rates were carried out with a UV/visible spectrometer (SHIMADZU UV-2200). k_{off} was determined by analyzing the replacement reaction in which ligated CO was replaced by NO as described in detail by Lambright et al. (1989). The

concentrated myoglobin stocks were converted to the carbonmonoxy form by stirring under CO followed by reduction with sodium dithionite. NO saturated buffer (100 mM sodium phosphate, pH 7.0) was prepared by bubbling NO through 3 ml of buffer in a sealed 1 cm path-length UV cell. About 20 μl of the concentrated MbCO solution was then injected into the cell at 20 °C, and the reaction was followed by monitoring the absorbance at 424 nm. Association equilibrium constants were calculated as the ratio of the rate constants.

NMR Spectroscopy. ^{1}H NMR spectra were recorded by using a GE OMEGA 500 spectrometer equipped with a SUN 3 workstation. Hyperfine-shifted NMR spectra were obtained with an 8-kilobyte data transform of 125 kHz and 7.0 μs 90° pulse by using a conventional WEFT[4] pulse sequence (180–τ–90 degrees) in order to minimize the strong solvent resonances in H_2O solution. An appropriate setting of the τ value (typically 120–130 ms) can eliminate H_2O signal under rapid repetition of the sequence. The probe temperature was 23 ± 0.5 °C. The concentration was about 1 mM in 100 mM sodium phosphate, pH 7.0, and the sample volume was about 500 μl. Proton shifts were referenced with respect to the signal from the proton resonance of tetramethylsilane (TMS). ^{15}N NMR spectra of the $C^{15}N$ derivatives were taken at 50.67 MHz. Chemical shifts are given in ppm with reference to the resonance of external $^{15}NH_3$. Sample conditions for the ^{15}N NMR spectra were the same as those for ^{1}H NMR spectra (Adachi et al., 1992).

Near-infrared Absorption Spectra of Deoxy Myoglobins. Deoxy myoglobin was prepared by reduction of met myoglobin with a small amount of solid sodium dithionite under an argon atmosphere. The met myoglobin solution was calmly stirred under the argon atmosphere on ice more than 30 min before reducing. The sample concentration was 1 mM and we used 100 mM sodium phosphate buffer, pH 7.0, at 20 °C. Near-infrared absorption spectra were recorded on a SHIMADZU UV 2200 UV/visible spectrophotometer over the range of 700 to 800 nm.

RESULTS

Electronic Absorption Spectra in Carbonmonoxy Form. The peak positions of the Soret bands for the wild type and mutant myoglobins are listed in Table I. The carbonmonoxy form of wild type myoglobin has the Soret band at 423.0 nm. In the absorption spectra of the mutants, subtle but significant deviations of the absorption maxima were observed. The

L29A and L29S mutants exhibited the Soret peak at 423.2 and 423.8 nm, whereas the peaks for L29G and L29F mutants were blue-shifted to 422.8 and 422.4 nm, respectively.

TABLE I: Peak position of Soret band, IR stretching band, population of conformers and ^1H chemical shifts for CO bound wild type and mutant myoglobins.

Myoglobin	λ_{max}	A_0	A_1	A_3	Val68 $C_\gamma H_3$
	nm		cm^{-1} (%)		ppm
Wild Type	423.0	1967 (3)	1945 (97)	ND[a]	- 2.4
L29G	422.8	1965 (11)	1948 (50)	1932 (39)	- 2.5
L29A	423.2	1965 (18)	1948 (38)	1934 (44)	- 2.4
L29F	422.4	ND	ND	1933 (100)	- 2.5
L29S	423.8	ND	1950 (75)	1936 (25)	- 2.6

[a] ND, not detected.

Laser Photolysis of Bimolecular Binding for Carbonmonoxy- and Oxy- Myoglobins. Table II shows the bimolecular association rate constants for CO and O_2 rebinding to wild type and mutant myoglobins. The second-order rate constants (k_{on}) were determined by milli- and microsecond laser photolysis measurements. Figure 2 shows the time courses for CO rebinding to wild type and mutant myoglobins. The time courses were fitted to a simple exponential curve and the bimolecular association rates were calculated. Compared to wild type, the CO association rates of the mutants were largely decreased; k_{on}^{CO} for the L29G mutant was 0.11 $\mu M^{-1}s^{-1}$ and k_{on}^{CO} for the L29G mutant was 0.072 $\mu M^{-1}s^{-1}$ at pH 7.0, 20 °C. The rate constant for the L29S mutant is extremely small (0.069 $\mu M^{-1}s^{-1}$)[5].

In our previous paper (Adachi et al., 1992), we speculated that increasing the space in the immediate vicinity of the heme in the L29A mutant allows more water molecules to enter the heme pocket, resulting in decrease of the CO binding rate. In the present results, L29G, in which the space in the vicinity of heme pocket would be larger than that in L29A, also exhibited a smaller CO rebinding rate (0.11 $\mu M^{-1}s^{-1}$) than L29A (0.15 $\mu M^{-1}s^{-1}$) (Table II). Furthermore, it is rather surprising that an

extremely slow ligand binding (0.069 $\mu M^{-1}s^{-1}$) was observed for the serine mutant (L29S), since the replacement of alanine by serine would

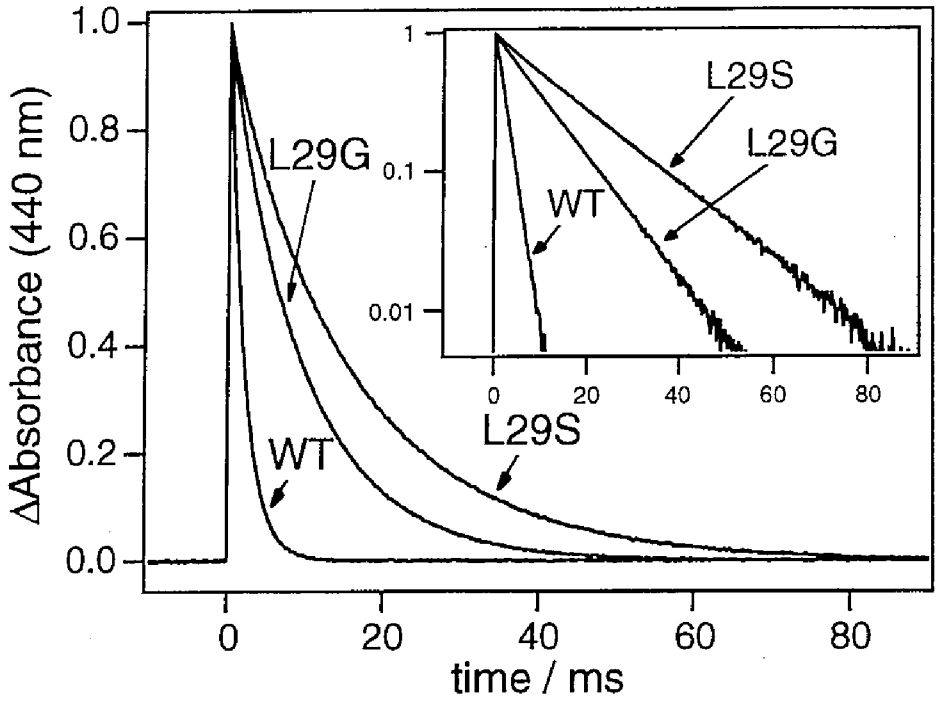

Figure 2. Bimolecular association kinetics of CO to wild type and L29G, L29S mutant myoglobins at CO concentration of 1.0 mM and 20 °C. The change in absorbance has been normalized to unity at the end of the geminate processes. Inset: semilogarithmic plots of the same data.

not increase the space of heme pocket. The comparison of the ligand binding rates for the L29S and L29G mutants clearly indicates that the decrease in CO binding rate in the Leu29 mutants (Adachi et al., 1992) is not simply due to the increasing space in the vicinity of the heme (see Figure 5A). It is quite interesting that the CO association rate constants depend on the hydrophobicity for the amino acid at the 29 position as plotted in Figure 5B[6]. Figure 5B also includes the rebinding data of the sperm whale mutant myoglobins previously reported (Carver et al., 1992; Springer et al., 1994). The mutant having the most hydrophilic residue at the 29 position, L29S, shows the slowest CO association rate constant, followed by the L29G and L29A mutants. Wild type myoglobin, in which the most hydrophobic residue, leucine, is occupied at the 29 position, exhibits a much faster rebinding rate. These observations strongly suggest that the hydrophobicity at the position of 29 is one of the crucial

TABLE II: Rate and Equilibrium Constants for CO and O_2 Binding in Wild Type and Mutant Myoglobins, and Hydrophobic Index of the Residue at the Position of Leu29. All of the Data Were Determined in 0.1 M phosphate buffer, pH 7.0, at 20 °C. Equilibrium Constants, K_{CO}, Were Calculated as k_{on}^{CO}/k_{off}^{CO}.

	k_{on}^{CO}	k_{off}^{CO}	K_{CO}	$k_{on}^{O_2}$	hydrophobicity[c]
	$\mu M^{-1}s^{-1}$	s^{-1}	μM^{-1}	$\mu M^{-1}s^{-1}$	kcal mol^{-1}
Wild type	1.1 ± 0.0	0.018 ± 0.001	61 ± 5	16.0 ± 0.5	+2.31
L29G	0.12 ± 0.01	0.022 ± 0.001[a]	5.0 ± 0.7	2.1 ± 0.1	0.0
L29A	0.15[b] ± 0.01	0.019 ± 0.001[a]	7.9 ± 1.0	4.3[b] ± 0.1	+0.42
L29F	0.072 ± 0.004	0.0015 ± 0.0002	51 ± 9	5.1 ± 0.3	+2.43
L29S	0.069 ± 0.006	0.019 ± 0.006[a]	3.6 ± 1.4	2.2 ± 0.1	–0.05

[a] For these mutants, the dissociation kinetics were observed to be best fit with two exponentials. The table entry is the best single-exponential fit to facilitate comparison. [b] Adachi et al. (1992). [c] Fauchère & Pliska (1983).

factors for the ligand binding process. However, the ligand binding rates of the L29F, L29W(sperm whale) and L29I mutants are not along this line. In these mutants, the effects of the steric hindrance of the side chains would be a dominant factor for regulating CO rebinding and overwhelm the hydrophobic effect (Springer et al., 1991, 1994)[7].

The O_2 association rate constants for the mutants were also largely decreased. $k_{on}^{O_2}$ for the L29F mutant was 5.1 $\mu M^{-1}s^{-1}$. The rate constants for the L29G and L29S mutants are smallest (2.1 $\mu M^{-1}s^{-1}$ and 2.2 $\mu M^{-1}s^{-1}$). Although the oxygen binding in human myoglobin is sensitive to volume and/or hydrophobicity at the position of B10, the oxygen binding is little affected by decreasing the size of the B10 residue in sperm whale myoglobin (Carver et al., 1992), suggestive of the different regulation mechanism between the CO and O_2 rebinding[8].

Dissociation Rates of Carbon Monoxide. The dissociation rates, k_{off}, of the carbon monoxide from wild type and mutant myoglobins were obtained by the NO replacement method (Antonini & Brunori, 1971; Lambright et al., 1989; Rohlfs et al., 1990) and are compiled in Table II. k_{off} of human wild type myoglobin (0.018 s^{-1}) was virtually identical to that reported previously (Dou et al., 1995). As listed in Table II, the dissociation rates for the mutants bearing a less hydrophobic amino acid residue at B10, L29A, L29G, and L29S mutants, are almost identical to that of wild type myoglobin. However, the dissociation rate of the L29F mutant was markedly decreased to 0.0014 s^{-1}, which is a more than 10-fold decrease as compared to that of wild type myoglobin. We also calculated the carbon monoxide affinity ($K_{CO} = k_{on}/k_{off}$) of the wild type and mutant myoglobins (Table II). The affinity to carbon monoxide is markedly reduced in the L29A, L29G, and L29S mutants, whereas that for the L29F mutant is almost equal to that for wild type myoglobin.

Infrared and ^1H NMR Spectra of Carbonmonoxy Myoglobins. The IR absorption spectra in the iron-ligated C-O stretching region, 1900–2000 cm^{-1}, of wild type and mutant myoglobins are illustrated in Figure 3. Table I summarizes parameters of the C-O stretching mode infrared band. The spectral patterns of the L29A and L29F mutants correspond to those of Leu29 mutants of sperm whale myoglobin (Li et al., 1994). The two or three distinguishable bands were observed at around 1932, 1945, and 1965 cm^{-1} for all mutants except for the L29F mutant. The intensity of the peak around 1945 cm^{-1} in the Leu29 mutants decreased and the peak around 1932 cm^{-1} gained its intensity. A single broad IR band at 1933 cm^{-1} for the

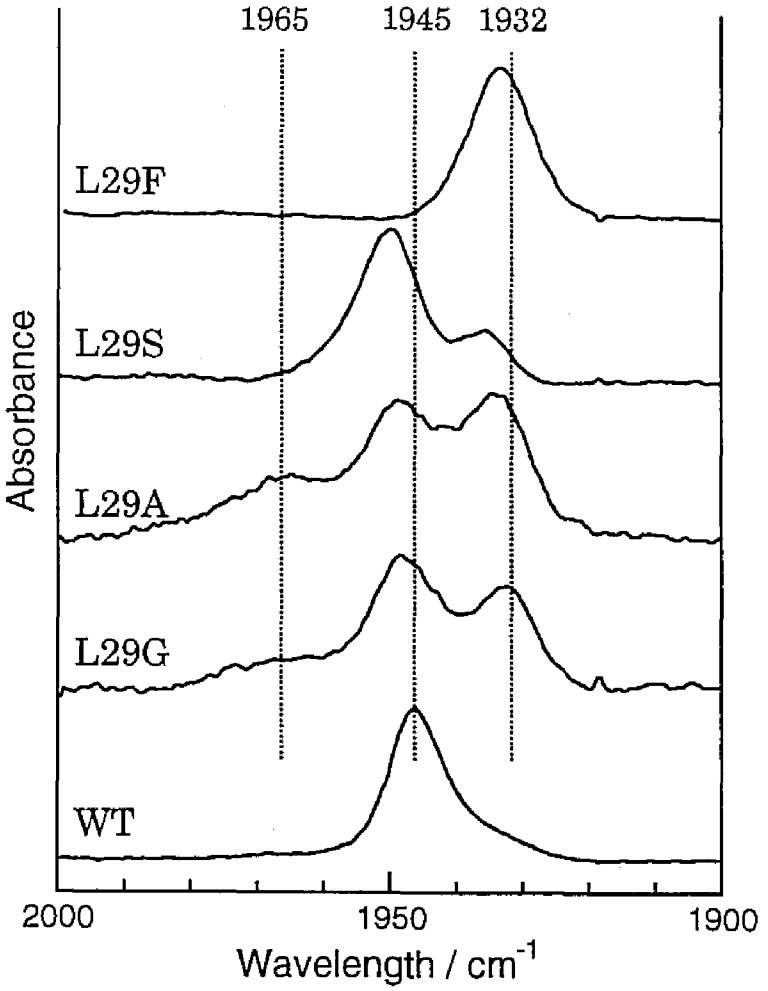

Figure 3. IR spectra of CO stretching region of wild type and mutant myoglobins in carbonmonoxy form. Samples contain about 1 mM protein in 0.1 M sodium phosphate buffer, pD 7.0.

L29F mutant implies the complete conversion from the conformer A_1 of wild type (Moore et al., 1988; Ormos et al., 1988) to the other conformer by the substitution for leucine by phenylalanine. The IR band for the L29S mutant is composed of two distinct bands centered at 1950 and 1936 cm^{-1}. Although they correspond to A_1 and A_3 conformers of wild type, the positions of these peaks show a shift to high frequency by 4–5 cm^{-1}.

By using ^1H NMR spectra, we also investigated the structural changes around the heme. A ring-current shifted signal observed at –2.5 ppm has been assigned to $C_\gamma H_3$ in Val68, which has served as a sensitive marker for the structural changes near the basic heme (Shulman et al., 1970; Lindstorm, 1972; Dalvit & Wright, 1987; Moore et al., 1988; Li et al., 1994; Wakasugi et al., 1994). As shown in Table I, the mutation at the position of Leu29 has little effect on this marker, indicating that the heme

environmental structures in CO bound forms are essentially the same as those found in wild type myoglobin.

Infrared, ^1H NMR, and ^{15}N NMR Spectra of Cyanomet Myoglobins. The prominent resonances in ^1H NMR spectra of cyanide adducts of wild type and mutant myoglobins are summarized in Table III. As listed in Table III, the resonance positions of 1-, 5-, 8-heme methyl protons were almost insensitive to the amino acid substitution. This indicates that the orientation of the axial histidine is little affected by this mutation (Yamamoto et al., 1990; Yamamoto & Suzuki, 1993). In the L29F mutant, however, the signal of the distal histidine $N_\varepsilon H$ (**b**) appeared at 28.9 ppm, which was about 5.8 ppm downfield shifted from that for wild type myoglobin, implying a perturbation in the orientation of the distal histidine by the amino acid substitution.

The signals of the proximal histidine $C_\varepsilon H$ (**d**) in L29A and L29G were downfield shifted by 2.7 and 2.9 ppm, respectively, and such shifts were also encountered in the signal position of the proximal histidine $C_\delta H$ (**g**). Since the hyperfine shifts of these two protons depend on the tilting angle of the magnetic z axis (Emerson & La Mar, 1990), the tilting angle of bound cyanide from the heme normal would be increased in these mutants. The resonance from $C_\gamma H$ (**h**) in Ile99 (FG5) is also one of the useful proximal side structural markers (38). As shown in Table III, the resonance positions of $C_\gamma H$ (**h**) in Ile99 (FG5) are almost independent of the mutation at the B10.

Table III: ^1H NMR chemical shifts for selected resonances of wild type and mutant myoglobins in the cyanomet form at pH 7.0 and 23 °C (ppm from TMS).

Resonance	Myoglobin					
	peak	Wild type	L29G	L29A	L29F	L29S
Heme 1-CH_3	**e**	18.8	18.1	18.5	18.4	18.7
Heme 5-CH_3	**a**	27.7	27.9	28.1	27.0	28.5
Heme 8-CH_3	**f**	13.4	13.5	13.9	14.3	13.8
His (E7) $N_\varepsilon H$	**b**	23.1	25.2	24.2	28.9	25.9
His (F8) $N_\delta H$	**c**	21.7	21.4	21.5	22.0	21.3
His (F8) $C_\varepsilon H$	***d***	20.8	23.7	23.5	22.5	25.0
His (F8) $C_\delta H$	**g**	- 5.9	- 11.3	-11.2	- 8.3	-12.8
Ile (FG5) $C_\gamma H$	**h**	- 10.2	- 10.1	-10.4	- 10.8	-10.5

The ^{15}N NMR spectra of cyanomet myoglobins were measured in the presence of excess cyanide ion ($C^{15}N^-$), which are illustrated in Figure 4, and the resonance positions are summarized in Table IV. The resonance from the liganded $C^{15}N^-$ in wild type human myoglobin appeared at 1342 ppm from $^{15}NH_3$, which corresponds to that of wild type sperm whale and horse myoglobin (Morishima et al., 1977; Morishima & Inubushi, 1977). The L29F mutants exhibited the resonance at 1306 ppm, which is relatively close to that of human wild type myoglobin. However, the substitution of leucine for the smaller and less hydrophobic amino acid residues, glycine or alanine, induced large upfield shifts, 1227 and 1236 ppm, respectively. The L29S mutant showed the largest upfield shifts, 1202 ppm as compiled in Table IV.

The C-N stretching band of wild type myoglobin appeared at 2125 cm^{-1} (McCoy & Caughey, 1970; Yoshikawa et al., 1985), whereas leucine-29 mutants, L29G, L29A, and L29S, exhibited the corresponding band at 2126–2128 cm^{-1}, which is shifted by 2–3 cm^{-1} to slightly higher frequencies, as listed in Table IV. Since the ν_{C-N} stretching is one of the indicators for the configuration of the liganded cyanide in hemoproteins (McCoy & Caughey, 1970; Yoshikawa et al., 1985), the slight shifts of the C-N stretching mode in these mutants imply that the bending in the C-N bond for the mutants is not so seriously affected by the amino acid substitution. On the other hand, in the IR spectra of the cyanomet phenylalanine mutant, L29F, the C-N stretching mode shifts 10 cm^{-1} to higher frequencies.

Table IV: Infrared parameters for the C-N stretch band and ^{15}N chemical shift of wild type and mutant myoglobins in cyanomet form at pH 7.0.

Myoglobin	ν_{C-N}	^{15}N Chemical Shift
	cm^{-1}	ppm
Wild type	2125	1342
L29G	2128	1227
L29A	2128	1236
L29F	2135	1306
L29S	2126	1202

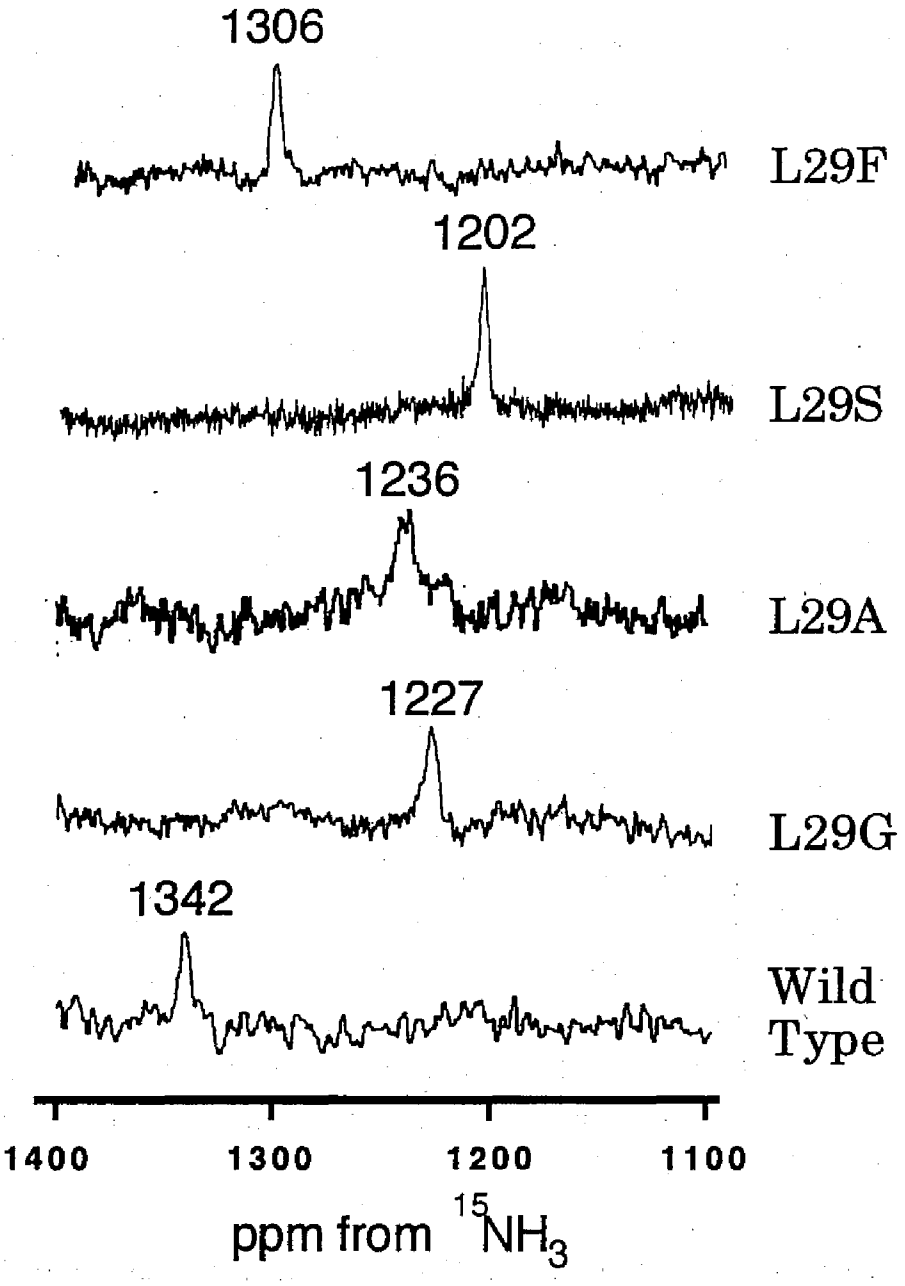

Figure 4. ^{15}N NMR spectra of wild type and mutant myoglobins in cyanomet form. Samples contain about 3 mM protein in 0.1 M sodium phosphate buffer, pD 7.0 at 23 °C.

^1H NMR and Near-infrared Absorption Spectra of Deoxy Myoglobins. A resonance of exchangeable proton in the far downfield region observed at 80.6 ppm in wild type deoxy myoglobin has been assigned to the $N_\delta H$ proton of the proximal histidine (Goff & La Mar, 1977; La Mar et al., 1977). These signals of all the mutant myoglobins showed a downfield shift. The signals for the L29G and L29A mutants appeared at 82.2 ppm and that of the L29F mutant was at 84.2 ppm. The L29S mutant exhibited the largest downfield shift at 85.1 ppm (Table V).

The near-infrared absorption spectra (band III) for wild type and Leu29 mutant myoglobins in the deoxy form are examined to investigate the structural change around the heme proximal site. These spectra are well described by a single Gaussian function on top of a cubic polynomial background (Iizuka et al., 1977; Jackson et al., 1994). The center frequency, 763.9 nm, for wild type myoglobin is identical with the previous data (Iizuka et al., 1977). The range of the center frequencies for the Leu29 mutants was from 763.0 to 765.8 nm (Table V). The band III has been assigned to charge transfer transition of $a_{2u} \rightarrow d_{xy}$, porphyrin to iron (Eaton et al., 1978; Eaton & Hofrichter, 1981), and the center frequency of band III reflects the position of the iron relative to the plane of the porphyrin (Jackson et al., 1994). The red-shift for the L29G, L29A, and L29S mutants suggests that the heme iron in these mutants is less out of the heme plane than that of wild type, whereas, in the L29F mutant, the deviation of the heme iron from the heme plane is larger.

Table V: ^1H chemical shift and center frequency of Band III in wild type and mutant myoglobins in deoxy form at pH 7.0.

Myoglobin	^1H Chemical Shift of Proximal His $N_\delta H$	Center Frequency of Band III
	ppm	nm
Wild type	80.6	763.9
L29G	82.2	764.1
L29A	82.2	765.8
L29F	84.2	763.0
L29S	85.1	764.7

DISCUSSION

The Ligand Environment Structure of the Less Hydrophobic Leucine 29 (L29A, L29G and L29S) Mutants. Although the structural deviations in the less hydrophobic mutants, L29S, L29A and L29G, from wild type myoglobin would be subtle as shown by their spectroscopic data, the environmental changes around heme ligand are suggested by IR, electronic and NMR spectra. In the IR spectra of L29G, L29A, and L29S mutants (Figure 3), the stretching mode at 1933 cm^{-1} was enhanced, while the intensity of the band at 1945 cm^{-1} was decreased. These changes in the intensity of the stretching mode were also detected in various myoglobin mutants (Li et al., 1994) and the appearance of the stretching mode at the lower frequency region has been ascribed to the destabilization of the partial negative charge at the oxygen atom by positive electrostatic environment near the CO ligand (Li et al., 1994).

Electronic absorption spectra of the carbon monoxide complexes of the L29S mutant myoglobin can be another marker for the polarity of the heme vicinity (Slichter & Drickamar, 1980; Laird & Skinner, 1989). In the polar environment, the excited state is more effectively polarized than the ground state and stabilized, which lowers the heme π-π^* transition energy and shifts the Soret maximum to red. The peaks of the Soret band maximum for less hydrophobic mutants, L29S and L29A, were observed at 423.8 and 423.2 nm, respectively, while that of wild type myoglobin appears at 423.0 nm. These red shifts in the Soret peak of the mutant would correspond to the increase of the polarity in the heme pocket, implying that the replacement of Leu29 by a less hydrophobic residue reduces the hydrophobicity of the heme pocket. Although the L29G mutant has less hydrophobic residue at the 29 position, the Soret band is slightly blue shifted, suggesting that some other electronic factors affect the peak position of the Soret band in this mutant. We are now trying to identify the fine structural differences in these mutants by multidimensional NMR measurements.

The environmental changes around the ligand in the less hydrophobic mutants are also reflected in ^{15}N NMR spectra of the $C^{15}N$-bound form. The replacement of the less hydrophobic amino acid residue at position 29 induced a large upfield shift as illustrated in Figure 4 (1342, 1236, 1227, and 1202 ppm for wild type, L29A, L29G, and L29S, respectively). One of the major factors to determine the resonance position of ^{15}N in liganded cyanide is the steric hindrance around the ligand. Using the strapped heme model, Avilés and Chang (1992) have indicated that the increase in the steric hindrance around liganded cyanide causes tilting and/or

bending of the cyanide ligand, resulting in an upfield shift. In contrast to the large upfield bias of the resonance position of the liganded $C^{15}N$ in the mutants from that of wild type myoglobin, the deviations of the stretching mode of cyanide in the less hydrophobic mutants are within 3 cm^{-1}. Since the C-N stretching mode is affected by the perturbation of the bending of the liganded CN^-, but not so much by the tilting (Yoshikawa et al., 1985), the mutation at the 29 position to glycine, alanine, or serine might induce the tilting of the liganded cyanide rather than the bending. Tilting of the cyanide ligand is also supported by ^1H NMR. The resonance positions of the proximal histidine ring protons, $C_\varepsilon H$ (**d**) and $C_\delta H$ (**g**), have been considered to be sensitive to the local structure of the liganded cyanide (Emerson & La Mar, 1990). Table III indicates that the difference of these signal positions for the L29A (35 ppm), L29G (35 ppm), and L29S (38 ppm) mutants is significantly larger than that for wild type myoglobin (27 ppm), which indicates that tilting of the liganded cyanide increased (Emerson & La Mar, 1990).

The Effect of Heme Pocket Hydrophobicity on CO Bimolecular Binding Rate. Although the heme environmental structure was affected by the replacement of Leu29 by alanine, glycine, and serine, the structural changes are subtle and it is unlikely that the remarkably reduced CO binding rate in these less hydrophobic mutants can be ascribed solely to the conformational changes in the heme cavity induced by the mutation. One of the key features in these mutants is the dependence of their rebinding rate on the hydrophobicity index of the amino acid residue at position 29 as depicted in Figure 5B. The reduced hydrophobicity at position 29 decelerates the rebinding rate.

The decreased hydrophobicity of the heme cavity allows us to speculate that the contribution of water molecules inside the heme pocket to the ligand binding process is affected by the mutation. As previous studies have shown, the replacement of noncovalently bound water molecule, which is hydrogen bonded to N_ε of His64(E7) in deoxy myoglobin, would be the major factor of regulating the carbon monoxide binding to the heme iron (Rohlfs et al., 1990; Carver et al., 1990; Smerdon et al., 1991; Quillin et al., 1993). In the CO-bound form, the possibility of water in the heme pocket might effectively increase the local water concentration, which is possibly an additional factor that contributes to decreasing the ligand rebinding rate. It is, therefore, most plausible that the decreased hydrophobicity in the heme pocket introduces the extra water molecules

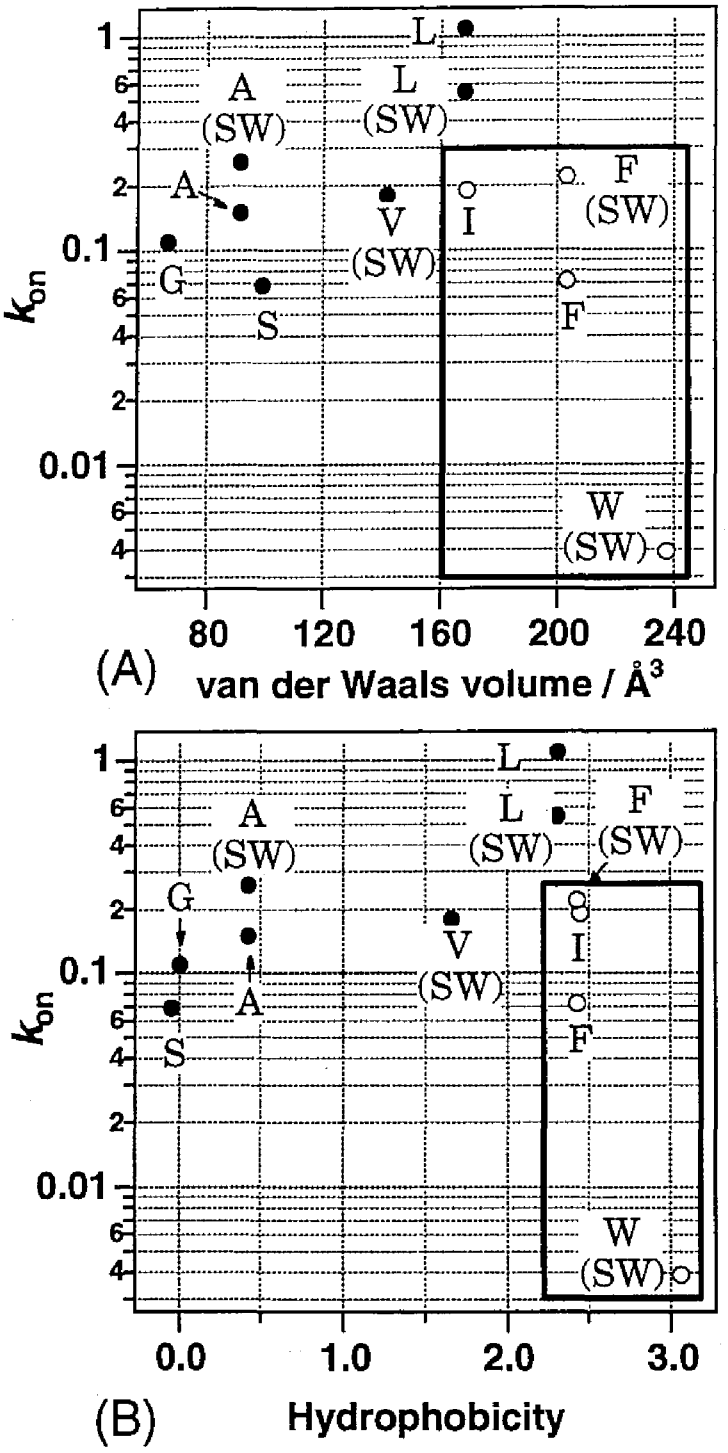

Figure 5. (A) Dependence of CO bimolecular rebinding rate constants on the volume at position 29. The values of amino acid volume were referred from Chothia (1975). This value was obtained from average of 15 protein structures. (B) Dependence of CO bimolecular rebinding rate constants on the hydrophobicity at the position of leucine-29. The mutants whose CO rebinding rate is dominated mainly by steric size are shown by a symbol (O) and demarcated by a square, and the others are (●). SW means sperm whale myoglobin.

into the heme cavity or increases the density of water molecules around the heme iron in the L29A, L29G, and L29S mutants.

Although it is quite difficult to estimate the position of the labile water molecules inside the heme pocket, even by crystallography, the present spectroscopic data suggest that the position and/or number of the water molecule inside the heme pocket is changed by the mutation at Leu29. As discussed above, the infrared spectra of carbon monoxide myoglobins (Figure 3) indicates the positive charge near the heme ligand in the L29G, L29A, and L29S mutants. Since the conformational changes around the heme iron are small, the presence of a positive charge can be derived from water molecules near the heme iron that are not observed for native myoglobin, as discussed by Li et al. (1994). The presence of water molecules near the heme iron also corresponds to the upfield shift of the ^{15}N resonance in the mutants (Figure 4). The interaction between the nitrogen atom of the ligated cyanide and water molecule, possibly a hydrogen bond between the ligated cyanide and water molecule, would cause upfield shift in the resonance position of ^{15}N (Morishima & Inubushi, 1978). The red-shift in the Soret peak might also imply the invasion of water molecules into the heme pocket by the replacement of leucine-29 with the less hydrophobic amino acid residue. On the basis of the microscopic theory of solvent–solute interactions (Laird & Skinner, 1989), Jung et al. (1995) suggested that the red-shift and broadening of the Soret band observed for cytochrome P450 by pressurization indicates a higher water content in the heme environment. In myoglobin, however, the red-shift of the Soret transition was not accompanied by a broadening, which is in sharp contrast to that in cytochrome P450 (Jung et al. 1995). Since the heme environmental structure of myoglobin is significantly different from that of cytochrome P450, the higher water content in the heme pocket would not be the only factor for the reduced hydrophobicity in the heme pocket of the mutants.

Thus, we can suggest that the hydrophobicity at position B10 is one of the factors to control the ligand binding process and the reduced hydrophobicity could favor the easy access of the water molecules into the heme pocket, which raises the barrier to CO binding and decreases the CO binding rate. The effects of hydrophobicity in the heme pocket on the ligand binding process were also manifested in the sperm whale mutant myoglobin (H64G) bearing a glycine residue at the position of the distal histidine (Rohlfs et al., 1990, Quillin et al., 1993). The x-ray structure of the

sperm whale myoglobin mutant clearly showed that approximately two water molecules are located adjacent to the coordinated ligand in the CO form in its highly polar heme pocket and the ligand binding rate for the mutant was markedly retarded (Quillin et al., 1993).

Ligand Binding and Heme Environmental Structure in the L29F Mutant. As clearly shown by the spectroscopy used here, the structural changes around the heme active site for the L29F mutant are more prominent than those for the other mutants. The IR stretching mode of carbonmonoxy L29F mutant consists of almost one component, while two or three components in the stretching modes were found for other mutants (Table I). The ^{1}H NMR signal of the distal histidine $N_{\varepsilon}H$ in the mutant was detected in the far downfield region (Table III), whereas the deviation of the ^{15}N resonance is much smaller than other mutants (Table IV). These spectral changes show that the effects of the substitution of phenylalanine for leucine at the 29 position is quite different from those of alanine, glycine and serine. In the crystallographic structures of the sperm whale mutant myoglobin, the large benzene ring of phenylalanine occupies at the CO binding site (Carver et al., 1992). Since the edge of the benzene ring has been proposed to be a partial positive charge and favors interactions with the negative charged face (Thomas et al., 1982), this electrostatic interaction would affect the C-O stretching mode of the carbonmonoxy form (Figure 3) and the C-N stretching mode of cyanide adduct (Table IV). However, the NMR signal from the methyl group of Val68 was insensitive to the L29F mutation, implying that the structural changes in the L29F mutant might be localized near the ligand. Although the detailed conformational changes are not yet clear, it can be safely said that these conformational changes around the ligand, which are not observed for the other mutants in this study, would lead to the extremely slow CO rebinding rate of the L29F mutant.

In summary, the mutants, in which Leu29 is substituted for a less hydrophobic amino acid residue, exhibited a substantial decrease in the carbon monoxide binding rates and their binding rates were dependent on the hydrophobicity of the amino acid residue at position 29. Although the volume of amino acid at that position is one of the factors that affect the ligand binding kinetics of myoglobin, we propose a contribution of the hydrophobicity at the 29 position to the control mechanism of the ligand binding process. In spite of the limited structural information, it can be concluded that the amino acid substitutions would introduce water

molecules inside or near the heme cavity and these noncovalently bound water molecules would perturb the barrier of CO binding to heme iron.

FOOTNOTES

[1] Alphanumeric codes (e.g. B10 etc.) refer to the position of the residue within the helices and loops of the myoglobin folding pattern. That is, B10 means the 10th residue in the B helix.

[2] The mutations are listed in the text using the single amino acid abbreviations. Leu29(B10)→Gly, Leu29(B10)→Ala, Leu29(B10)→Phe, and Leu292(B10)→Ser, substitution are designated as the L29G, L29A, L29F, and L29S mutations, respectively.

[3] Varadarajan et al. (1989) replaced Cys110(G11) of human myoglobin by alanine to prevent difficulties in protein purification. In this study, we denote this mutant (Cys110→Ala) of human myoglobin as "wild type".

[4] The abbreviations used are: WEFT, water-eliminated Fourier transform; TMS, tetramethylsilane; ppm, parts per million; SW, sperm whale.

[5] By freeze-thawing, a minor component appeared in the rebinding reaction for L29S mutant and the time course was biphasic. However, the fraction amplitude of the minor process is less than 10 % and the rate constant of the major component estimated by a single exponential fitting does not seriously deviated from a double exponential fitting.

[6] The hydrophobicity index we used here was proposed by Fauchère and Pliska (1983). This value was defined as the partitioning of N-acetyl-amino-acid amides between water and octanol, which are probably the most commonly used for estimating the contribution of the hydrophobic effect. We confirmed that the similar relationship between the hydrophobicity and the rebinding rate was observed by use of other hydrophobic index (Chothia, 1975; Wolfenden et al., 1981; Kyte & Doolittle, 1982).

[7] For the L29I mutant, the association rate constant (k_{on} = 0.19 $\mu M^{-1}s^{-1}$) is smaller than that of wild type (k_{on} = 1.1 $\mu M^{-1}s^{-1}$), whereas the hydrophobicity index and molecular volume of isoleucine are almost the

same as those of leucine. By inspection of the X-ray structure, Ile29(B10) $C_\gamma H_3$ branching at $C_\beta H$ would interfere with the motion of the E-heliix, which perturbs the dynamic interactions for the packing between the B and E helices and induced the steric effects as suggested in the L29F and L29W(SW) mutants (Carver et al., 1992)

[8] All of the mutant myoglobins showed no CO geminate binding (geminate recombination yields are less than 2%) under this condition (data not shown). This result for the L29S mutant of human myoglobin is significantly different form that of sperm whale myoglobin reported by Huang and Boxer (1994), although the time course for O_2 binding to the human L29S mutant is quite similar to that of the sperm whale L29S mutant (1994). They showed that about 20% of photodissociated carbon monoxide geminately rebinds to the heme and there were two phases in bimolecular recombination ranging from 10 μs to 10 ms for the sperm whale L29S mutant. On the other hand, the mutant human myoglobins we prepared here exhibits no CO geminate rebinding (geminate recombination yields are less than 2%) under this condition (data not shown). The different measurement conditions might be responsible for the different geminate rebinding. Our condition was 100 mM sodium phosphate pH 7.0 at 20 °C, whereas 50 mM Tris/Cl and 1 mM EDTA, pH 8.0 at 23 °C was used for the measurements by Boxer et al. (1994). In addition to the experiment conditions, we measured the rebinding kinetics for the purified *human* L29S mutant protein, while they used *sperm whale* L29S mutant in the crude lysate of *E. coli* (Boxer et al. 1994).

REFERENCES

Adachi, S., & Morishima, I. (1989) *J. Biol. Chem. 264*, 18896-18901.

Adachi, S., Sunohara, N., Ishimori, K., & Morishima, I. (1992) *J. Biol. Chem. 267*, 12614-12621.

Antonini, E., & Brunori, M. (1971) *Hemoglobin and Myoglobin in Their Reactions with Ligands*, North Holland Publishing Co., Amsterdam.

Avilés, , G., & Chang, C. K. (1992) *J. Chem. Soc., Chem. Commun.*, 31-32.

Carver, T. E., Rohlfs, R. J., Olson, J. S., Gibson, Q. H., Blackmore, R. S., Springer, B. A., & Sligar, S. G. (1990) *J. Biol. Chem. 265*, 20007-20020.

Carver, T. E., Olson, J. S., Smerdon, S. J., Krzywda, S., Wilkinson, A. J., Gibson, Q. H., Blackmore, R. S., Ropp, J. D., & Sligar, S. G. (1991) *Biochemistry 30*, 4697-4705.

Carver, T. E., Brantley Jr, R. E., Singleton, E. W., Arduini, R. M., Quillin, M. L., Phillips Jr, G. N., & Olson, J. S. (1992) *J. Biol. Chem. 267*, 14443-14450.

Case, D. A., & Karplus, M. (1979) *J. Mol. Biol. 132*, 343-368.

Chothia, C. (1975) *Nature 254*, 304-308.

Dalvit, C., & Wright, P. E. (1987) *J. Mol. Biol. 194*, 313-327.

Dou, Y., Admiraal, S. J., Ikeda-Saito, M., Krzywda, S., Wilkinson, A. J., Li, T. S., Olson, J. S., Prince, R. C., Pickering, I. J., & George, G. N. (1995) *J. Biol. Chem. 270*, 15993-16001.

Eaton, W. A., Hanson, L. K., Stephens, P. J., Sutherland, J. C., & Dunn, J. B. R. (1978) *J. Am. Chem. Soc. 100*, 4991-5003.

Eaton, W. A., & Hofrichter, J. (1981) *Methods Enzymol. 76*, 175-261.

Egeberg, K. D., Springer, B. A., Sligar, S. G., Carver, T. E., Rohlfs, R. J., & Olson, J. S. (1990) *J. Biol. Chem. 265*, 11788-11795.

Elber, R., & Karplus, M. (1990) *J. Am. Chem. Soc. 112*, 9161-9175.

Emerson, S. D., & La Mar, G. N. (1990) *Biochemistry 29*, 1556-1566.

Fauchère, J. L., & Pliska, V. (1983) *Eur. J. Med. Chem. 18*, 369-375.

Gibson, Q. H., Olson, J. S., McKinnie, R. E., & Rohlfs, R. J. (1986) *J. Biol. Chem. 261*, 10228-10239.

Gibson, Q. H., Regan, R. R., Elber, R., Olson, J. S., & Carver, T. E. (1992) *J. Biol. Chem. 267*, 22022-22034.

Gibson, Q. H., Regan, R., Olson, J. S., Carver, T. E., Dixon, B., Pohajdak, B., Sharma, P. K., & Vinogradov, S. N. (1993) *J. Biol. Chem. 268*, 16993-16998.

Goff, H. M., & La Mar, G. N. (1977) *J. Am. Chem. Soc. 99*, 6599-6606.

Huang, X., & Boxer, S. G. (1994) *Nature Struct. Biol. 1*, 226-229.

Iizuka, T., Yamamoto, H., Kotani, M., & Yonetani, T. (1971) *Biochim. Biophys. Acta. 371*, 126-139.

Jackson, T. A., Lim, M., & Anfinrud, P. A. (1994) *Chem. Phys. 180*, 131-140.

Jung, C., Hui Bon Hoa, G., Davydov, D., Gill, E., & Heremans, K. (1995) *Eur. J. Biochem. 233*, 600-606.

Kunkel, T. A. (1985) *Proc. Natl. Acad. Sci. U.S.A. 82*, 488-492.

Kyte, J., & Doolittle, R. F. (1982) *J. Mol. Biol. 157*, 105-132.

La Mar, G. N., Budd, D. L., & Goff, H. M. (1977) *Biochem. Biophys. Res. Commun. 77*, 104-110.

Lai, H. H., Li, T. S., Lyons, D. S., Phillips Jr, G. N., Olson, J. S., & Gibson, Q. H. (1995) *Protein-Struct. Funct. Genet. 22*, 322-339.

Laird, B. B., & Skinner, J. L. (1989) *J. Chem. Phys. 90*, 3274-3281.

Lambright, D. G., Balasubramanian, S., & Boxer, S. G. (1989) *J. Mol. Biol. 207*, 289-299.

Lambright, D. G., Balasubramanian, S., & Boxer, S. G. (1993) *Biochemistry 32*, 10116-10124.

Lambright, D. G., Balasubramanian, S., Decatur, S. M., & Boxer, S. G. (1994) *Biochemistry 33*, 5518-5525.

Li, T., Quillin, M. L., Phillips Jr., G. N., & Olson, J. S. (1994) *Biochemistry 33*, 1433-1446.

Lindstorm, T. R., Noren, I. B. E., Charache, S., Lehmann, H., & Ho, C. (1972) *Biochemistry 9*, 1677-1681.

Lim, M., Jackson, T. A., & Anfinrud, P. A. (1993) *Proc. Natl. Acad. Sci. U.S.A. 90*, 5801-5804.

McCoy, S., & Caughey, W. S. (1970) *Biochemistry 9*, 2387-2393.

Moore, T., Hansen, P. A., & Hochstrasser, R. M. (1988) *Proc. Natl. Acad. Sci. U.S.A. 85*, 5062-5066.

Morishima, I., & Inubushi, T. (1977) *J. Chem. Soc., Chem. Commun.*, 616-617.

Morishima, I., Inubushi, T., Neya, S., Ogawa, S., & Yonezawa, T. (1977) *Biochem. Biophys. Res. Commun. 78*, 739-745.

Morishima, I., & Inubushi, T. (1978) *J. Am. Chem. Soc. 100*, 3568-3574.

Nozaki, Y., & Tanford, C. (1971) *J. Biol. Chem. 246*, 2211-2217.

Olson, J. S., Mathews, A. J., Rohlfs, R. J., Springer, B. A., Egeberg, K. D., Sligar, S. G., Tame, J., Renaud, J.-P., & Nagai, K. (1988) *Nature 336*, 265-266.

Ormos, P., Braunstein, D., Frauenfelder, H., Hong, M. K., Lin, S.-L., Sauke, T. B., & Young, R. D. (1988) *Proc. Natl. Acad. Sci. U.S.A. 85*, 8492-8496.

Phillips, S. E. V. (1980) *J. Mol. Biol. 142*, 531-554.

Quillin, M. L., Arduini, R. M., Olson, J. S., & Phillips Jr., G. N. (1993) *J. Mol. Biol. 234*, 140-155.

Ramaprasad, S., Johnson, R. D., & La Mar, G. N. (1984) *J. Am. Chem. Soc. 106*, 5330-5335.

Rohlfs, R. J., Mathews, A. J., Carver, T. E., Olson, J. S., Springer, B. A., Egeberg, K. D., & Sligar, S. G. (1990) *J. Biol. Chem. 265*, 3168-3176.

Schulman, B. A., & Kim, P. S. (1994) *Protein Sci. 3*, 2226-2232.

Slichter, C. P., & Drickamer, H. G. (1980) *Phys. Rev. B. 22*, 4097-4108.

Smerdon, S. J., Dodson, G. G., Wilkinson, A. J., Gibson, Q. H., Blackmore, R. S., Carver, T. E., & Olson, J. S. (1991) *Biochemistry 30*, 6252-6260.

Springer, B. A., Sligar, S. G., Olson, J. S., & Phillips Jr., G. N. (1994) *Chem. Rev. 94*, 699-714.

Thomas, K. A., Smith, G. H., Thomas, T. B., & Feldmann, R. J. (1982) *Proc. Natl. Acad. Sci. U.S.A. 79*, 4843-4847.

Varadarajan, R., Szabo, A., & Boxer, S. G. (1985) *Proc. Natl. Acad. Sci. U.S.A. 82*, 5681-5684.

Varadarajan, R., Lambright, D. G., & Boxer, S. G. (1989) *Biochemistry 28*, 3771-3781.

Wakasugi, K., Ishimori, K., Imai, K., Wada, Y., & Mrishima , I. (1994) *J. Biol. Chem. 269*, 18750-18756.

Wolfenden, R., Andersson, L., Cullis, P. M., & Southgate, C. C. B. (1981) *Biochemistry 20*, 849-855.

Yamamoto, Y., Nakai, N., Chujo, R., & Suzuki, T. (1990) *FEBS Lett. 264*, 113-116.

Yamamoto, Y., & Suzuki, T. (1993) *Biochim. Biophys. Acta. 1163*, 287-296.

Yoshikawa, S., O'Keeffe, D. H., & Caughey, W. S. (1985) *J. Biol. Chem. 260*, 3518-3528.

CHAPTER 2.

The Role of Interaction between Distal Histidine and Thr67 on the Ligand Binding Dynamics in Myoglobin

ABSTRACT

Site-directed mutations at the E10 position (Thr67) have been introduced to investigate the roles of the electrostatic interaction between the distal histidine (His64) and Thr67 in the heme environmental structure and ligand binding kinetics. Replacement of Thr67 with Val induced only subtle alternations in the IR spectra of carbonmonoxy form and kinetic parameters for O_2 and CO rebinding, suggesting that the polarity of the γ-hydroxyl group of Thr67 neither contribute to the hydrophobicity of the heme pocket through the distal histidine and nor participate in the ligand binding kinetics. However, IR spectra of carbomonoxy T67D (Thr67→Asp) and T67N (Thr67→Asn) mutants exhibit an increase in the A_0 conformer, which suggests the presence of the steric interaction between the distal histidine and amino acid at position 67. The CO and O_2 association rates were also changed in the T67D and T67N mutants; the geminate rebinding for CO and O_2 increased by 2–3-fold. The calculation of the rate constants of the each elementary step for the ligand binding reaction shows that the bond formation barrier is lowered, while the ligand entry barrier is raised. These results can be understood that the electrostatic and/or steric interaction between the distal histidine and amino acid at E10 are one of the factors which regulate the heme environmental structure and ligand binding kinetics.

INTRODUCTION

Many hemoproteins, such as myoglobin (Mb[1]), hemoglobin, catalase, and peroxidase have a histidine in the distal heme pocket. The histidine is referred to as the distal histidine. It has long been known that the distal histidine is of functional importance in these proteins. One of the importance of the distal histidine in its biological function is to form a hydrogen bond with the adjacent amino acid. In cytochrome *c* peroxidase (CCP), the distal histidine forms a hydrogen bond with Asn82 adjacent to the distal histidine (Poulos & Kraut, 1980; Finzel et al., 1984). This hydrogen bond plays a crucial role in a peroxidase activity. Many other peroxidases also possess such hydrogen bonds (Poulos et al., 1993; Edwards et al., 1993; Kunishima et al., 1994; Fukuyama et al., 1995; Sundaramoorthy et al., 1994; Petersen et al., 1994; Patterson & Poulos, 1995) and utilize it to enhance the proton acceptance ability of the distal histidine. The disruption of this hydrogen bond reduces the basicity of the distal histidine and substantially decreases the rate of active species formation because of a decrease in the deprotonation rates of hydrogen peroxidases by the distal histidine (Nagano et al., 1996).

In myoglobin, the distal histidine does not form such a hydrogen bond with other amino acid residues, which would be one of the reasons for a weak peroxidase activity in myoglobin (Phillips, 1980; Nagano et al., 1996). Thr at position 67 (E10[2]) in myoglobin is located in the position corresponding to Asn82 in CCP (Figure 1). Although the distance between the distal histidine and Thr67 is too long to form a hydrogen bond between them, the presence of the electrostatic interaction between the distal histidine and Thr67 was suggested by the pK_a value of the distal histidine (Nagano et al., to be submitted).

In our previous study, the pK_a value for the Thr67→Asn mutant was 8.50, which is lower than that for wild type (8.72), Thr67→Asp mutation increased the pK_a value to 9.58 (Nagano et al., to be submitted). The pK_a value is given by the acid-base transition of the distal histidine (scheme 1). The decreased pK_a value of the T67N mutant from that of wild type implies that this mutant favors the alkaline form (scheme 1) at the transition pH of wild type, while the increased pK_a value of the T67D mutant indicates that the protein more favors the acidic form (scheme 1). This difference in the pK_a value of the distal histidine is attributed to the shift of the equilibrium between the two tautomers of the distal histidine. Since Thr67 is located adjacent to the N_δ atom of the distal histidine, substitution

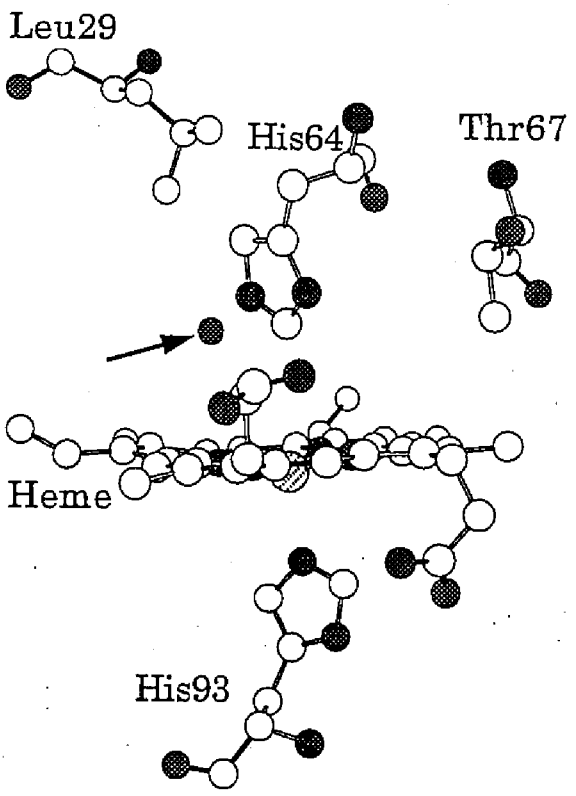

Figure 1. Heme environmental structure of human aquo-met myoglobin (Hubbard et al., 1990). The heme and some selected myoglobin residues constituting the heme pocket are shown. The arrow points to the water molecule hydrogen bonded to the distal histidine.

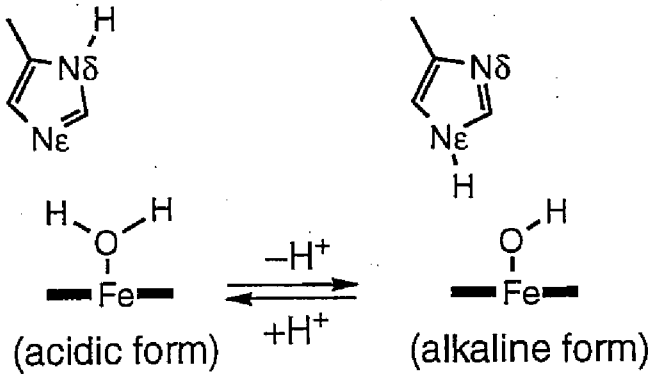

SCHEME 1

at position 67 could change the equilibrium through the interaction between the distal histidine and amino acid at E10. If the carboxylate of Asp67 interacts with the proton attached to the N_δ atom of the distal histidine, the acidic form in scheme 1 is stabilized and the pK_a value of the

histidine is increased, implying the presence of the electrostatic interaction between the N_δ atom and amino acid at position 67.

The mutation at Thr67 also resulted in changes of the cyanide binding rates (k_{CN}) to ferric myoglobin at pH 7.0 (Nagano et al., to be submitted). Cyanide binding rates of the Thr67 mutants, in which Thr67 was replaced with Asn, Asp, and Val, were proportional to the pK_a value. The T67N mutant, which favors the acidic form in scheme 1 due to the low pK_a value (8.50), increased k_{CN} from 0.15 to 0.27 $mM^{-1}s^{-1}$, while T67D mutant, which favors the alkaline form in scheme 1 due to the high pK_a value (9.58), decreased k_{CN} from 0.15 to 0.084 $mM^{-1}s^{-1}$ (Nagano et al., to be submitted). Since previous mutational studies revealed that the cyanide binding rates to myoglobin depend on the deprotonation step of HCN by the N_ε atom of the distal histidine (Brancaccio et al., 1994; Dou et al., 1996), an ability of protonation of the N_ε atom of the distal histidine influences the cyanide binding rates. Thus, the feasibility of protonation of the N_ε atom of the distal histidine in the T67N mutant (alkaline from, scheme 1) related to the increase in k_{CN}, while low affinity of proton to the N_ε atom of the distal histidine in the T67D mutant (acidic from, scheme 1) related to the decrease in k_{CN}.

As the electrostatic interaction between the distal histidine and amino acid at E10 changes k_{CN}, it is expected that the CO rebinding rate to these mutants would be changed. The CO rebinding rate is regulated by the water molecule hydrogen bonded to the N_ε atom of the distal histidine (Rohlfs et al., 1990; Quillin et al., 1993; Springer et al., 1994; Olson & Phillips, 1996, 1997). In wild type deoxy myoglobin, a water molecule is hydrogen bonded to the N_ε atom of the distal histidine (Figure 1) (Quillin et al., 1993). This water molecule has been recently considered to control the ligand binding reaction to ferrous myoglobin (Rohlfs et al., 1990; Springer et al., 1994; Olson & Phillips, 1996, 1997). The perturbation of the electrostatic interaction induced by mutation at E10 could change the coordination of the hydrogen bonded water, resulting in the change of the ligand association rates.

In this paper, to investigate the role of the electrostatic interaction between the distal histidine and Thr67 in the ligand binding properties, Thr67 was substituted with Asp and Asn to enhance the interaction with the distal histidine and substituted with Val to disrupt the interaction. We utilized a laser photolysis and stopped flow techniques to characterize the ligand association and dissociation rate constants for CO and O_2 for these mutants. Furthermore, we examined the effect of the interaction

between the distal histidine and Thr67 on hydrophobicity of the heme pocket, since our previous study proposed that the hydrophobicity of the heme pocket is one of the key factors in regulating the ligand binding to the heme iron (Uchida et al., 1997). To study the effect, we measured IR spectra of the carbomonoxy myoglobins.

EXPERIMENTAL PROCEDURE

Preparation of Mutant Myoglobins. The original expression vector of human myoglobin[3], pMb3 (pLcIIFXMb), is a gift from Varadarajan and Boxer (1985). The procedures for site-directed mutagenesis are described in previous papers (Kunkel, 1985; Varadarajan et al., 1985; Adachi *et al.*, 1992). Protein preparation and purification were followed by the method described previously (Adachi *et al.*, 1992; Nagano et al., to be submitted).

Electronic Absorption and Infrared Spectra. Electronic absorption spectra of purified proteins in 100 mM sodium phosphate buffer, pH 7.0, were recorded on a Shimadzu UV 2200 UV/visible spectrophotometer. The sample concentration was 5 μM. The peak maxima of deoxy-, oxy- and carbonmonoxy forms did not shift for more than 1 nm by the mutations. Infrared spectra for the carbonmonoxy forms were measured at 1 cm^{-1} resolution on a Bio-Rad FTS-30 spectrophotometer. The protein solution was loaded into a CaF_2 cell with 0.1 mm path length. The spectral ranges were recorded from 1850 to 2000 cm^{-1}. We used equimolar aquo-met form of human wild type myoglobin as a reference. An average of 512 scans was used for each spectrum. The sample concentration was about 1 mM, pH 7.0 at room temperature. Spectrum analysis was carried out using IGOR Pro software (WaveMetrics, Inc.). The constituent bands were fitted with Gaussian functions.

Near-infrared Absorption Spectra of Deoxy Myoglobins. Deoxy myoglobin was prepared by reduction of aquo-met myoglobin with a small amount of solid sodium dithionite under an argon atmosphere. The aquo-met myoglobin solution was calmly stirred under the argon atmosphere on ice for more than 30 min before reducing. The sample concentration was 1 mM and we used 100 mM sodium phosphate buffer, pH 7.0, at 20 °C. Near-infrared absorption spectra were recorded on a Shimadzu UV 2200 UV/visible spectrophotometer over the range of 700 to 850 nm.

Kinetic Measurements of CO and O_2 Binding. The association rate constants of CO and O_2 were obtained by a laser photolysis apparatus as previously described in detail (Adachi & Morishima, 1989; Adachi et al.,

1992; Uchida et al., 1997). We used 6-ns full-width at half-maximum (FWHM) pulses from a Q-switched Nd:YAG laser for the experiments. The incident energy was about 10 mJ at the wavelength maximum of 532 nm. The absorption changes were monitored by a continuous, weak probe beam from a 150-W xenon arc lamp passed through a monochromator. The probe light at 440 nm was focused onto the slit of a monochromator (Unisoku USP-501). Signals were detected in transmission using a photomultiplier (Hamamatsu Photonics, R2949) and the transient signals were digitized by a Tektronix TDS-520A oscilloscope. The data were transferred to a NEC PC-9801BX4/U2 computer for further data analysis. No smoothing artifact affected the results of the following data analysis. The protein concentration was about 5 μM. The buffer conditions were 100 mM sodium phosphate, pH 7.0, at 20 °C.

The time courses for milli- to microsecond experiments were analyzed by fitting to the equation 1,

$$\Delta A_t = \Delta A_0 \exp(-k_{app}\, t) \tag{1}$$

where ΔA_t is the absorbance change at any time t, ΔA_0 is the total absorbance change (absorbance at $t = 0$ minus absorbance at $t = \infty$). k_{app} is the observed first-order rate constant and satisfies the equation (2) (Antonini & Brunori, 1971),

$$k_{app} = k_{on}[L] \tag{2}$$

where k_{on} is the bimolecular ligand binding rate constant and [L] is ligand concentration. The time courses from nano- to milli second were analyzed by fitting to the following equations (equation 3 for CO and equation 4 for O_2 due to 1 and 2 phases geminate rebinding, respectively),

$$\Delta A_t = \phi_g \exp(-k_g\, t)+C \tag{3}$$

$$\Delta A_t = \phi_{g1} \exp(-k_{g1}\, t)+\phi_{g2} \exp(-k_{g2}\, t)+C \tag{4}$$

where k_g is the geminate rate constant, ϕ_g is the geminate yield, C is a constant.

The kinetics measurements of the CO dissociation rates (k_{off}) were carried out with a UV/visible spectrometer (Shimadzu UV-2200). k_{off} was determined by analyzing the replacement reaction in which ligated CO was replaced by NO as previously described (Lambright et al. 1989). The

concentrated aquo-met myoglobin stock was converted to the carbonmonoxy form by addition of a small amount of sodium dithionite in the CO saturated buffer with stirring. NO saturated buffer (100 mM sodium phosphate, pH 7.0) was prepared by bubbling NO through deoxygenated buffer solution in a sealed 1 cm path-length UV cell (3 ml). About 20 μl of the concentrated Mb-CO solution was then injected into the cell at 20 °C, and the reaction was followed by monitoring the absorbance at 424 nm.

Dissociation rate constants for O_2 were estimated by use of CO replacement reaction method with a stopped-flow apparatus (Antonini & Brunori, 1971; Rohlfs et al., 1990). In our experiments, oxymyoglobin solution which was saturated with 1 atm of O_2 was mixed with a CO saturated solution. The observed replacement rate is given by equation 5,

$$k_{obs} = k_{off(O_2)} \frac{1}{1+\frac{k_{on(O_2)}[O_2]}{k_{on(CO)}[CO]}} \tag{5}$$

(Rohlfs et al., 1990). The CO and O_2 bimolecular association rates ($k_{on(CO)}$ and $k_{on(O_2)}$) were independently measured. Absorption changes were monitored at 429 nm. CO and O_2 association equilibrium constants were calculated from the ratio of the association and dissociation rate constants.

Kinetic Models for CO and O_2 Binding. In this study, we used the three-state sequential model (Henry et al., 1983) for the CO rebinding in myoglobin (equation 6).

$$\underset{1}{\mathrm{MbCO}} \underset{k_{21}}{\overset{h\nu}{\rightleftharpoons}} \underset{2}{\mathrm{Mb:CO}} \underset{k_{32}}{\overset{k_{23}}{\rightleftharpoons}} \underset{3}{\mathrm{Mb + CO}} \tag{6}$$

where the states 1 and 3 are referred to as the CO bound and the deoxy states, respectively. The state 2 is the geminate state in which the iron-CO bond has been photolyzed but the ligand is still trapped within the protein matrix (Henry et al., 1983). The observable k_g, $\phi_{g(CO)}$, $k_{on(CO)}$, and $k_{off(CO)}$ are related to the rate constants for the three-state sequential scheme (Henry et al., 1983) by the following equations,

$$k_g = k_{21}+k_{23} \tag{7}$$

$$\phi_{g(CO)} = k_{21}/k_g \quad (8)$$

$$k_{on(CO)} = k_{32}\,\phi_g \quad (9)$$

Since the geminate process of the CO rebinding could be fitted with a single exponential within our experimental error, the model was adequate to our experiments under the present conditions.

In the geminate process for O_2 rebinding, the 4-state sequential model has been proposed as one of the possible models (Sommer et al., 1985; Gibson et al., 1986; Lambright et al., 1994),

$$\underset{1}{MbO_2} \underset{k_{21}}{\overset{h\nu}{\rightleftharpoons}} \underset{2}{Mb : O_2} \underset{k_{32}}{\overset{k_{23}}{\rightleftharpoons}} \underset{3}{Mb ::: O_2} \underset{k_{43}}{\overset{k_{34}}{\rightleftharpoons}} \underset{4}{Mb + O_2} \quad (10)$$

where the state 1 is oxymyoglobin, 2 and 3 represent species in which the O_2 is still inside the protein, but not ligated to the heme iron. The state 3 is distinct from the state 2 where the ligand is still in the protein but presumably away from the iron atom. The state 4 is deoxymyoglobin (Sommer et al., 1985). The observable $k_{g1(O_2)}$, $k_{g2(O_2)}$, $\phi_{g1(O_2)}$, $\phi_{g2(O_2)}$, and $k_{on(O_2)}$ are related to the rate constants for the four-state sequential scheme (Lambright et al., 1994) by the following equations,

$$k_{g1(O_2)} \equiv k_{21}+k_{23} \quad (11)$$

$$k_{g2(O_2)} \cong k_{32}\phi_2+k_{34} \quad (12)$$

$$\phi_{g1(O_2)} \cong \phi_2 \quad (13)$$

$$\phi_{g2(O_2)} \cong \phi_3(1-\phi_2) \quad (14)$$

$$k_{on} = k_{43}\,\phi_3 \quad (15)$$

$$\phi_2 = k_{21}/(k_{21}+k_{23}) \quad (16)$$

$$\phi_3 = k_{32}\phi_2(k_{32}\phi_2+k_{34}) \quad (17)$$

RESULTS

Infrared Spectra of Carbonmonoxy Myoglobins. To gain insights into the role of the electrostatic interaction between the distal histidine and Thr67 in hydrophobicity of the heme environmental structure, we measured infrared (IR) spectra of carbomonoxy wild type and Thr67 mutant myoglobins. Figure 2 shows the IR spectra with the results of curve-fitting in the C-O stretching region, 1900–2000 cm^{-1}, for wild type and T67V, T67D, and T67N mutant myoglobins at pH 7.0, room temperature.

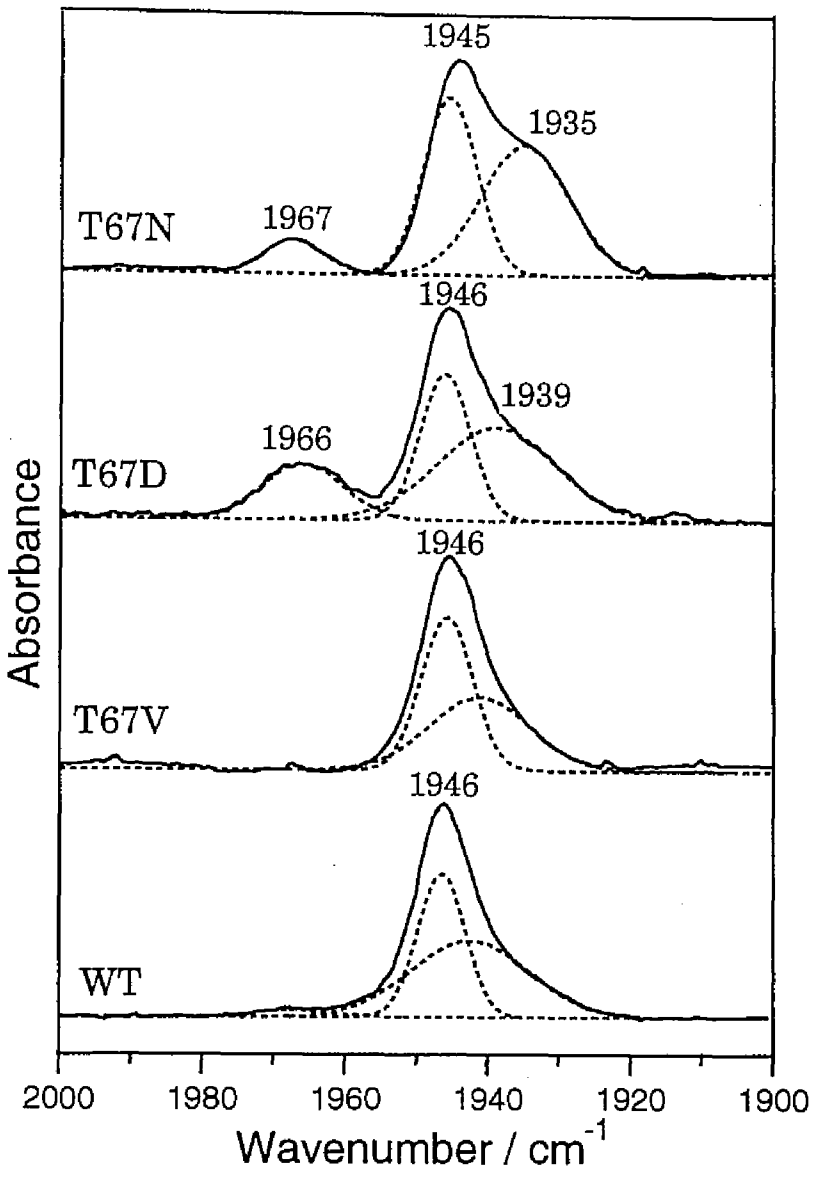

Figure 2. IR spectra of C-O stretching region of the wild type and the Thr67 mutant myoglobins (solid line). Component bands are shown as broken lines. Samples contain 1 mM protein in 0.1 M sodium phosphate buffer at pH 7.0 at room temperature.

The peak positions and relative intensities of the ν(C-O) band are summarized in Table I. For human wild type myoglobin, the IR spectrum consists of three bands; main bands at 1946 and 1943 cm^{-1} and a minor band at 1967 cm^{-1}, referred to as A_1 A_2, and A_0, respectively (Ansari et al., 1987; Oldfield et al., 1991). The spectral pattern of the T67V mutant is similar to that of wild type myoglobin, indicating that the polarity of Thr67 little affected the IR spectra of myoglobin. The mutation to Asp or Asn leads to a significant increase in the band around 1966 cm^{-1}, which is

assigned to the A_0 conformer. The A_0 conformer, being the predominant conformer at low pH, has been assigned to an open conformer (Morikis et al., 1989; Oldfield et al., 1991; Ray et al., 1994; Li et al., 1994). The T67D and T67N mutants have a conformer in which the distal histidine does not interact with iron-bound CO. In the T67D mutant, the A_2 band slightly shifted from 1943 to 1939 cm^{-1}. In addition, the T67N mutant shows a disappearance of the A_2 band and an increase in the A_3 conformers at 1935 cm^{-1}. The increase in the A_3 conformer for the T67N mutant suggests that the positive interaction between the amino acid within the heme pocket and iron-bound CO exists (Li et al., 1994; Jewsbury & Kitagawa, 1994). The increases in the A_0, A_2, and A_3 conformers of the T67N and T67D mutants imply that the heterogeneity of the heme pocket is increased in these mutants.

TABLE I: IR Stretching Frequencies and Population of the Conformers for CO-bound Forms of Wild Type and Mutant Myoglobins.

Myoglobin	A_0	A_1	A_2	A_3
	cm^{-1}			
WT	1967 (3)[a]	1946 (63)	1943 (34)	ND[b]
T67V	ND	1946 (67)	1941 (33)	ND
T67D	1966 (19)	1946 (50)	1939 (31)	ND
T67N	1967 (10)	1945 (52)	ND	1935 (38)

[a] Values in parentheses represents percentages of the relative population of the conformers. [b] ND, not detected.

CO Association and Dissociation Reactions. To examine the functional relevance of the electrostatic interaction between the distal histidine and Thr67, we have studied the kinetics of CO rebinding after photolysis at room temperature. A series of the time courses for CO bimolecular recombination to the wild type and Thr67 mutant myoglobins is illustrated in Figure 3. The bimolecular association rate constants ($k_{on(CO)}$) were determined by fitting the time course to the equation 1 and are summarized in Table II. The rate constants of the T67V and T67N mutants are 0.90 and 0.81 $\mu M^{-1}s^{-1}$, respectively, which are close to that of wild type myoglobin (0.84 $\mu M^{-1}s^{-1}$). In contrast, $k_{on(CO)}$ for the Asp mutant was a 1.5-fold increase (1.33 $\mu M^{-1}s^{-1}$) from that of wild type, although the mutant has an isosteric side chain as does the Asn mutant. This

indicates that the difference in $k_{on(CO)}$ between the T67N and T67D mutants are not attributed to steric hindrance of the side chain at E10.

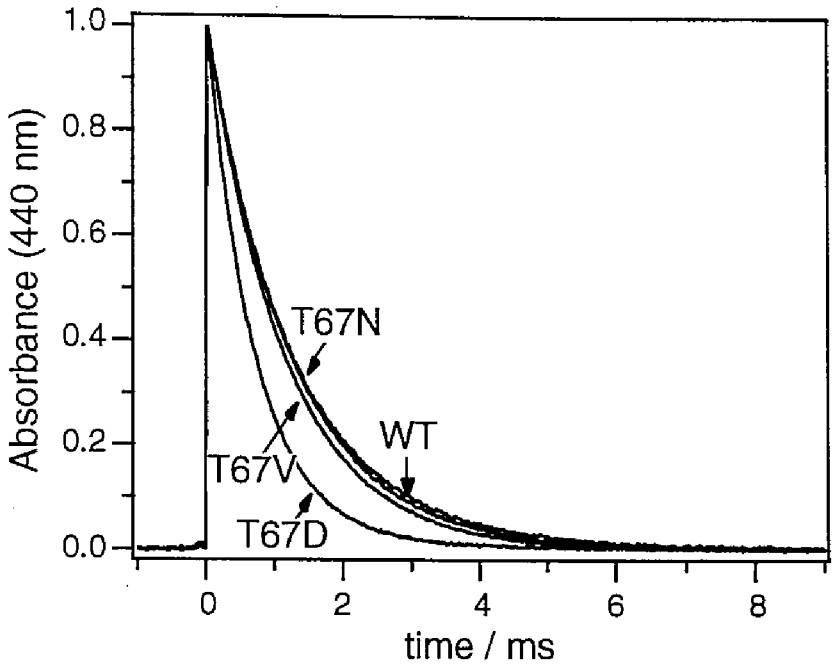

Figure 3. Bimolecular association kinetics of CO to wild type and Thr67 mutant myoglobins at CO concentration of 1.0 mM and 20 °C (solid line). The broken lines are fits to a exponential. The change in absorbance has been normalized to unity at the end of the geminate processes. The time course were monitored at 440 nm.

The geminate rebinding processes within 2 microsecond for wild type and the Thr67 mutants are shown in Figure 4. We fitted the time courses of CO rebinding in the geminate region by equation 3 and obtained the parameters of the geminate kinetic, which are compiled in Table II. The geminate recombination rates for the T67V mutant, $k_{g(CO)}$ = 2.9 μs^{-1}, is similar to that of wild type myoglobin (2.7 μs^{-1}) and the fraction of the geminate recombination ($\phi_{g(CO)}$) for the T67V mutant (0.050) is also almost the same as that of wild type myoglobin (0.047) within experimental error. On the other hand, the geminate recombination rates ($k_{g(CO)}$) for the other mutants are increased; $k_{g(CO)}$ for 3.4 and 3.9 μs^{-1} for the T67N, and T67D mutants, respectively. The geminate yields ($\phi_{g(CO)}$) are also affected in the T67N, and T67D mutants, $\phi_{g(CO)}$ increased to 0.089 and 0.14, respectively.

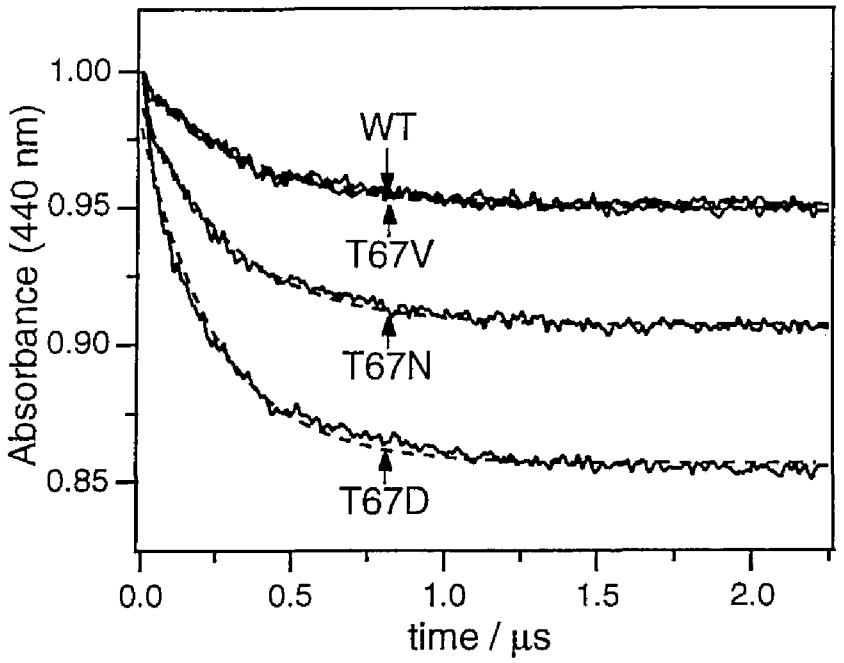

Figure 4. Time courses for CO geminate rebinding to wild type and Thr67 mutant myoglobins (solid line). The broken lines are fits to a exponential. The time course are monitored at 440 nm at 20 °C. Traces for 2000 shots were averaged.

The time courses of CO dissociation reaction for the wild type and Thr67 mutants were measured by the conventional NO replacement method (Lambright et al., 1989; Rohlfs et al., 1990) and the obtained values of the CO dissociation rates ($k_{off(CO)}$) are listed in Table II.

TABLE II: Kinetic Rate Constants for CO Binding to the Wild Type and Mutant Myoglobins at 20 °C.

	$k_{on(CO)}$	$k_{off(CO)}$	$K_{(CO)}$	$k_{g(CO)}$	$\phi_{g(CO)}$
	$\mu M^{-1}s^{-1}$	s^{-1}	μM^{-1}	μs^{-1}	
WT	0.84±0.01	0.018±0.001	47±4	2.7±0.3	0.047±0.005
T67V	0.90±0.02	0.017±0.001	53±3	2.9±0.0	0.050±0.001
T67D	1.3±0.0	0.016±0.001	85±5	3.9±0.1	0.14±0.00
T67N	0.81±0.03	0.016±0.001	50±6	3.4±0.1	0.089±0.004

The rates were little affected by the substitution at position 67. CO association equilibrium constants were calculated from the ratio of the

association and dissociation rate constants and listed in Table II. The increases in CO association equilibrium constants for all the mutants mainly reflect the change of the association rate constants, since the dissociation rates are little changed by mutation at E10.

O_2 Association and Dissociation Reactions. Figure 5 shows the time courses for O_2 bimolecular recombination to the Thr67 mutants. The time courses of O_2 bimolecular rebinding can be fitted with a single exponential and the obtained rate constants are compiled in Table III-A. The Val mutant shows almost similar O_2 association rate constants ($k_{on(O_2)}$) (16.7 $\mu M^{-1}s^{-1}$) to that of wild type myoglobin (16.0 $\mu M^{-1}s^{-1}$). The Asn mutant shows a decrease in the association rates for O_2 (9.78 $\mu M^{-1}s^{-1}$). The $k_{on(O_2)}$ are also decreased by the replacement of Thr67 with Asp (12.4 $\mu M^{-1}s^{-1}$).

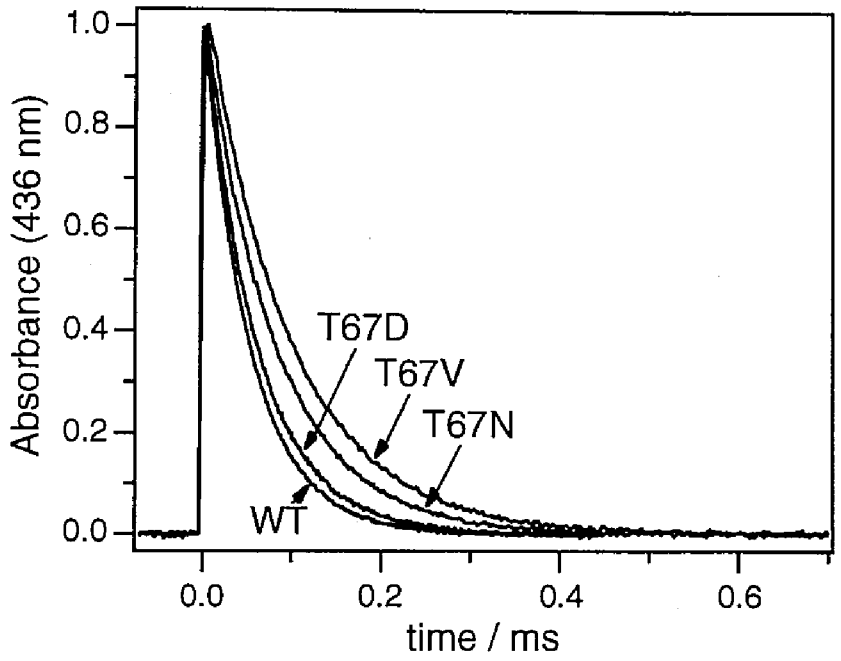

Figure 5. Bimolecular association kinetics of O_2 to wild type and mutant myoglobins at CO concentration of 1.0 mM and 20 °C (solid line). The broken lines are fits to a exponential. The change in absorbance has been normalized to unity at the end of the geminate processes. The time course were monitored at 436 nm.

The time courses of the geminate rebinding for wild type and the Thr67 mutants are depicted in Figure 6. The fraction of the geminate rebinding for the O_2 binding is larger than that of the CO binding and about half of the photolyzed CO rebinding in the geminate region. For wild type and all the Thr67 mutants, the geminate process for the O_2

rebinding cannot be described by a single exponential, but well by sum of two exponentials. The fitted parameters to the equation 4 are summarized in Table III-B. The geminate rebinding rates ($k_{g1(O_2)}$, $k_{g2(O_2)}$) for the T67V and T67N mutants are close to those of wild type, while the Asp67 mutant exhibited larger geminate rate constants ($k_{g1(O_2)}$, $k_{g2(O_2)}$). The geminate rebinding yields ($\phi_{g1(O_2)}$, $\phi_{g2(O_2)}$) for the T67V and T67N mutants are also similar to those of wild type. On the other hand, the fast geminate yield ($\phi_{g1(O_2)}$) for the T67D mutant is larger than that of wild type.

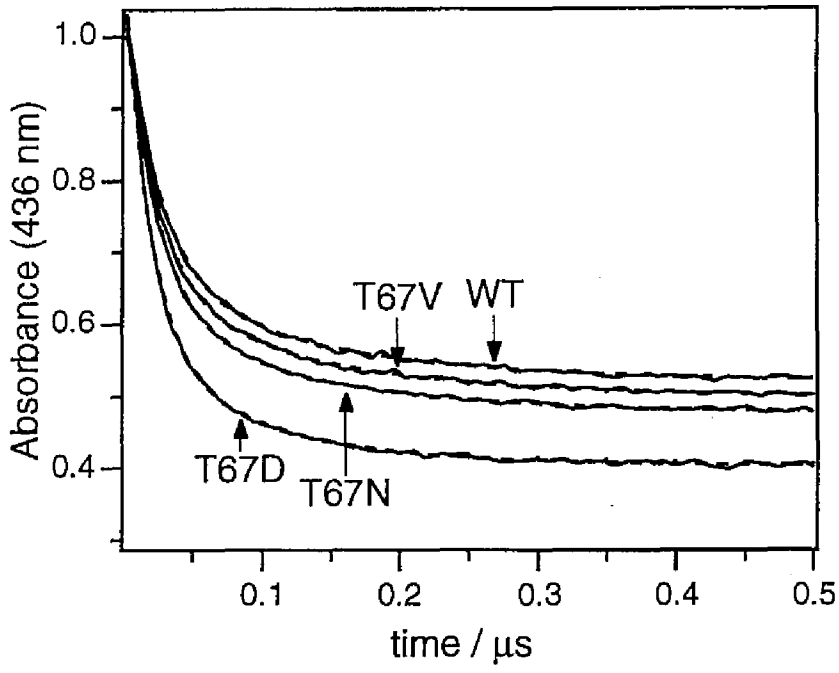

Figure 6. Time courses for O_2 geminate rebinding to wild type and Thr67 mutant myoglobins (solid line). The broken lines are fits to double exponentials. The time course are monitored at 436 nm at 20 °C. Traces for 2000 shots were averaged.

The O_2 dissociation rate constants ($k_{off(O_2)}$) were measured by the CO replacement reactions in the stopped flow apparatus and presented in the Table III-A. $k_{off(O_2)}$ for the T67V mutant (16.7 s^{-1}) is almost identical to that of wild type (16.0 s^{-1}). The dissociation rate constants for O_2 of the mutants are decreased 9.78 (T67N) and 12.4 s^{-1} (T67D). The decrease in the O_2 dissociation rates was unusual. Most of the distal pocket mutation of myoglobins increased the O_2 dissociation rates, since most mutations perturb or disrupt the hydrogen bond between the distal histidine and

iron-bound oxygen (Olson et al., 1988; Rohlfs et al., 1990; Springer et al., 1994). The electrostatic interaction of the distal histidine and Thr67 changed the O_2 dissociation rates.

TABLE III-A: Kinetic Rate Constants for O_2 Binding to the Wild Type and Mutant Myoglobins at 20 °C.

	$k_{on(O_2)}$	$k_{off(O_2)}$	$K_{(O_2)}$
	$\mu M^{-1}s^{-1}$	s^{-1}	μM^{-1}
WT	16.0 ± 0.5	20.7 ± 0.2	0.773 ± 0.02
T67V	16.7 ± 0.4	14.9 ± 0.9	1.12 ± 0.10
T67D	12.4 ± 0.3	12.4 ± 0.3	1.53 ± 0.11
T67N	9.78 ± 0.4	6.87 ± 0.43	1.42 ± 0.11

TABLE III-B: Fitted Parameter for O_2 Geminate Rebinding for CO Binding to the Wild Type and Mutant Myoglobins at 20 °C.

	$k_{g1(O_2)}$	$\phi_{g1(O_2)}$	$k_{g2(O_2)}$	$\phi_{g2(O_2)}$
	μs^{-1}		μs^{-1}	
WT	37 ± 1	0.37 ± 0.02	7.4 ± 0.1	0.13 ± 0.01
T67V	38 ± 1	0.40 ± 0.03	7.1 ± 0.1	0.12 ± 0.01
T67D	47 ± 3	0.51 ± 0.03	8.5 ± 0.1	0.12 ± 0.01
T67N	40 ± 1	0.44 ± 0.02	6.8 ± 0.1	0.11 ± 0.01

Near-infrared Absorption Spectra of Deoxymyoglobins. The near-infrared absorption spectra (band III) for the wild type and Thr67 mutant myoglobins in the deoxy form are measured to investigate the role of the structural of the heme proximal site in regulating the geminate recombination and shown in Figure 7. These spectra were well described by a single Gaussian function on top of a cubic polynomial background (Lim et al., 1993; Jackson et al., 1994). The center frequencies of the bands are compiled in Table IV. The center frequencies of the band III are 763.0 nm

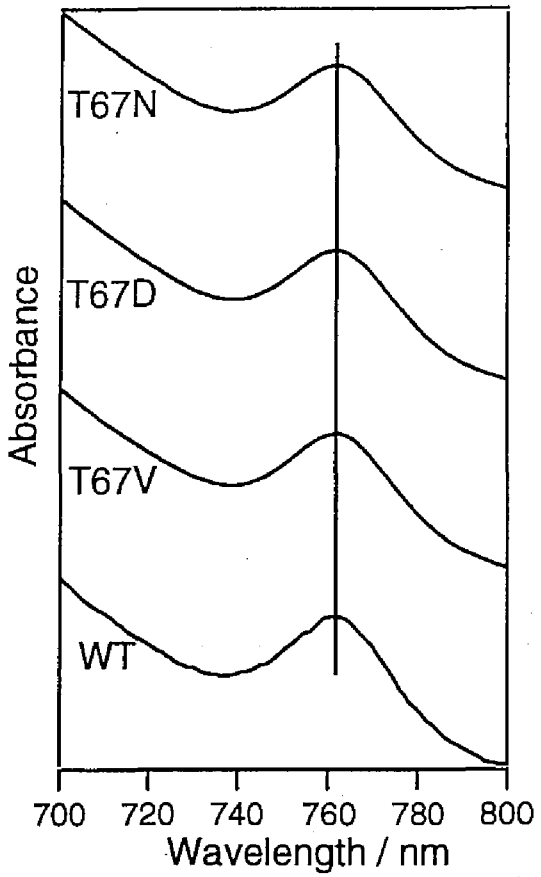

Figure 7. Near-infrared absorption spectra of the deoxy wild type and Thr67 mutant myoglobins. The data were modeled with a Gaussian function plus a cubic polynomial function. Samples contain 1 mM protein in 0.1 M sodium phosphate buffer at pH 7.0.

TABLE IV: pK_a Values of the Acid-base Transition in the Ferric Form and Center Frequency of Band III in Wild Type and Mutant Myoglobins in Deoxy Form at pH 7.0.

	Center frequency of band III	pK_a
	nm	
WT	763.9	8.72±0.01
T67V	763.0	8.94±0.01
T67D	763.2	9.58±0.03
T67N	763.0	8.50±0.02

for the T67V and T67N mutants and 763.2 nm for the T67D mutant, which are a little blue-shifted from that for wild type myoglobin (763.9 nm). Since

the center frequency of band III is sensitive to the position of the iron relative to the plane of the porphyrin (Jackson et al., 1994), the slightly blue-shifted center frequencies of the band III for the Thr67 mutants suggest that the heme iron moves more out of heme plane than wild type.

DISCUSSION

The Effects of the Electrostatic Interaction between the Distal Histidine and Thr67 in Polarity of the Heme Pocket. We investigated the effects of the electrostatic interaction between the distal histidine and amino acid residue at position 67 on the polarity of the heme pocket by IR spectra of carbonmonoxy myoglobins. IR spectra of the C-O stretching region serve as a sensitive marker for the polarity of the heme pocket, since they reflect the electrostatic field near the ligand binding site (Ray et al., 1994; Li et al., 1994; Decatur & Boxer, 1995). Substitution of the γ-hydroxyl group with γ-methyl group in the Thr67 (T67V) caused no effects on the IR spectra of the carbonmonoxy forms (Figure 2, Table I). Since the isosteric valine mutation serves as a particularly useful probe to the role of the hydroxyl group of Thr (Smerdon et al., 1991, 1995; Cameron et al., 1993; Fronticelli et al., 1993), it was concluded that the polarity of Thr67 in wild type myoglobin exerts no interaction on the coordinated CO.

On the other hand, the IR spectra of carbomonoxy myoglobins were changed by Thr→Asp and Thr→Asn mutations (Figure 2, Table I). The alterations of the IR spectra induced by the T67N and T67D mutants are mainly attributed to the change of the polarity in the heme pocket, since ^{1}H NMR spectra of the cyano-met forms of the mutants showed that the heme environment structure of these mutants were not changed (Nagano et al., to be submitted). In the T67D mutant, the intensity of the A_0 bands at ~1966 cm^{-1} was much increased (Figure 2, Table I). In the A_0 conformer, there is no significant positive interaction between the iron-coordinated CO and amino acids within the heme pocket, and the conformer is also observed for wild type myoglobin under acidic pH, in which the distal histidine rotates far away from the bound ligand and exerts no interaction with the iron-bound CO (Morikis et al., 1989; Li et al., 1994; Ray et al., 1994; Jewsbury & Kitagawa, 1994). In the Asp67 mutant, since Asp residue is expected to be deprotonated at the neutral pH (-COOH, pK_a = ~4) and a potent hydrogen bond acceptor, Asp interacts with the proton attached to the N_δH, and stabilizes the N_ε/N_δH form (i, scheme 2), resulting in the increase in the A_0 conformer. In the T67D mutant, the distal histidine

exerts no positive interaction with the iron-bound CO, which coincides with the increase in the A_0 conformer. This implies that the side chain of Asp67 electrostatically interacts with the distal histidine.

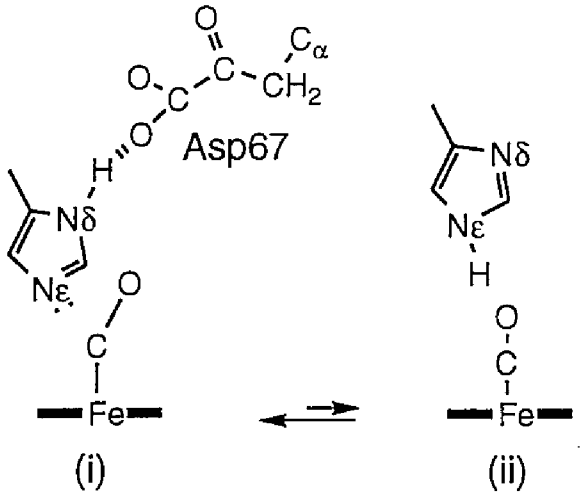

SCHEME 2

On the other hand, Thr67→Asn mutant leads to a significant increase in the band at 1935 cm^{-1}, which is assigned to the A_3 conformer. Although some controversy exists on the interpretation of the A_3 conformer (Oldfield et al., 1991; Ray et al., 1994; Li et al., 1994), the proximity of the protonated distal nitrogen ($N_\varepsilon H$) would be attributed to the A_3 conformer. The positive interaction by the distal histidine polarizes the C-O bond, resulting in weakening the C-O bond (Li et al., 1994; Jewsbury & Kitagawa, 1994). In the T67N mutant, the N_ε atom of the distal histidine is more protonated, estimating from the pK_a value of the distal histidine. Thr67→Asn substitution decreased the pK_a value from 8.72 to 8.50 (Table IV) (Nagano et al., to be submitted). This indicates that T67N mutant more favors the $N_\varepsilon H$ form (ii, scheme 3) than wild type. Since Asn can be a potent hydrogen bond donor, Asn is likely to interact with the lone pair of the N_δ atom of the distal histidine and favors the $N_\varepsilon H/N_\delta$ form, resulting in the increase in the A_3 conformer. Thus, Asn or Asp at position 67 exerts the electrostatic interaction with the distal histidine and changed the polarity of the heme pocket.

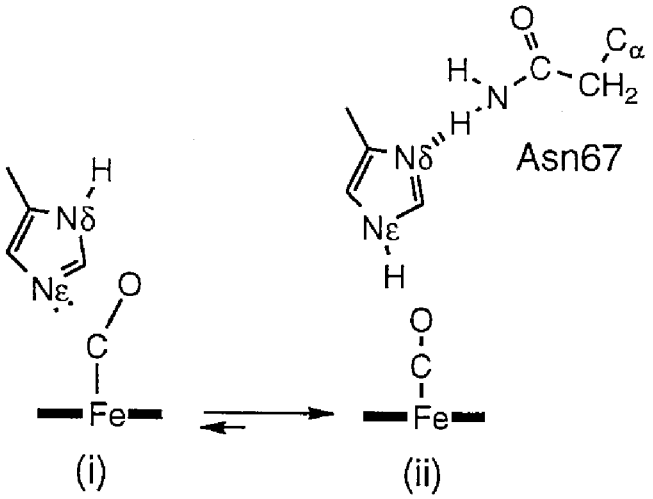

SCHEME 3

Relation with Conformational Changes of the Distal Histidine and Ligand Binding Rates. We investigated the effects of the alternation in the polarity within the heme pocket induced by Thr67 mutations on the ligand binding kinetics. As described in RESULTS section, the T67D mutant increased the CO association rate, while the T67N mutant decreased it (Table II). On the other hand, O_2 association rates were decreased in both the T67D and T67N mutants (Table III-A). The effects of replacement of Thr67 with Asp or Asn on the ligand binding kinetics were further examined by calculating the rate constants of the bond formation (k_{21}) and ligand entry (k_{entry}) rates from the solvent to protein interior based on the equations 8, 9 and 12–18. Values for k_{21} and k_{entry} for the wild type, T67V, T67N, and T67D mutant myoglobins are summarized in Table V. The T67D and T67N mutants increased the bond formation rates (k_{21}) for both CO and O_2 by 2–5-fold. On the contrary, the ligand entry rates (k_{entry}) for CO and O_2 binding decreased for both the mutants by about 2-fold. Both changes were independent of ligands (CO or O_2), which means that these changes are related to the steric interaction between ligand and amino acid residue, but not polarity in the protein. It is concluded that the substitution of Thr67 by Asp and Asn increased the barrier for ligand entry, while decreased the barrier for bond formation. Although hydrophobic interaction between the distal histidine and the T67N mutant is different from that between the distal histidine and the T67D mutant as revealed by IR spectra of carbomonoxy forms, energy barriers for CO and O_2 binding to the T67N mutant resemble those of the T67D mutant (Figure

8). This suggests that isosteric side chains of Asn67 and Asp67 sterically interact with the distal histidine.

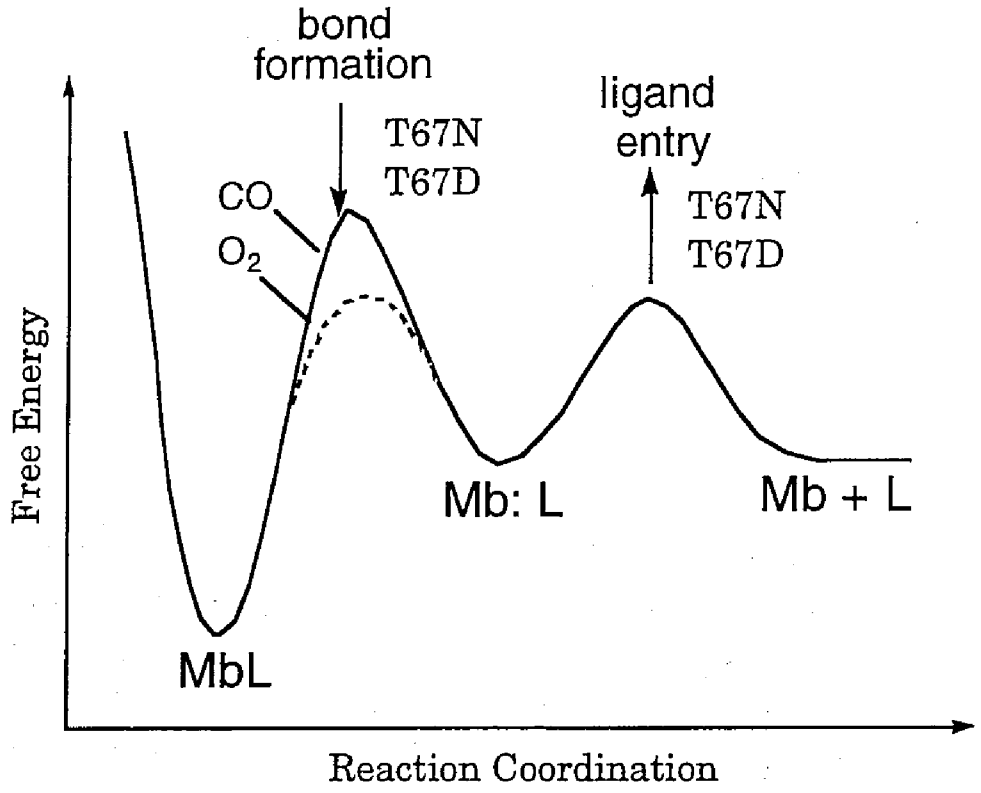

Figure 8. Relative free energy diagram schematically plotted vs the reaction coordinate. The solid and dashed curves represent for the CO and O_2 binding respectively.

TABLE V: Calculated Rate Constants for CO Rebinding to the Wild Type and Thr67 Mutant Myoglobins at 20 °C.

Myoglobin	$k_{21(CO_2)}$	$k_{entry(CO)}$	$k_{21(O_2)}$	$k_{entry(O_2)}$
	μs^{-1}	$\mu M^{-1}s^{-1}$	μs^{-1}	$\mu M^{-1}s^{-1}$
WT	0.13	17.2	14	57
T67V	0.14	17.3	15	59
T67D	0.57	9.0	24	37
T67N	0.30	8.8	18	35

The standard deviation for k_g and ϕ_g were within 10% as described in Table I.

Relation of the Inner Kinetic Barrier and Interaction between the Distal Histidine and Thr67. To understand a manner of the changes of the kinetic barrier for the ligand binding in the T67N and T67D mutants, we inquire the possibility of the previous reported three factors which regulate the inner kinetic barrier. Quillin et al. summarized the three ways of controlling the bond formation barrier (Quillin et al., 1995). First, the movement of the proximal histidine to the plane of the heme regulates the geminate recombination (Rohlfs et al., 1988; Petrich et al., 1988, 1991; Gibson et al., 1989). The degree of the displacement of the heme iron from the heme plane can be estimated from the center frequency of the band III. This band has been assigned to the charge transfer transition of $a_{2u} \rightarrow d_{xy}$, porphyrin to the heme iron (Eaton et al., 1978; Eaton & Hofrichter, 1981) and the increased transition energy would cause band III to shift to the blue. This band was little affected by the mutation at Thr67 (Figure 7), compared with other distal mutants (Christian et al., 1997; Uchida et al., 1997) and the differences in the band III of the three mutants were small (Table IV). This indicates that the effects of the movement of the proximal histidine to the heme on lowering the bond formation barrier of the T67D and T67N are small (Figure 8). Second, inhibition of the movement of the dissociated ligand increases the geminate rebinding (Gibson et al., 1992; Quillin et al., 1995). Insertion of the sterically hindered side chains into the heme pocket drastically increased the geminate yield, such as Val68→Phe (Quillin et al., 1995) and Leu29→Phe (Gibson et al., 1992). Since Thr67 is located in the opposite site to the movement of the photodissociated CO (Schlichting et al., 1994; Teng et al., 1994; Hartmann et al., 1996; Srajer et al., 1996), Thr67 cannot directly inhibit the movement of the dissociated ligand (Phillips, 1980). In addition, Thr67 mutation caused no structural changes which induce the inhibition of the ligand movement in the heme pocket, considering the ^{1}H NMR spectra (Nagano et al., to be submitted). These indicate that the inhibition of the movement of the dissociated ligand is not a factor for the increase in bond formation rate of the T67N and T67D mutants. Third, sterical restriction next to the heme iron inhibits the geminate recombination. The removal of the heme contact side chain by Val68→Ala mutant significantly increased the geminate recombination (Lambright et al., 1994). The signals of the side chain of Val68 were not affected by the Thr67 mutation in the ^{1}H NMR spectra (Nagano et al., to be submitted), indicating that the heme environmental structure are essentially the same as those found in wild type. It is concluded that the sterical restriction by Val68 cannot be a

factor which contributes to the increase in the geminate recombination of the T67N and T67D mutants. The previous proposed factors are not the case for the decrease in the kinetic barrier for the bond formation in the T67N and T67D mutants (Figure 8). These results raise the possibility of regulation of the inner kinetic barrier by the electrostatic and/or steric interactions between the distal histidine and side chain at position 67 .

The time resolved x-ray crystal structure of carbonmonoxy myoglobin photoproduct revealed that the distal histidine is displaced toward the outside of the heme pocket on photolysis (Schlichting et al., 1994; Srajer et al., 1996). Although photolyzed CO moves to the docking site surrounded by residues Ile107, Val68, and Leu29, which is opposite to the distal histidine, the geometry of the distal histidine is altered with the CO dissociation from the heme iron. It has been suggested that Thr67 and a water molecule which is located between the distal histidine and Thr67 are connected to the flexibility of the distal histidine (Johnson et al., 1989). The flexibility for the displacement of the distal histidine would be attributed to the inner kinetics barrier through the electrostatic interaction between the distal histidine and amino acid at E10. Since the side chain at position 67 interact with the distal histidine in the T67N and T67D mutants (schemes 3 and 4), these interactions may reduce the flexibility of the distal histidine and sterically inhibit photolyzed ligand movement into the ligand docking site, which increased the geminate yield of ligand binding in the T67N and T67D mutants.

In summary, IR spectra and kinetic results of the isosteric mutant T67V showed that the polarity of Thr67 does not affect the heme environmental structure and ligand binding kinetics. On the contrary, Thr67→Asn and Asp mutants changed the polarity of the heme pocket revealed by IR spectra of carbonmonoxy forms. Furthermore, kinetic analysis of CO and O_2 binding in the T67N and T67D mutants showed the alternation of the kinetic barrier. These results suggested that the electrostatic and steric interaction between the distal histidine and Asn67 or Asp67. Although wild type myoglobin has little interaction between the distal histidine and Thr67, a larger and polar side chain at E10 would interact with the distal histidine and change hydrophobicity of the heme pocket and ligand binding kinetics. This raises the possibility of regulation of the property in the distal histidine by mutation of the adjacent amino acid.

FOOTNOTES

[1] The abbreviations used are: Mb, myoglobin; WT, wild type.

[2] Alphanumeric codes (*e.g.* E10) refer to the position of the residue within the helices and loops of the myoglobin folding pattern. *i.e.* E7 denotes the 10th residue in the E helix.

[3] Varadarajan *et al.* (1989) replaced Cys110(G11) of human myoglobin by alanine to prevent difficulties in protein purification. In this study, we denote this mutant (Cys110 → Ala) of human myoglobin as "wild type".

REFERENCES

Adachi, S., & Morishima, I. (1989) *J. Biol. Chem. 264*, 18896-18901.

Adachi, S., Sunohara, N., Ishimori, K., & Morishima, I. (1992) *J. Biol. Chem. 267*, 12614-12621.

Ansari, A., Berendzen, J., Braunstein, D., Cowen, B. R., Frauenfelder, H., Hong, M. K., Iben, I. E. T., Johnson, E. T., Ormos, P., Sauke, T. B., Scholl, R., Schulte, A., Steinbach, P. J., Vittitow, P. J., & Young, R. D. (1987) *Biophys. Chem. 26*, 337-355.

Antonini, E., & Brunori, M. (1971) *Hemoglobin and Myoglobin in Their Reactons with Ligands*, North Holland, Amsterdam.

Brancaccio, A., Cutruzzola', F., TravagliniAllocatelli, C., Brunori, M., Smerdon, S. J., Wilkinson, A. J., Dou, Y., Keenan, D., Ikeda-Saito, M., Brantley, R. E., & Olson, J. S. (1994) *J. Biol. Chem. 269*, 13843-13853.

Cameron, A. D., Smerdon, S. J., Wilkinson, A. J., Habash, J., Helliwell, J. R., Li, T., & Olson, J. S. (1993) *Biochemistry 32*, 13061-13070.

Christian, J. F., Unno, M., Sage, J. T., Champion, P. M., Chien, E., & Sligar, S. G. (1997) *Biochemistry 36*, 11198-11204.

Decatur, S. M., & Boxer, S. G. (1995) *Biochem. Biophys. Res. Commun. 212*, 159-164.

Dou, Y., Olson, J. S., Wilkinson, A. J., & Ikedasaito, M. (1996) *Biochemistry 35*, 7107-7113.

Eaton, W. A., Hanson, L. K., Stephens, P. J., Sutherland, J. C., & Dunn, J. B. R. (1978) *J. Am. Chem. Soc. 100*, 4991-5003.

Eaton, W. A., & Hofrichter, J. (1981) *Methods Enzymol. 76*, 175-261.

Edwards, S. L., Raag, R., Waruushu, H., Gold, M. H., & Poulos, T. L. (1993) *Proc. Natl. Acad. Sci. U.S.A. 90*.

Finzel, B. C., Poulos, T., & Kraut, J. (1984) *J. Biol. Chem. 259*, 13027-13036.

Fronticelli, C., Bringar, W. S., Olson, J. S., Bucci, E., Gryczynski, Z., O'Donnell, J. K., & Kowalczyk, J. (1993) *Biochemistry 32*, 1235-1242.

Fukuyama, K., Kunishima, N., Amada, F., Kubota, T., & Matsubara, H. (1995) *J. Biol. Chem. 270*, 21884-21892.

Gibson, Q. H., Olson, J. S., McKinnie, R. E., & Rohlfs, R. J. (1986) *J. Biol. Chem. 261*, 10228-10239.

Gibson, Q. H. (1989) *J. Biol. Chem 264*, 20155-20158.

Gibson, Q. H., Regan, R. R., Elber, R., Olson, J. S., & Carver, T. E. (1992) *J. Biol. Chem. 267*, 22022-22034.

Hartmann, H., Zinser, S., Komninos, P., Schneider, R. T., Nienhaus, G. U., & Parak, F. (1996) *Proc. Natl. Acad. Sci. U.S.A. 93*, 7013-7016.

Henry, E. R., Sommer, J. H., Hofrichter, J., & Eaton, W. A. (1983) *J. Mol. Biol. 166*, 443-451.

Jackson, T. A., Lim, M., & Anfinrud, P. A. (1994) *Chem. Phys. 180*, 131-140.

Jewsbury, P., & Kitagawa, T. (1994) *Biophys. J. 67*, 2236-2250.

Johnson, K. A., Olson, J. S., & Phillips Jr., G. N. (1989) *J. Mol. Biol. 207*, 459-463.

Kunkel, T. A. (1985) *Proc. Natl. Acad. Sci. U.S.A. 82*, 488-492.

Kunishima, N., Fukuyama, K., Matsubara, H., Hatanaka, H., Shibano, Y., & Amachi, T. (1994) *J. Mol. Biol. 235*, 331-344.

Lambright, D. G., Balasubramanian, S., & Boxer, S. G. (1989) *J. Mol. Biol. 207*, 289-299.

Lambright, D. G., Balasubramanian, S., Decatur, S. M., & Boxer, S. G. (1994) *Biochemistry 33*, 5518-5525.

Lim, M., Jackson, T. A., & Anfinrud, P. A. (1993) *Proc. Natl. Acad. Sci. U.S.A. 90*, 5801-5804.

Li, T., Quillin, M. L., Phillips Jr., G. N., & Olson, J. S. (1994) *Biochemistry 33*, 1433-1446.

Morikis, D., Champion, P. M., Springer, B. A., & Sligar, S. G. (1989) *Biochemistry 28*, 4791-4800.

Nagano, S., Tanaka, M., Ishomori, K., Watanabe, Y., & Morishima, I. (1996) *Biochemistry 35*, 14251-14258.

Oldfield, E., Guo, K., Augspurger, J. D., & Dykstra, C. E. (1991) *J. Am. Chem. Soc. 113*, 7537-7541.

Olson, J. S., Mathews, A. J., Rohlfs, R. J., Springer, B. A., Egeberg, K. D., Sligar, S. G., Tame, J., Renaud, J.-P., & Nagai, K. (1988) *Nature 336*, 265-266.

Olson, J. S., & Phillips Jr, G. N. (1996) *J. Biol. Chem. 271*, 17593-17596.

Olson, J. S., & Phillips Jr, G. N. (1997) *J. Biol. Inorg. Chem 2*, 544-552.

Patterson, W. R., & Poulos, T. L. (1995) *Biochemistry 34*, 4331-4341.

Petersen, J. F. W., Kadziola, A., & Larsen, S. (1994) *FEBS Lett. 339*, 291-296.

Petrich, J. W., Poyart, C., & Martin, J. L. (1988) *Biochemistry 27*, 4049-4060.

Petrich, J. W., Lambry, J.-C., Kuczera, K., Karplus, M., Poyart, C., & Martin, J.-L. (1991) *Biochemistry 30*, 3975-3987.

Phillips, S. E. V. (1980) *J. Mol. Biol. 142*, 531-554.

Poulos, T. L., & Kraut, J. (1980) *J. Biol. Chem. 255*, 8199-8205.

Poulos, T. L., Edwards, S. L., Wariishi, H., & Gold, M. H. (1993) *J. Biol. Chem. 268*, 4429-4440.

Quillin, M. L., Arduini, R. M., Olson, J. S., & Phillips Jr., G. N. (1993) *J. Mol. Biol. 234*, 140-155.

Quillin, M. L., Li, T. S., Olson, J. S., Phillips Jr, G. N., Dou, Y., Ikeda-Saito, M., Regan, R., Carlson, M., Gibson, Q. H., Li, H. Y., & Elber, R. (1995) *J. Mol. Biol. 245*, 416-436.

Ray, G. B., Li, X.-Y., Ibers, J. A., Sessler, J. L., & Spiro, T. G. (1994) *J. Am. Chem. Soc. 116*, 162-176.

Rohlfs, R. J., Olson, J. S., & Gibson, Q. H. (1988) *J. Biol. Chem. 263*, 1803-1813.

Rohlfs, R. J., Mathews, A. J., Carver, T. E., Olson, J. S., Springer, B. A., Egeberg, K. D., & Sligar, S. G. (1990) *J. Biol. Chem. 265*, 3168-3176.

Schlichting, I., Berendzen, J., Phillips, G. N., & Sweet, R. M. (1994) *Nature 371*, 808-812.

Smerdon, S. J., Dodson, G. G., Wilkinson, A. J., Gibson, Q. H., Blackmore, R. S., Carver, T. E., & Olson, J. S. (1991) *Biochemistry 30*, 6252-6260.

Smerdon, S. J., Krzywda, S., Brzozowski, A. M., Davies, G. J., Wilkinson, A. J., Brancaccio, A., Cutruzzola', F., TravagliniAllocatelli, C., Brunori, M., Li, T. S., Brantley, R. E., Carver, T. E., Eich, R. F., Singleton, E., & Olson, J. S. (1995) *Biochemistry 34*, 8715-8725.

Sommer, J. H., Henry, E. R., & Hofrichter, J. (1985) *Biochemistry 24*, 7380-7388.

Springer, B. A., Sligar, S. G., Olson, J. S., & Phillips Jr., G. N. (1994) *Chem. Rev. 94*, 699-714.

Srajer, V., Teng, T. Y., Ursby, T., Pradervand, C., Ren, Z., Adachi, S., Schildkamp, W., Bourgeois, D., Wulff, M., & Moffat, K. (1996) *Science 274*, 1726-1729.

Sundaramoorthy, M., Choudhury, K., Edwards, S. L., & Poulos, T. L. (1994) *J. Am. Chem. Soc. 113*, 7755-7757.

Teng, T. Y., Srajer, V., & Moffat, K. (1994) *Nature Struct. Biol. 1*, 701-705.

Uchida, T., Unno, M., Ishimori, K., & Morishima, I. (1997) *J. Biol. Chem.* *272*, 30108-30114.

Varadarajan, R., Szabo, A., & Boxer, S. G. (1985) *Proc. Natl. Acad. Sci. U.S.A.* *82*, 5681-5684.

Varadarajan, R., Lambright, D. G., & Boxer, S. G. (1989) *Biochemistry* *28*, 3771-3781.

PART IV.

STRUCTURAL AND FUNCTIONAL INVESTIGATION OF A NOVEL HEME PROTEIN THAT ACT AS A TRANSCRIPTIONAL ACTIVATOR

CHAPTER 1.

Coordination Structure of CO to the Transcriptional Activator, CooA, Studied by Resonance Raman Spectroscopy and Ligand Binding Kinetics

ABSTRACT

CooA is the first example of heme proteins which act as a DNA-binding transcriptional activator. In order to investigate the gene activation mechanism triggered by the CO binding to CooA, the heme environmental structure and the dynamics of CO rebinding to CooA have been examined in the absence and presence of its target DNA. Resonance Raman spectra confirm that the heme iron of ferrous CooA is six-coordinated low-spin. One of the axial ligands in ferrous CooA is replaced by CO to form CO-bound CooA. In the absence of DNA, the Fe-CO and C=O stretching lines of the CO-bound CooA were observed at 487 and 1969 cm^{-1}, respectively, suggesting that a neutral histidine is an axial ligand trans to CO. The frequency of ν(Fe-CO) at 487 cm^{-1} implies an open conformation of the distal heme pocket, and suggests that the ligand replaced by CO is located away from the bound CO. When the target DNA was added to the CO-bound CooA, the appearance of a new ν(Fe-CO) line at 519 cm^{-1} and the narrowing of the main line at 486 cm^{-1} were observed. This alteration at the heme distal site is further substantiated by the observation that the CO rebinding was decelerated in the presence of the target DNA, but not in the presence of the nonsense DNA. Thus, the heme distal site of CooA changes its conformation drastically by the CO binding and is susceptible to the change of its DNA binding domain. These observations support the activation mechanism proposed for CooA, which is triggered by the movement of the heme distal ligand to modify the conformation of the DNA binding domain.

INTRODUCTION

CooA is one of the heme proteins which act as a DNA-binding transcriptional activator (Aono et al., 1996; Shelver et al., 1997). The purple, nonsulfur, phototrophic bacterium *Rhodospirillum rubrum* synthesizes a series of enzymes that oxidize carbon monoxide (CO^1) into carbon dioxide which is coupled to the evolution of molecular hydrogen (Bonam et al., 1989). Unlike other bacteria capable of oxidizing CO anaerobically, *R. rubrum* expresses the CO-oxidizing enzymes only in the presence of atmospheric CO (Kerby et al., 1995). A gene region designated as *cooA* was demonstrated to be responsible for the regulation, whose product protein, CooA, shows high homology with the known transcriptional regulators, such as cyclic AMP receptor protein (CRP) (28% identical, 51% similar) (Kerby et al., 1995). Like the mechanism of CRP activation by cyclic AMP, CO is assumed to bind with CooA (Bonam et al., 1989; Kerby et al., 1992, 1997; Fox et al., 1996; Shelver et al., 1997), which causes the protein-CO complex to bind specifically to the target DNA, resulting in the expression of CO oxidizing enzymes (He et al., 1996; Shelver et al., 1997).

CooA is a homodimer containing 222 amino acid residues in each subunit (Shelver et al., 1995, 1997). Recent success of high-level expression of CooA in *Escherichia coli* has enabled us and other researchers to obtain the homogeneous protein enough for spectroscopic investigations (Aono et al., 1996; Shelver et al., 1997). It was revealed that each subunit of CooA contains a single *b*-type heme as a prosthetic group, which can bind exogenous CO reversibly as is evidenced by its optical absorption spectra (Aono et al., 1996; Shelver et al., 1997). The significant homology between CooA and CRP suggests that CooA may consist of two domains, N-terminal effector binding domain and C-terminal DNA-binding domain containing the helix-turn-helix motif (McKay & Steitz, 1981; Weber & Steitz, 1984, 1987). Our recent mutagenesis work confirmed that the N-terminal region of CooA consisting of amino acid residues from Met1 to Met131 is the heme binding domain (Aono et al., 1997). Alteration at the heme center caused by the CO binding should be transmitted to the DNA-binding domain, which increases the association constant of CooA specifically with the target DNA. The molecular mechanism of this process remains to be elucidated and would be an important contribution to the understanding of the transcriptional activation in prokaryotes. The presence of heme makes CooA especially attractive to investigate using various spectroscopic methods.

The CO binding to the heme has special importance for the characterization of heme proteins. The vibrational frequencies of the Fe-CO unit detected by resonance Raman and infrared spectroscopies are used to characterize the axial ligand trans to the bound CO as well as the polarity of the distal heme pocket. The rebinding kinetics of CO after photodissociation from CO-bound hemes reflects the environment around the hemes. The characterization of CO-bound CooA is of special interest, since it is the CO-bound form of CooA that plays crucial and physiological role in its gene activation (Bonam et al., 1989; Shelver et al., 1995, 1997; Kerby et al., 1992, 1995, 1997; Fox et al., 1996; Aono et al., 1996), and provides a clue to elucidate the activation mechanism of CooA by CO. We have therefore undertaken the resonance Raman investigation on the CO-bound and reduced forms of CooA due to their physiological importance. CO rebinding kinetics of CooA was also determined by a laser photolysis method. It has been confirmed that the ferrous protein is in a six-coordinated form with two axial ligands, one of which is suggested to be a histidine. The addition of CO to the reduced protein causes the replacement of the other axial ligand by CO and creates the open distal pocket. The conformation of the distal heme site was modulated by the specific interaction with the target DNA. These results are consistent with the signal transduction mechanism proposed for CooA that the specific DNA binding is induced by the movement of the distal ligand triggered by the CO binding (Aono et al., 1996; Shelver et al., 1997).

EXPERIMENTAL PROCEDURES

The protein expression and preparation were performed as previously described (Aono et al., 1996, 1997). Reduced CooA was prepared by adding a slight excess of freshly prepared dithionite solution under argon atmosphere into the protein solution. CO-bound CooA was prepared by introducing gaseous CO into the reduced sample.

The resonance Raman spectra were obtained by excitation with 413.1 nm of a Kr^+ laser (Spectra Physics, Model 2016). The scattered light were dispersed with a single polychromator (Ritsu, DG-1000) equipped with a cooled CCD camera (Astromed, CCD3200). The spectral slit width was ca. 6 cm^{-1}. The sample solutions for Raman measurements were sealed in quartz cells which were rotated at ca. 1000 rpm at room temperature. Typically, the sample aliquots were 5 μM on the basis of heme content dissolved in 50 mM Tris/HCl buffer at pH 8.0. Raman shifts were

calibrated with indene and CCl_4 as standards to an accuracy of 1 cm^{-1} for intense isolated lines. Absorption spectra were measured both prior to and after Raman measurements, and no degradation was detected under the experimental condition applied in this study.

The kinetics of CO rebinding were obtained by a laser photolysis apparatus as previously described (Uchida et al., 1997). The absorption changes were monitored at 420 nm using a photomultiplier (Hamamatsu, R2949) and digitized by a storage oscilloscope (Tektronix, TDS-520A). The sample solution was the same as that used for Raman measurements.

A representative DNA sequence recognized by CooA is as follows (He et al., 1996),

5' AACTGTCATCTGGCCGACAGACGGGGCC

TTGACAGTAGACCGGCTGTCTGCCCCGG 5'

The two strands of the purified 28mer oligonucleotides were purchased from Takara and used without further purification. The two strands were annealed at room temperature for about 3 hours after heating for five minutes at 80 °C. Nonsense DNA of 34 mer double-stranded oligonucleotides was prepared by the same method. Resonance Raman spectra and CO rebinding kinetics of the DNA bound CooA were measured after incubating the protein solution with the DNA at room temperature for more than 30 min.

RESULTS AND DISCUSSION

The high frequency resonance Raman spectra (1200-1700 cm^{-1}) of the dithionite-reduced (*spectrum* A), and CO-bound (*spectrum* B) forms of CooA are presented in Figure. 1 and the observed frequencies of the major lines are compared to those of cytochrome *c* (Hu et al., 1993), cytochrome *c* with Met80-Cys mutation (Smulevich et al., 1994), cytochrome b_5 and myoglobin (Mb) (Takahashi et al., 1994) in Table I. It is established that the lines in the high-frequency region can be used as sensitive markers of the oxidation state (ν_4) and spin and coordination states (ν_2 and ν_3) of the heme iron (Spiro & Li, 1988). The polarized lines at 1579 and 1491 cm^{-1} observed for the dithionite-reduced form can be assigned to ν_2 and ν_3, respectively (polarization data not shown), whose frequencies indicate that the heme iron is six-coordinate low-spin as found for cytochrome b_5. As we will discuss later, the CO-bound CooA has a histidine as a fifth ligand, which should also be one of axial ligands in the reduced protein. The similarity of the frequencies of marker bands between ferrous CooA and

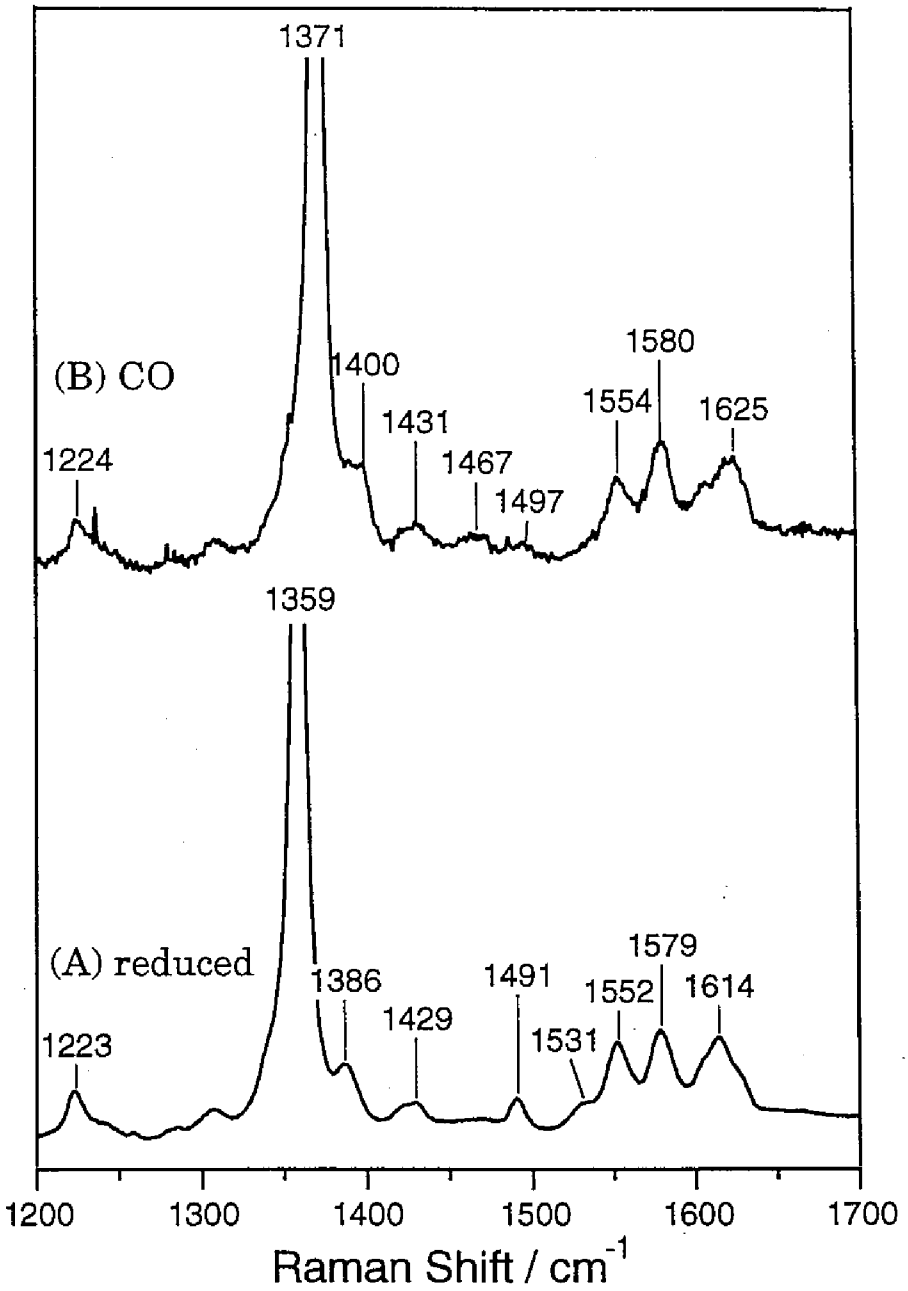

Figure 1. The high-frequency resonance Raman spectra of CooA in the dithionite-reduced (A) and CO-bound (B) states.

cytochrome b_5 suggests that the other ligand is neutral, such as histidine, methionine and lysine. Coordination of methionine or cysteine can be probably excluded, since the frequency of ν_2 usually appears at around 1590 cm^{-1} for His/Met or His/Cys ligand pairs, 10 cm^{-1} higher than that for CooA (Hu et al., 1993; Lou, et al., 1993; Smulevich et al., 1994). Furthermore, the absorption maxima of the Soret, α- and β- bands for ferrous CooA are 425, 559 and 529 nm, respectively (Aono et al., 1996), which are different from those of cytochrome *c* (414, 550 and 522 nm)

(Wallace & Clark-Lewis, 1992) or imidazole-bound cytochrome P450 (445, 566 and 538 nm) (Dawson et al., 1983).

Table I: Frequencies of Raman Lines from the Ferrous and CO-bound Forms of CooA, Cytochrome *c*, Cytochrome b_5 and Myoglobin (in cm^{-1}).

Protein	ν_2	ν_3	ν_4	ν(Fe-C)	ν(C=O)	Ref.
CooA (Fe^{2+})	1579	1491	1359			*a*
CooA-CO	1580	ND[b]	1371	487	1969	*a*
Cytochrome *c* (Fe^{2+})	1592	1489	1363			*c*
Cytochrome *c* M80C (Fe^{2+})	1592	1494	1360			*d*
Cytochrome b_5 (Fe^{2+})	1583	1493	1360			*e*
Myoglobin (Fe^{2+})	1564	1473	1356			*f*
Myoglobin-CO	1585	1501	1373	507	1945	*f*

[a] this work. [b] ND, not detected. [c] Hu et al., 1993. [d] Smulevich et al., 1994. [e] Shiro et al., private communication. [f] Takahashi et al., 1994

The addition of CO to the reduced CooA forms a stable CooA-CO complex, which is indicated by a strong Soret absorption band at 422 nm (Aono et al., 1996; Shelver et al., 1997). The resonance Raman spectrum for the CooA-CO complex (*spectrum* B, Figure 1) is characteristic of a low spin six-coordinated heme and resembles that of Mb-CO. The frequency of the ν_2 mode is located at 1580 cm^{-1}, showing a slight low frequency shift compared to that of Mb-CO at 1585 cm^{-1}. The observation suggests that the porphyrin core of CooA-CO is slightly expanded compared to that of Mb-CO, since the ν_2 frequency is linearly correlated with the distance between the porphyrin center and its pyrrole nitrogen atom (Choi et al., 1982; Spiro & Li, 1988). Figure 2 shows resonance Raman spectra in the Fe-CO stretching and the C=O stretching frequency regions of the natural abundance (*spectrum* A) and ^{13}CO-labeled CO (*spectrum* B) adducts of CooA. A line at 487 cm^{-1} can be assigned to the stretching mode of Fe-CO, ν(Fe-CO), on account of its 4 cm^{-1} low-frequency shift upon $^{13}C\,O$ substitution. The C=O stretching frequency, ν(C=O), appeared at 1969 cm^{-1} for natural abundance CO and at 1927 cm^{-1} for ^{13}CO. There is a well-known inverse correlation between the frequencies of Fe-CO and C=O stretching modes (Li & Spiro, 1988; Yu & Kerr, 1988; Oldfield et al., 1991), which is explained by the different contribution of the electron back-donation from Fe($d\pi$) to CO(π^*) orbitals on the Fe-CO bond. As the back-donation increases, the Fe-C bond is strengthened and the C=O bond is

donation increases, the Fe-C bond is strengthened and the C=O bond is weakened. Since the σ-character of the Fe-CO bond controls ν(Fe-CO) exclusively, depending on the σ-basicity of the proximal ligand, the points (ν(Fe-CO) and ν(C=O)) for proteins possessing a similar proximal ligand fall on the same correlation line. Thus, the correlation between ν(Fe-CO) and ν(C=O) can be used to identify the strength of the proximal ligand. The frequencies measured for CooA-CO fall on the line composed by heme proteins with neutral histidine as a proximal ligand (correlation plot not shown). This result as well as the appearance of the Soret absorption maximum at 422 nm provide evidences that the heme iron in CO-bound CooA ligates to a histidine.

The vibrational frequency of ν(Fe-CO) displays a wide range of frequencies (450-550 cm^{-1}) reflecting the polarity of the distal heme pocket (Uno et al., 1987; Li & Spiro, 1988; Morikis et al., 1989; Oldfield et al., 1991; Park et al., 1991; Ray et al., 1994; Li et al., 1994). The isolated Fe-CO unit as is observed for model compounds and for Mb-CO in the acidic solution shows frequencies at ~490 and ~1965 cm^{-1} for ν(Fe-CO) and ν(C=O), respectively, and is labeled as the A_0 conformer in Mb (Morikis et al., 1989). It is considered that the distal His swings out of the heme pocket in the acidic Mb (Morikis et al., 1989; Ray et al., 1994; Li et al., 1994; Yang & Phillips, 1996). The appearances of the ν(Fe-CO) and ν(C=O) lines at 487

and 1969 cm^{-1}, respectively, for the CO bound CooA demonstrate that the Fe-CO unit has the conformation similar to the A_0 conformer of Mb. This observation indicates the absence of any significant interaction between the bound CO and the distal heme pocket, that is, the absence of the distal histidine or any positively and sterically interacting residues around the iron-bound CO. Since ferrous CooA has a six-coordinated iron, CO should replace one of the axial ligands to form CO-bound CooA. The replaced ligand, whose identity has not been specified, moves away and affords no interaction with the bound CO. The absence of the distal ligands that interact with CO is consistent with the observation that the stable oxygen bound CooA is not formed (Aono et al., 1996), because the interaction with the positively charged residue would stabilize the iron-bound oxygen. In the spectrum A of Figure 3, Fe-C-O bending mode, δ(Fe-C-O), was not observed. The low intensity of δ(Fe-C-O) is characteristic of heme proteins with an unconstrained heme pocket (Yu & Kerr, 1988), further supporting the open conformer of the CO-bound CooA.

Figure 3 depicts the RR spectra of natural abundance (*spectrum* B) and $^{13}C^{18}O$-labeled (*spectrum* C) CO-bound CooA in the presence of the

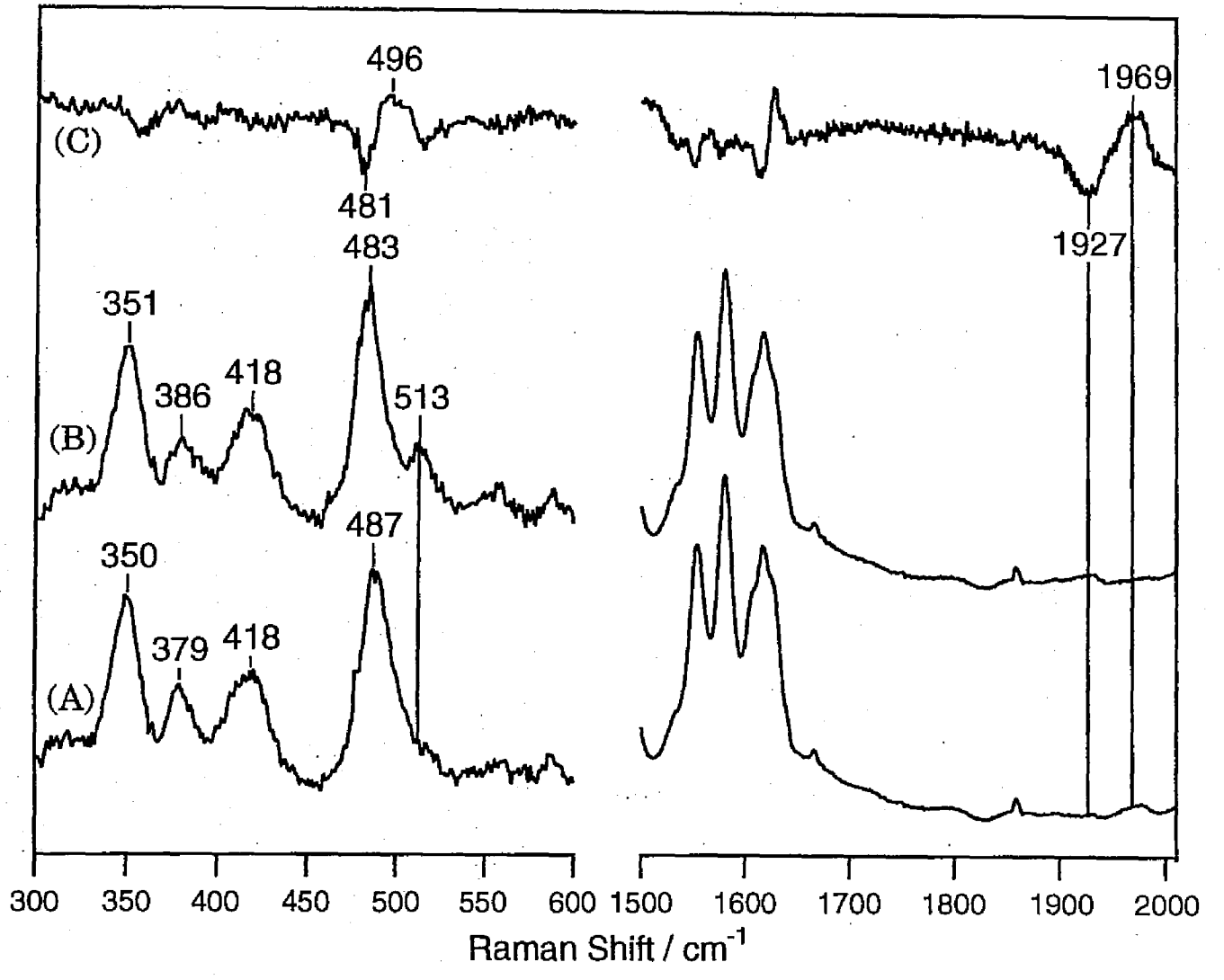

Figure 2. Resonance Raman spectra of CooA in the CO-bound state. (A) $^{12}C^{16}O$-bound and (B) $^{13}C^{16}O$-bound CooA in the absence of the target DNA; (C) difference spectrum between traces A and B.

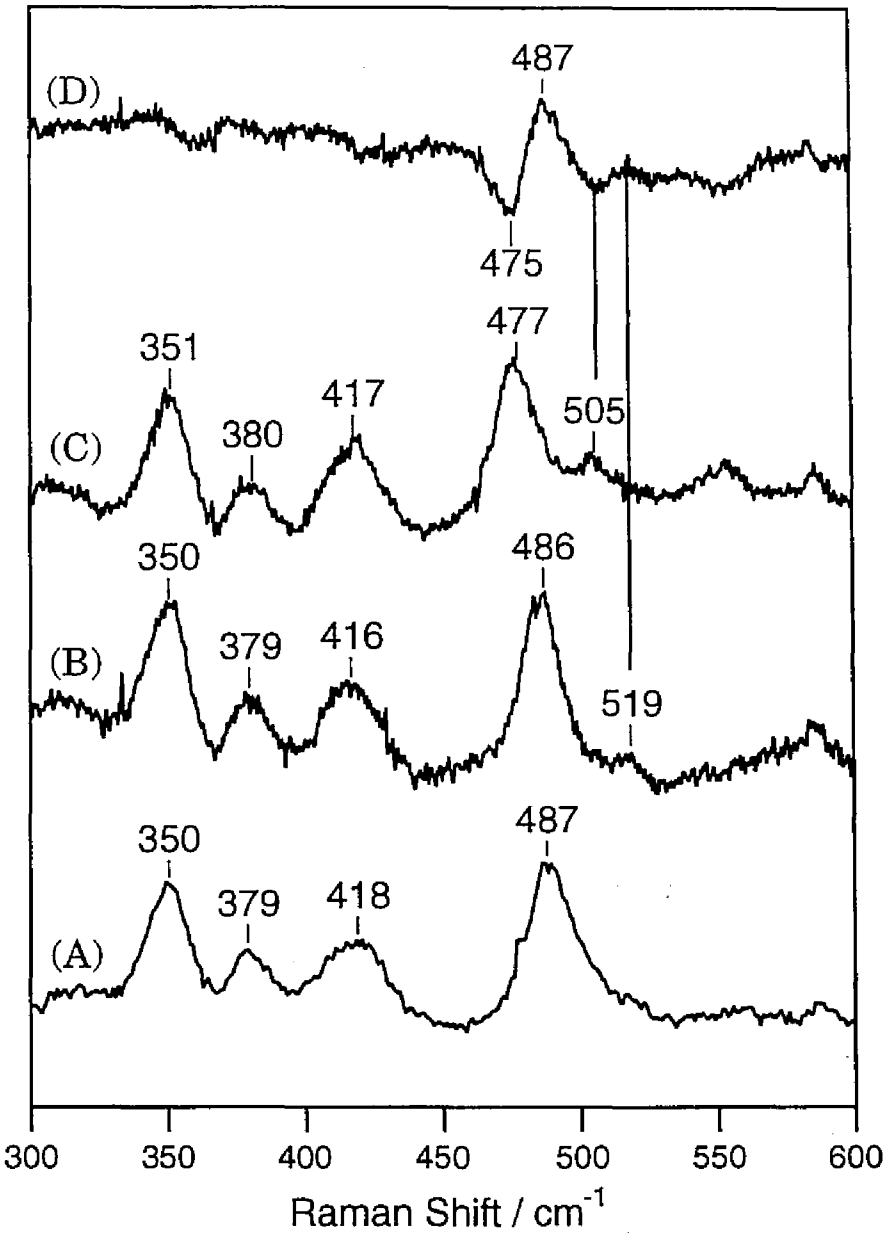

Figure 3. Effect of the target DNA binding on the Resonance Raman spectra of CooA in the CO-bound state. (A) $^{12}C^{16}O$-bound CooA in the absence of the target DNA; (B) $^{12}C^{16}O$-bound and (C) $^{13}C^{18}O$-bound CooA in the presence of the target DNA; (D) difference spectrum between traces B and C.

target DNA. Comparing with the spectrum obtained in the absence of DNA (*spectrum* A), the addition of 20 equiv. of the target DNA per monomeric CooA results in the narrowing of the major ν(Fe-CO) line at 486 cm^{-1} (from 20 to 15 cm^{-1} measured as full widths at half heights) concomitant with the appearance of a weak line at 519 cm^{-1}. Both of the lines are assigned as Fe-CO stretching modes, because the isotopic shifts

for both lines are observed (*spectrum* D)[2]. The frequency at 519 cm^{-1} corresponds to the A_3 conformer of Mb-CO (Morikis et al., 1989). Thus, the binding of the target DNA causes the decrease in the A_0 conformer along with the appearance of the A_3 conformer. Although some controversy exists on the interpretation of the A_3 conformer (Oldfield et al., 1991; Park et al., 1991; Li et al., 1994), it is considered that a strong hydrogen bonding would increase the back-donation and enhance the Fe-C stretching frequency to ~520 cm^{-1} (Jewsbury & Kitagawa, 1994). These observations demonstrate that the specific DNA binding causes the structural change around the distal heme environment which increases the polar interaction with the bound CO. This is the first experimental observation that shows the structural link between the distal heme site and DNA binding domain of CooA.The kinetics of CO recombination to ferrous CooA after the photolysis of CO in the presence and absence of the target DNA are illustrated in Figure 4. The observed dynamics is complex and consists of at least three exponential decays. The transient spectra after the photodissociation show that CO binds to a five-coordinated heme produced by the laser photolysis (data not shown). The observed heterogeneity, hence, suggests the presence of conformational transitions that compete with the CO rebinding within the five-coordinated protein. The conformational transition between the activated and inactivated forms and/or the allosteric interaction between the two subunits are possibly responsible for the observed heterogeneity. Addition of the target DNA decelerated the CO association (*trace* B), while addition of nonsense DNA showed exactly the same kinetic trace (*trace* C) as that in the absence of DNA (*trace* A). The DNA titration experiment shows that the change reached a maximum with the 10 equiv. of the target DNA per monomeric CooA (data not shown). The slow CO association demonstrates that the CO binding site is more crowded in the conformer which is bound to the DNA, and is consistent with the observed conformational transition of Fe-CO unit in the presence of the DNA.

It is proposed that the activation of CooA as the transcriptional activator is induced by the displacement of the distal ligand by CO which in turn modifies the conformation of the DNA binding domain (Aono et al., 1996; Shelver et al., 1997). The present resonance Raman and kinetic data afford the first experimental observation that supports the proposed mechanism. First, the Fe-CO and C=O stretching frequencies were observed at 487 cm^{-1} and 1969 cm^{-1}, respectively, for CO-bound CooA in the absence of DNA. These frequencies show the absence of polar or steric

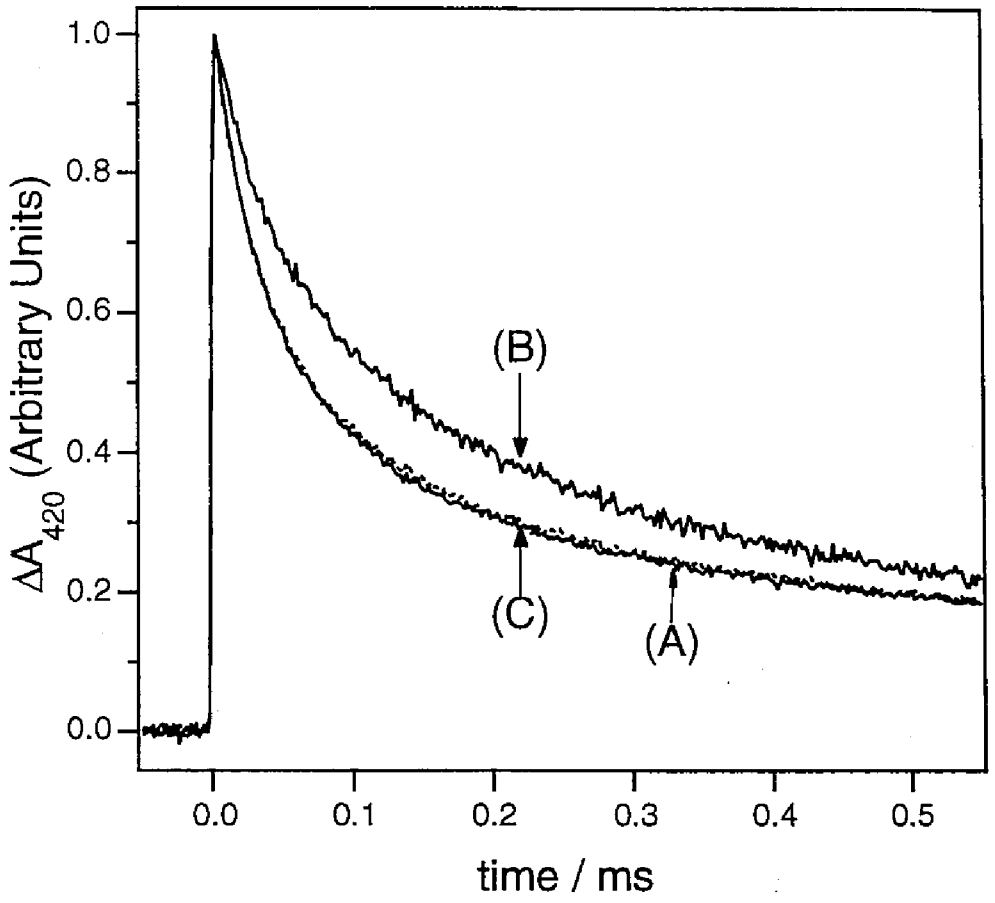

Figure 4. Time courses for the CO rebinding to CooA following laser photolysis in the absence (A) and presence (B) of the target DNA. (C) The time course observed in the presence of nonsense DNA. Traces A and C overlap each other. Ordinate scales are normalized.

interaction between the distal residues and the bound-CO, implicating that the distal ligand in the ferrous form is replaced by CO with a rather large conformational transition by the CO binding. Secondly, the structure of the heme distal site of CooA-CO is susceptible to the conformational transition at the DNA binding domain, which is evidenced by the changes in the ν(Fe-CO) as well as in the ligand binding kinetics caused by the addition of the target DNA. This suggests that the structural alteration around the heme distal site can be efficiently transmitted to the DNA-binding domain of CooA. A conformational change of CRP has been demonstrated to be induced by the cAMP binding which includes the reorganization of its secondary structure (DeGrazia et al., 1990; Baichoo & Heyduk, 1997). The CRP-cAMP dimer also shows a conformational change by the DNA binding (Schultz et al., 1991). The

present findings on CooA thus resemble very much the features reported for CRP.

It is interesting to compare the coordination structure of CooA with those of soluble guanylate cyclase (Ignarro et al., 1982) and FixL (Gilles-Gonzalez et al., 1991). Soluble guanylate cyclase detects NO at the five-coordinated heme, and the binding of NO to the heme causes a break of the trans Fe-His bond (Yu et al., 1994, Stone & Marletta, 1994). FixL detects also O_2 at the sixth open position of the heme (Gilles-Gonzalez et al., 1994, 1995; Tamura et al., 1996). On the contrary, CooA detects CO at the six-coordinate heme. This is an unique feature of CooA, since no hemeproteins having six-coordinated hemes have been reported to have an exogenous ligand binding properties at the physiological condition. One of the axial ligands is shown to be a histidine from the current spectroscopic results, which can be compared to the recent mutagenesis studies demonstrating His77 as a possible candidate for the ligand (Shelver et al., 1997, Aono et al., submitted). Further spectroscopic investigation combined with the site-directed mutagenesis is in progress to clarify the other axial ligand as well as the mechanism of the signal transduction between the heme binding and DNA binding domains of CooA.

FOOTNOTES

[1] The abbreviations used are: CO, carbon monoxide; CRP, cyclic AMP receptor protein; Mb, myoglobin.

[2] We could not detect the C=O stretching line in the presence of the DNA due to its fluorescence background.

REFERENCES

Aono, S., Nakajima, H., Saito, K., & Okada, M. (1996) *Biochem. Biophys. Res. Commun. 228*, 752-756.

Aono, S., Matsuo, T., Shimono, T., Ohkubo, K., Takasaki, H., & Nakajima, H. (1997) *Biochem. Biophys. Res. Commun.*

Baichoo, N., & Heyduk, T. (1997) *Biochemistry 36*, 10830-10836.

Bonam, D., Lehman, L., Roberts, G. P., & Ludden, P. W. (1989) *J. Bacteriol. 171*, 3102-3107.

Choi, S., Spiro, T. G., Langry, K. C., Budd, D. L., & LaMar, G. N. (1982) *J. Am. Chem. Soc. 104*, 4345-4351.

Dawson, J. H., Andersson, L. A., & Sono, M. (1983) *J. Biol. Chem. 258*, 13637-13645.

DeGrazia, H., Harman, J. G., Tan, G. S., & Wartell, R. M. (1990) *Biochemistry 29*, 3557-3562.

Fox, J. D., He, Y., Kerby, R. L., Ludden, P. W., & Roberts, G. P. (1996) *J. Bacteriol. 178*, 6200-6208.

Fox, J. D., Kerby, R. L., Ludden, P. W., & Roberts, G. P. (1996) *J. Bacteriol. 178*, 1515-1524.

Gilles-Gonzalez, M. A., Gonzalez, G., & Helinski, D. R. (1991) *Nature 350*, 170-172.

Gilles-Gonzalez, M. A., Gonzalez, G., & Perutz, M. F. (1995) *Biochemistry 34*, 232-236.

Gilles-Gonzalez, M. A., Gonzalez, G., Perutz, M. F., Kiger, L., Marden, M. C., & Poyart, C. (1994) *Biochemistry 33*, 8067-8073.

He, Y., Shelver, D., Kerby, R. L., & Roberts, G. P. (1996) *J. Biol. Chem. 271*, 120-123.

Hu, S. Z., Morris, I. K., Singh, J. P., Smith, K. M., & Spiro, T. G. (1993) *J. Am. Chem. Soc. 115*, 12446-12458.

Ignarro, L. J., Degnan, J. N., Baricos, W. H., Kadowitz, P. J., & Wolin, M. S. (1982) *Biochim. Biophys. Acta. 718*, 49-59.

Jewsbury, P., & Kitagawa, T. (1994) *Biophys. J. 67*, 2236-2250.

Kerby, R. L., Hong, S. S., Ensign, S. A., Coppoc, L. J., Ludden, P. W., & Roberts, G. P. (1992) *J. Bacteriol. 174*, 5284-5294.

Kerby, R. L., Ludden, P. W., & Roberts, G. P. (1995) *J. Bacteriol. 174*, 5284-5294.

Kerby, R. L., Ludden, P. W., & Roberts, G. P. (1997) *J. Bacteriol. 179*, 2259-2266.

Li, X.-Y., & Spiro, T. G. (1988) *J. Am. Chem. Soc. 110*, 6024-2033.

Li, W., & Palmer, G. (1993) *Biochemistry 32*, 1833-1843.

Lou, B.-S., Hobbs, J. D., Chen, Y.-R., Yu, L., Yu, C. A., & Ondrias, M. R. (1993) *Biochim. Biophys. Acta. 1144*, 403-410.

McKay, D. B., & Steitz, T. A. (1981) *Nature 290*, 744-749.

Morikis, D., Champion, P. M., Springer, B. A., & Sligar, S. G. (1989) *Biochemistry 28*, 4791-4800.

Oldfield, E., Guo, K., Augspurger, J. D., & Dykstra, C. E. (1991) *J. Am. Chem. Soc. 113*, 7537-7541.

Park, K. D., Guo, K., Adeboun, F., Chiu, M. L., Sligar, S. G., & Oldfield, E. (1991) *Biochemistry 30*, 2333-2347.

Ray, G. B., Li, X.-Y., Ibers, J. A., Sessler, J. L., & Spiro, T. G. (1994) *J. Am. Chem. Soc. 116*, 162-176.

Schultz, S. C., Shields, G. C., & Steitz, T. A. (1991) *Science 253*, 1001-1007.

Shelver, D., Kerby, R. L., He, Y., & Roberts, G. P. (1995) *J. Bacteriol. 177*, 2157-2163.

Shelver, D., Kerby, R. L., He, Y., & Roberts, G. P. (1997) *Proc. Natl. Acad. Sci. U.S.A. 94*, 11216-11220.

Smulevich, G., Bjerrum, M. J., Gray, H. B., & Spiro, T. G. (1994) *Inorg. Chem. 33*, 4629-4634.

Spiro, T. G., & Li, X.-Y. (1988) *Biological Application of Raman Spectroscopy*, Wiley, New York.

Stone, J. R., & Marletta, M. A. (1994) *Biochemistry 33*, 5636-5640.

Takahashi, S., Wang, J., Rousseau, D. L., Ishikawa, K., Yoshida, T., Takeuchi, N., & Ikeda-Saito, M. (1994) *Biochemistry 33*, 5531-5538.

Tamura, K., Nakamura, H., Tanaka, Y., Oue, S., Tsukamoto, K., Nomura, M., Tsuchiya, T., Adachi, S., Takahashi, S., Iizuka, T., & Shiro, Y. (1996) *J. Am. Chem. Soc. 118*, 9434-9435.

Uchida, T., Unno, M., Ishimori, K., & Morishima, I. (1997) *J. Biol. Chem. 272*, 30108-30114.

Uno, T., Nishimura, Y., Tsuboi, M., Makino, R., Isizuka, T., & Ishimura, Y. (1987) *J. Biol. Chem. 262*, 4549-4556.

Wallace, C. J. A., & Clark-Lewis, I. (1992) *J. Biol. Chem. 267*, 3852-3861.

Weber, I. T., & Steitz, T. A. (1984) *Proc. Natl. Acad. Sci. U.S.A. 81*, 3973.

Weber, I. T., & Steitz, T. A. (1987) *J. Mol. Biol. 198*, 311-326.

Yang, F., & Phillips Jr, G. N. (1996) *J. Mol. Biol. 256*, 762-774.

Yu, N.-T., & Kerr, E. A. (1988) *Biological Applications of Raman Spectroscopy*, Vol. III, John Wiley & Sons, New York.

Yu, A. E., Hu, S., Spiro, T. G., & Burstyn, J. M. (1994) *J. Am. Chem. Soc. 116*, 4117-4118.

CHAPTER 2.

A Kinetic Study of CO Binding to a CO-sensing Transcriptional Activator, CooA by Flash Photolysis

ABSTRACT

The carbon monoxide binding mechanism to ferrous CooA was investigated using stopped flow and laser photolysis methods. The overall CO association reaction to ferrous CooA by rapid mixing of ferrous CooA with CO is monophasic and depends on CO concentration. The CO association rate constant was 0.036 $m^{-1}M^{-1}$. Time-resolved transient difference spectra of this reaction showed an clear isosbestic point at 420 nm at a 100 ms resolution, indicating that no intermediates are involved in the CO association reaction. This implies that the five-coordinated heme produced by release of the axial ligand is substantially unstable to detect. The instability of the five-coordinated heme was also supported by the quite large geminate yield (~0.5) and fast geminate rate constants (~100 μs^{-1}) for CO rebinding after photolysis. The instability of the five-coordinated heme may be attributed to the crowded heme pocket of CooA. The crowded heme pocket is significant to rapid geminate rebinding and to prevent CooA from forming the five-coordinate heme, since the five-coordinated heme has no significance in function of CooA.

INTRODUCTION-

The first CO^1-sensing hemoprotein, CooA, acts as a DNA-binding transcriptional activator (Aono et al., 1996; Shelver et al., 1995, 1997). CooA is a homodimeric protein containing 222 amino acid residues (Shelver et al., 1995, 1997) and a *b*-type heme as a prosthetic group in each subunit (Aono et al., 1996; Shelver et al., 1997). In both ferrous and CO-bound CooA, the heme is six-coordinate low spin and has a histidine as one of the axial ligands (Shelver et al., 1997; Aono et al., submitted; Uchida et al., submitted). CooA can bind to the specific DNA site only in the presence of CO, but not in the absence of CO. Although the six-coordinated heme has been also encountered in cytochromes *b* and *c*, these cytochromes cannot bind CO to form a ferrous CO adduct under the physiological condition. For ligand binding, it is required that the ligand binding site is vacant in the absence of ligands. Hemoproteins involved in oxygen transport, such as hemoglobin and myoglobin, and in reduction or activation of oxygen, such as cytochrome *c* oxidase or cytochrome P450, have a heme in which the sixth position is vacant for exogenous ligand binding in a ferrous form. The six-coordinated heme in the absence of CO is unusual for reversible CO binding. However, CO binding to the ferrous heme induces the conformational change to the specific DNA binding form. Therefore, to know the CO binding mechanism to ferrous CooA is notable.

In this study, two approaches were applied to evaluate the CO binding mechanism of CooA. Overall CO association rate was obtained by a stopped flow method. Rapid mixing ferrous CooA with CO by the stopped flow apparatus can determine the overall rate of forming the CO-complex from ferrous CooA. Stopped flow method can give the rate constants for CooA in the DNA-unbound form. Laser photolysis method can provide the CO rebinding rate to photolyzed CooA. The rebinding reaction within 1 μs after photolysis, which is referred to as geminate recombination, gives an information on the distal heme pocket. Laser photolysis method provides CO binding rate constants in the DNA binding form of CooA. These approaches would revealed the CO association properties and the heme environmental structure of CooA.

MATERIALS AND METHODS

Protein Purification. The protein expression and preparation were performed as previously described (Aono et al., 1996, 1997; Uchida et al., submitted). The recombinant CooA was expressed in *E. coli* JM109 and

purified by FPLC using a Q-Sepharose (Pharmacia) ion-exchange column at the first step. The appropriate fractions were pooled, concentrated, and applied to a Chelating Sepharose (Pharmacia). The fractions containing CooA were concentrated and loaded to a HR 16/50 gel-filtration column (Pharmacia). Reduced CooA was prepared by adding a slight excess (ca. 10-fold) of freshly prepared dithionite solution (10 mM) to the protein solution (5 μM) under argon atmosphere. CO-bound CooA was prepared by introducing gaseous CO into the reduced sample.

Stopped Flow Experiment. Measurements of the overall CO association rate constants to ferrous CooA were carried out with a stopped flow spectrophotometer at 20 °C. Ferrous CooA (5 μM on the basis of heme content) in 50 mM Tris-HCl, 10 mM dithionite, pH 8.0 was mixed anaerobically with an equal volume of the same buffer containing various concentrations of CO (0.2, 0.4, 0.6, 0.8, and 1.0 mM). The dissolved O_2 in the sample solution was depleted by flowing N_2 gas in a reservoir of the stopped flow mixer. In another reservoir, the buffer solution containing 10 mM dithionite was bubbled with a gas mixture of N_2 and CO. CO concentration was controlled by using a gas mixer (ESTEC Model SGD-XC-0.5 L), for at least 15 min. The time courses were monitored at 431 nm (the absorption maximum in the difference spectra obtained by subtraction of the spectra for CO-bound form from fully reduced form). Signals were detected in transmission by using a photomultiplier (Hamamatsu Photonics, R2949) and the transient signals were digitized by a Tektronix TDS-520A oscilloscope. The data were transferred to a NEC PC-9801BX4/U2 computer for further data analysis.

The time courses were fitted with a single exponential curve,

$$\Delta A_t = \Delta A_0 \exp(-k_{app(ass)}\, t)+C \qquad (1)$$

where ΔA_t is the absorbance change at any time t, ΔA_0 is the total absorbance change (absorbance at $t = 0$ minus absorbance at $t = \infty$) and C is a constant. $k_{app(ass)}$ is the observed pseudo-first order rate constant.

Apparent rate constants satisfies the equation 2 (Antonini & Brunori, 1971),

$$k_{app(ass)} = k_{on(ass)}[CO]+k_{off} \qquad (2)$$

where $k_{on(ass)}$ is the CO association rate constants and k_{off} is the CO dissociation rate constants.

Laser Photolysis Experiment. The CO rebinding rate constants were obtained by a laser photolysis apparatus as previously described in detail (Adachi & Morishima, 1989; Adachi et al., 1992; Uchida et al., 1997). We used 4–6-ns full-width at half-maximum (FWHM) pulses from a Q-switched Nd:YAG laser for the experiment. The incident energy was about 10 mJ at the wavelength maximum of 532 nm. The absorption changes were monitored by a continuous, weak probe beam from a 150-W xenon arc lamp passed through a monochromator. The probe light at 420 nm (the absorption minimum in the difference spectra obtained by subtraction of the spectra for fully reduced form from CO-bound form) was focused onto the slit of a monochromator (UNISOKU USP-501) and was measured with a photomultiplier (Hamamatsu Photonics, R2949). The detector output was digitized with a 500 MHz oscilloscope (Tektronix TDS-520A). The data were transferred to a NEC PC-9801BX4/U2 computer for further data analysis and converted to change in absorbance. The protein concentration was about 5 μM on the basis of heme content. The buffer conditions were 50 mM Tris-HCl, pH 8.0, at 20 °C. Traces for 250 laser shots were averaged. The time courses for milli- to microsecond experiments were analyzed by fitting to the following equation,

$$\Delta A_t = \sum_{i=1}^{3} A_i \exp(k_{\mathrm{app}i} t) + C \qquad (3)$$

where ΔA_t is the absorbance change at any time t, A_i is amplitude factor, and C is a constant. $k_{\mathrm{app}i}$ is the observed pseudo-first order rate constant. The measurements were carried out under various CO concentrations (0.2, 0.4, 0.6, 0.8, and 1.0 mM) controlled by using the gas mixer.

Apparent rate constants satisfies the equation 4 (Antonini & Brunori, 1971),

$$k_{\mathrm{app}i} = k_i[\mathrm{CO}] \qquad (4)$$

where k_i is the CO rebinding rate constants.

Transient difference spectra were obtained to plot the absorbance changes which were observed at various single wavelength as a function of wavelength.

The time courses in the time range from 10 ns to 1 μs after photolysis, which were referred to geminate recombination, were analyzed by fitting to the following equation,

$$\Delta A_t = \phi_{g1} \exp(-k_{g1}\, t) + \phi_{g2} \exp(-k_{g2}\, t) + C \qquad (5)$$

where ϕ_{g1} and ϕ_{g2} are the geminate yields, k_{g1} and k_{g2} are the geminate rate constants, and C is a constant.

RESULTS

Overall CO Association Reaction to Ferrous CooA Observed by a Stopped Flow Apparatus. To obtain the overall CO association rate constants, we monitored the absorbance change after mixing the six-coordinated ferrous CooA solution with the CO-saturated buffer solution ([CO] = 1.0 mM) at pH 8.0, 20°C. The time course after the rapid mixing operated by a stopped flow apparatus is illustrated in Figure 1 (*lower panel*). The absorbance change was fitted with a single exponential and the residuals from a single exponential (equation 1) are also presented in Figure 1 (*upper panel*). They showed a random distribution. The apparent rate constant was estimated as 0.07 ± 0.01 s^{-1} at a CO concentration of 1.0 mM, which is abnormally slow association rate constant comparing with those of oxygen transport and storage proteins, hemoglobin and myoglobin (0.5–2 x 10^3 s^{-1}) (Antonini & Brunori, 1971). Although horseradish peroxidase also exhibits (3-4 s^{-1}) the slowest recombination rate among other hemoproteins (Coletta et al., 1986; Meunier et al., 1995), the apparent association rate of CO to ferrous CooA was still *ca.* 30-fold slower.

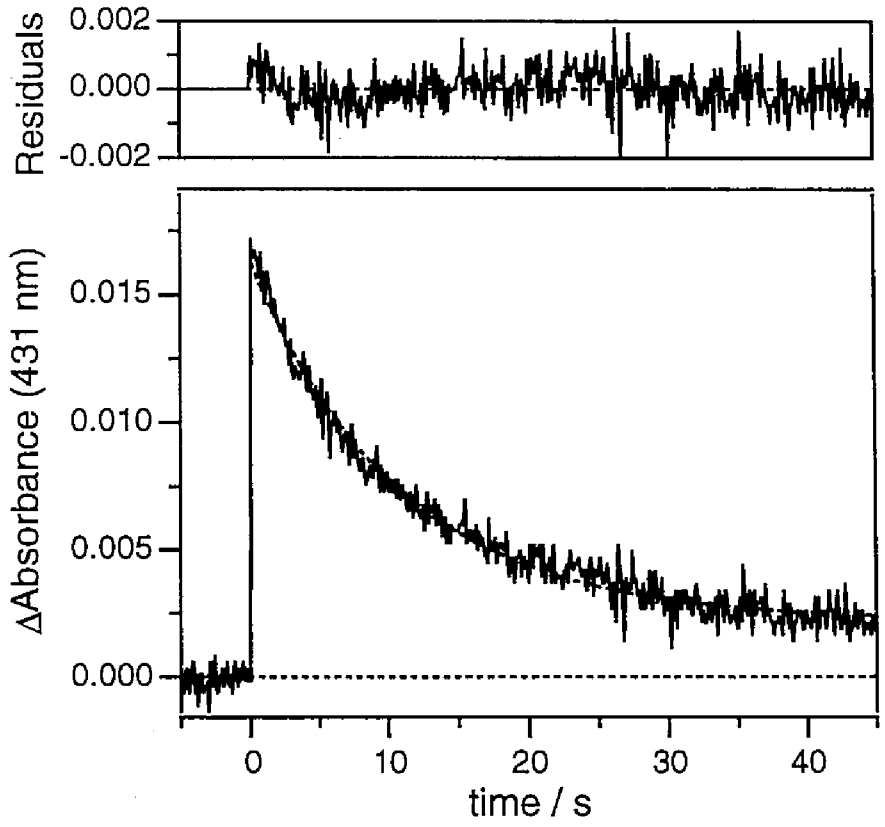

Figure 1. A solution of 5 μM ferrous CooA was rapid-mixed at 20 °C with 50 mM Tris-HCl, pH 8.0 buffer containing CO. *Bottom panel*, stopped flow traces for the reaction of ferrous CooA with CO saturated buffer. *Top panel*, residuals of 2-exponential fitting from the experimental data. The time course were monitored at 431 nm.

We investigated the dependence of the CO association rate constants on CO concentration under 0.2, 0.4, 0.6 and 0.8 mM as well as 1.0 mM to determine the rate-order of the overall CO association reaction. The apparent rate constants are plotted as a function of CO concentration in Figure 2. As shown in Figure 2, the apparent rebinding rates linearly changed with CO concentration, which indicates that the overall CO association reaction is the pseudo-first order reaction containing CO concentration because of excess of ligand concentration. The estimated overall association rate constant, $k_{on(ass)}$, by using the equation 2 is 0.036 ± 0.03 $mM^{-1}s^{-1}$, which is quite slower than CO rebinding rates of hemoglobin and myoglobin (0.5–2 x 10^3 $mM^{-1}s^{-1}$) by ~10^5-fold (Antonini & Brunori, 1971). The estimated dissociation rate constants is 0.035 ± 0.002 s^{-1}, which is comparable to those of myoglobin and hemoglobin (~0.02 ± 0.00 s^{-1}) (Antonini & Brunori, 1971).

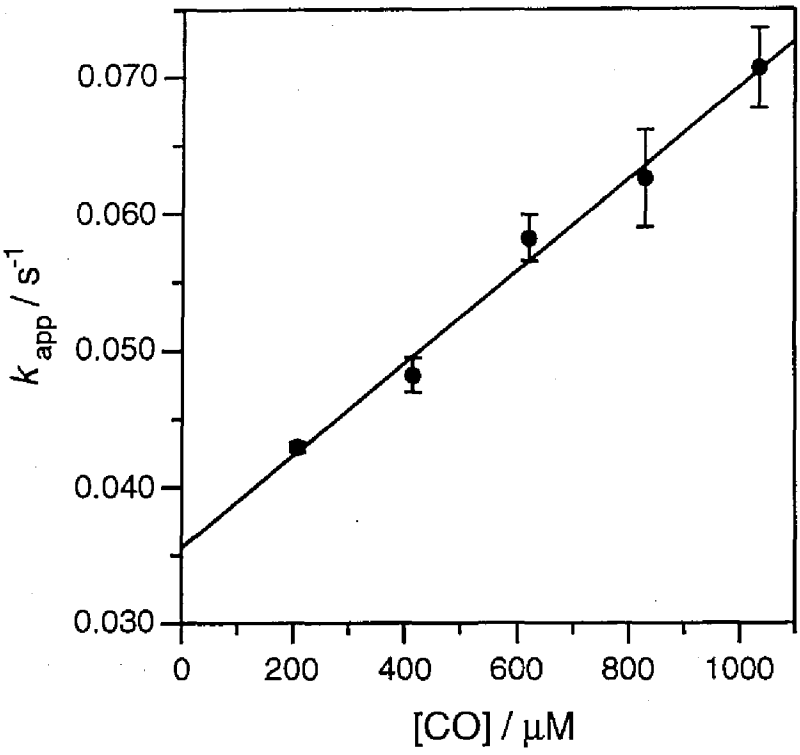

Figure 2. CO concentration dependence of the apparent CO association rate constants obtained by stopped flow apparatus.

Transient Spectra of CO Association to ferrous CooA by Stopped Flow Methods. To determine whether overall CO association reaction involves some intermediates, we observed the transient absorption difference spectra. The transient absorption difference spectra in the Soret region after mixing the ferrous CooA and CO saturated buffer solutions are shown in Figure 3. The transient difference spectra resemble the difference spectrum between ferrous and CO-bound CooA. There is bleaching near 420 nm, where CO-bound six-coordinated species would absorb, and positive absorbance at about 430 nm, which would be attributed to the absorption by the ferrous six-coordinated species. An isosbestic point was observed at 432 nm. The clear isosbestic point and monophasic decay of the CO association reaction suggest that the CO association reaction to ferrous CooA occurs without any detectable intermediate at 100 ms resolution.

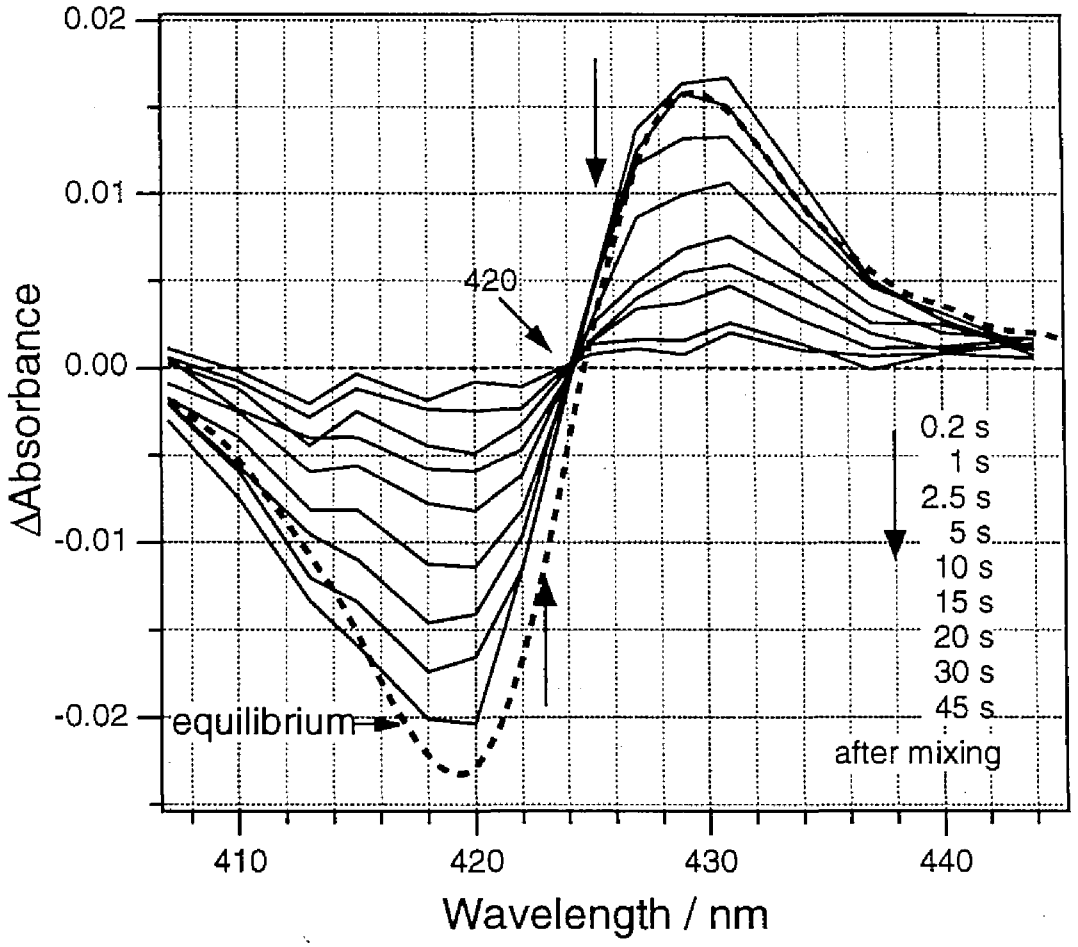

Figure 3. Transient difference spectra of CooA after rapid mixing with ferrous CooA and CO saturated buffer, which derived from single wavelength stopped flow analysis. The experimental conditions are same as those in Figure 1. The difference spectra is obtained by subtraction of the spectra for CO-bound CooA from fully reduced CooA. The transient spectra was illustrated at 2 nm resolution.

CO Rebinding Reaction to CooA Measured by Laser Photolysis. To determine the rate constants for CO binding to the five-coordinated heme, laser photolysis measurements were carried out. Time courses for CO recombination to photolyzed CooA are shown in Figure 4. As previously reported (Uchida et al., submitted), CO rebinding reaction in the range of 10^{-5}–10^{-3} s after photolysis consists of at least three exponential decays. The apparent rate constants are estimated by fitting the time courses to the 3-exponentials (equation 3)[2]. Figure 4 shows residuals from 2 or 3 exponentials in the middle and top panel, respectively, representing that better fitting can be obtained by the 3-exponentials[3]. Each apparent rate constant showed linear dependence on CO concentration, indicating that

all the three processes are bimolecular reaction (data not shown). The rate constants are k_1 = 32 $\mu M^{-1}s^{-1}$ (51%, relative population of the phase to total photolysis), k_2 = 6.8 $\mu M^{-1}s^{-1}$ (30%), and k_3 = 1.2 $\mu M^{-1}s^{-1}$ (15%). These rate constants are summarized in Table I. The three rate constants of CooA are close to those of other oxygen transport proteins, hemoglobin, myoglobin and their mutants (0.5–25 $\mu M^{-1}s^{-1}$) (Antonini & Brunori, 1971; Springer et al., 1994). This indicates that the reactivity of the heme iron for CooA itself is comparable to the other heme proteins, although the CO association reaction rate is substantially slower.

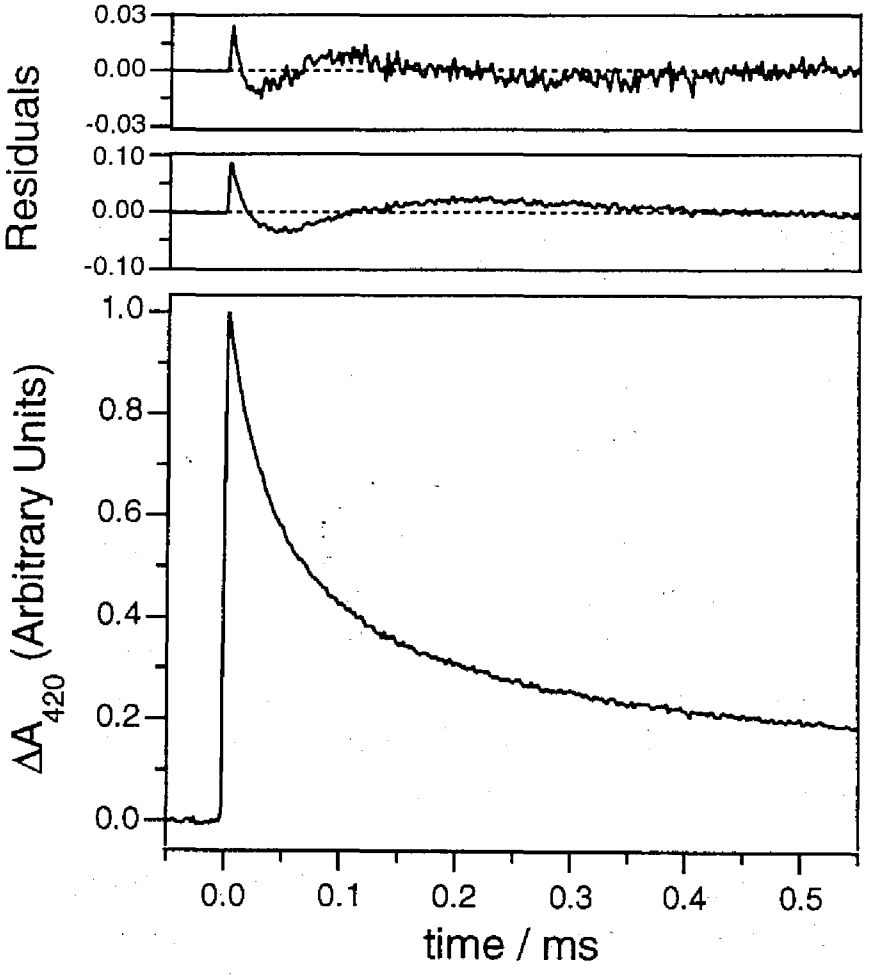

Figure 4. *Bottom panel*, observed time course for CO binding to CooA after photolysis. *Middle panel*, residuals of 2-exponential fitting from the experimental data. *Top panel*, residuals of 3-exponential fitting from the experimental data. The time course were monitored at 420 nm at 20 °C. Sample contains about 5 μM protein in 50 mM Tris-HCl, pH 8.0. Traces for 250 shots were averaged.

TABLE I: Kinetic Parameters for CO Bimolecular Rebinding to CooA and Other Heme Proteins at 20 °C.

Protein	k_1	k_2	k_3
		$\mu M^{-1}s^{-1}$	
CooA	32 ± 1	6.8 ± 0.5	1.2 ± 0.1
	$(51 \pm 4)^a$	(30 ± 2)	(15 ± 3)

[a] Values in parentheses represent percentage of the relative population.

There was a very fast rebinding process, referred to as geminate rebinding with a half-life on the order of 20 ns. Geminate rebinding reflects the heme distal pocket structure (Tian et al., 1995).

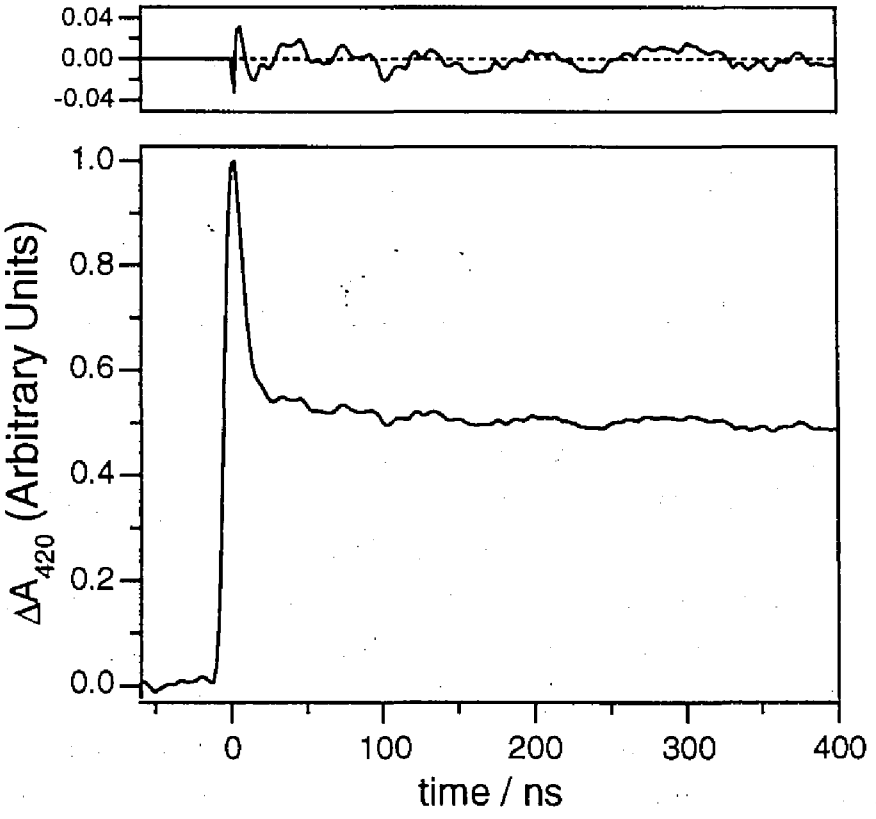

Figure 5. Time courses for CO binding to CooA after photolysis for the geminate region. The time course are monitored at 420 nm at 20 °C. Traces for 2000 shots were averaged. Sample contains about 5 μM protein in 50 mM Tris-HCl, pH 8.0.

The time course of the geminate reaction for the CO rebinding to CooA is illustrated in Figure 5 (*lower panel*). The time course was fitted to a double-exponential curve (equation 5). Residuals from double-exponentials are illustrated in Figure 5 (*upper panel*) and exhibit a random distribution, indicating that a sum of the two exponentials are required to fit the time course. The geminate rebinding rates and yields were calculated, and are listed in Table II. The first geminate rate (k_{g1} = ~130 μs^{-1}) is significantly faster than those for other heme proteins (3–46 μs^{-1}), such as myoglobin (Henry et al., 1983; Gibson et al., 1986), hemoglobin (Hofrichter et al., 1983; Campbell et al., 1984, 1985; Olson et al., 1987; Unno et al., 1990, 1991), and P450 (Tian et al., 1995). The geminate rate constants of CooA is comparable to that for P420 (150 μs^{-1}) (Tian et al., 1995). The geminate yield of CooA (~0.5) is much larger than those of myoglobin (~0.05) (Henry et al., 1983; Gibson et al., 1986) and P450 with camphor (~0.025) (Tian et al., 1995).

TABLE II: Kinetic Parameters for CO Geminate Rebinding to CooA and Other Heme Proteins at 20 °C

Protein	k_{g1}	ϕ_{g1}	k_{g2}	ϕ_{g2}
	μs^{-1}		μs^{-1}	
CooA	130	0.47	4.1	0.04

Transient Difference Spectra of CO Rebinding to CooA by Laser photolysis. To confirm whether CO rebinds to the five-coordinated heme following photolysis, we observed the transient absorption difference spectra. Figure 6 illustrates the transient absorption difference spectra in the Soret region, comparing with the two equilibrium difference spectra; between deoxy and CO-bound myoglobin, and between ferrous six-coordinated and CO-bound CooA. The transient difference spectra of CooA resemble the difference spectra between five-coordinated ferrous and carbonmonoxy myoglobins, rather than that between six-coordinated and CO-bound CooA. The bleaching around 420 nm for the transient spectra is caused by the dissociation of iron-bound CO from the heme by photolysis, since CO bound CooA has the Soret absorption maximum at 422 nm (Aono et al., 1996; Shelver et al., 1997). On the other hand, the positive absorption around 436 nm originated from the five-coordinated species, not from the six-coordinated species, since the Soret maximum of

the five-coordinated deoxy myoglobin which has a neutral histidine as an axial ligand same as CooA is 436 nm (Antonini & Brunori, 1971), while six-coordinated ferrous CooA has the Soret maximum at 426 nm (Aono et al., 1996; Shelver et al., 1997). The transient difference spectra of CO rebinding did not show an isosbestic point due to the three component with different association rates, which suggests heterogeneity of the CO binding sites.

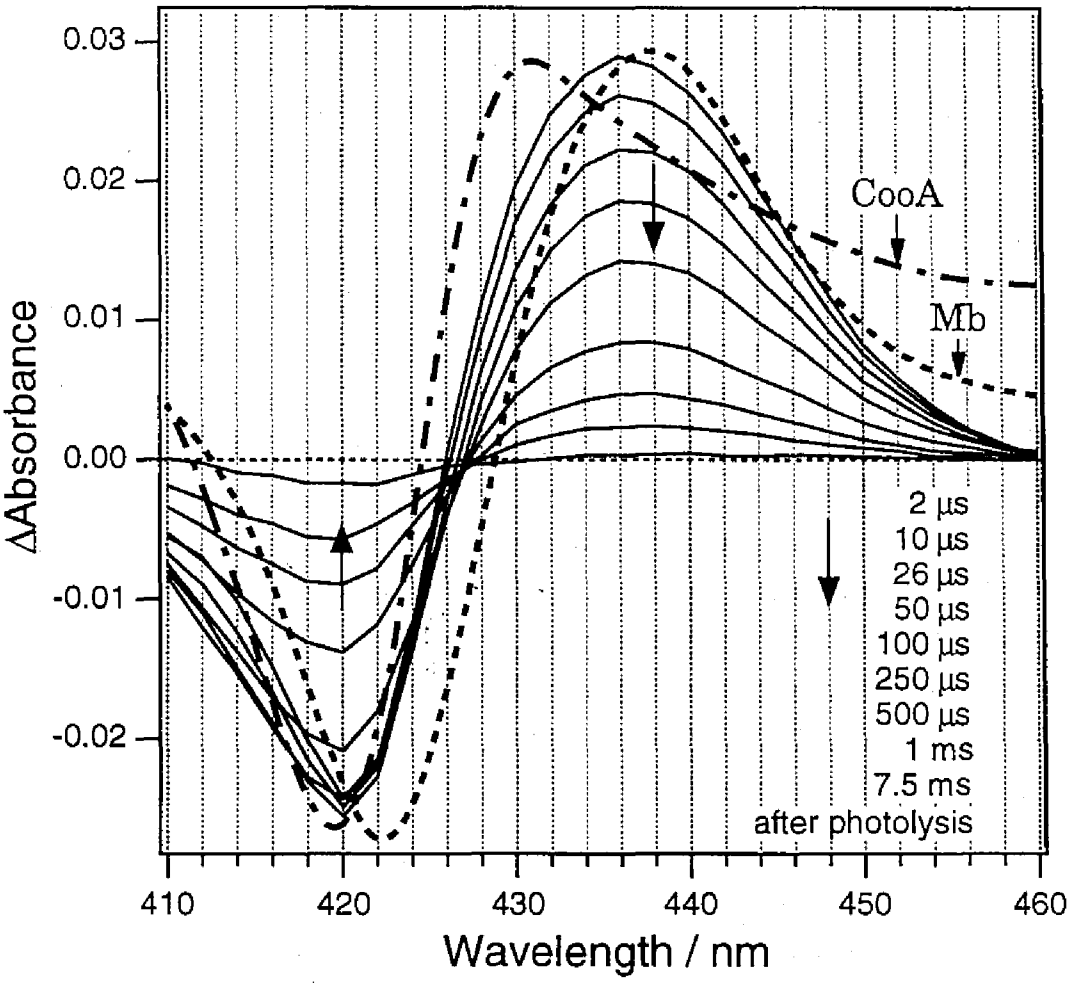

Figure 6. Transient difference spectra of CooA after photolysis derived from single wavelength analysis. The experimental conditions are same as those in Figure 4. The difference spectra is obtained by subtraction of the spectra for CO-bound CooA from fully reduced CooA. The transient spectra was illustrated at 2 nm resolution.

DISCUSSION

CO Association Mechanism to Ferrous CooA. The CO association reaction to ferrous CooA is substantially slower than those of the other hemoproteins, such as myoglobin, hemoglobin, and oxidases. However, bimolecular CO rebinding rates after photolysis is comparable to those of myoglobin. These indicate that the reactivity of the heme iron of CooA for CO is not low, and quite slow CO association of the CooA is attributed to the coordination structure of ferrous CooA, that is, replacement of the axial ligand.

For CO binding to the six-coordinated heme, the bond between the axial ligand and the heme iron must be disrupted. However, we could not observe the transient five-coordinated heme by the overall CO association reaction and resonance Raman spectra. Time-resolved difference spectra of CO association reaction to ferrous CooA has an clear isosbestic point at 420 nm at 100 ms resolution and no absorption maximum at 436 nm which corresponds to the Soret maximum of the five-coordinated myoglobin (Figure 3). In addition, an intense laser excitation without any rotations of the Raman cell produced no resonance Raman line for the five-coordinated Fe-His stretching and only increased the six-coordinated ferrous species, which showed the presence of ferrous six-coordinated species. (data not shown) These results indicate that the transient five-coordinated heme is so unstable that the dissociated axial ligand rapidly rebinds to the heme iron (k_{21} in scheme 1 is quite larger) and cannot be observed on millisecond order. CO association reaction to ferrous CooA revealed the instability of the five-coordinated heme in CooA.

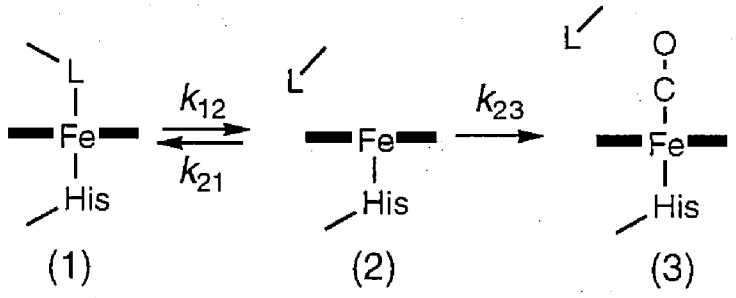

SCHEME 1

Significance of the Unstable Five-coordinated Heme of CooA. Instability of the five-coordinated heme in the bis-ligated hemoprotein has been already encountered in cytochromes b_5 and c. The disruption of the Fe-His and Fe-Met bonds in cytochromes b_5 and c, respectively, was observed after picosecond laser excitation (Jongeward et al., 1988).

However, the axial ligands rebind to the heme iron on the picosecond time region and CO rebinding could not compete with axial ligand rebinding. These results indicate that when one of the axial ligands is dissociated from the heme iron in these proteins, the axial ligand rebinds so fast that CO cannot bind to the heme iron. Indeed, photolysis of the ferrous CooA by 4–6 nanosecond laser pulse caused no absorbance changes from 10 nanosecond to ~1 second (data not shown). Even if the Fe-axial ligand bond of CooA is disrupted by photolysis, the five-coordinated heme is so unstable that the Fe-axial ligand rebinds within 10 ns prior to the CO association.

The fast geminate rebinding rate constants and large geminate yields of CooA (Figure 5) also reflect instability of the five-coordinated heme. The geminate yield for CooA (51%) is an important feature of the CO rebinding (Table II), comparing with that of myoglobin (~5%) (Henry et al., 1983; Gibson et al., 1986). Geminate rebinding to myoglobins has been extensively studied and it is proposed that the geminate yields mainly depend on the distal heme environment, rather than on the proximal axial ligand (Quillin et al., 1995; Olson & Phillips, 1996). The free space of the heme pocket can affect the geminate yields: Val68→Phe mutation reduced free space of the heme pocket, resulting in the increase in the geminate yield by about 50% (Quillin et al., 1995). In addition, benzohydroxamic acid (BHA) binding to horseradish peroxidase binds close to the heme iron, resulting in the picosecond geminate yields of the CO rebinding from 20 to 90% by binding (Berinstain et al., 1990). These indicate that the large geminate yield of CooA is attributed to the crowded heme pocket of CooA. The increase in geminate yield of CooA from 51 to 64% upon addition of the target DNA (results not shown) supports that the crowded heme pocket increase the geminate yield. Resonance Raman spectra of CO-bound CooA in the presence of the target DNA increased in the A_3 conformer and decrease in the A_0 conformer (Uchida et al., submitted). Previous studies with respect to the C-O stretching frequency of iron-bound CO in the resonance Raman and IR spectra revealed that the A_0 conformer is open conformer and the A_3 conformer is close conformer (Morikis et al., 1989; Oldfield et al., 1991; Ray et al., 1994; Li et al., 1994). The increase in the A_3 conformer in the presence of DNA implied that CooA converted the open conformer to the close conformer by the specific DNA binding, which indicates that the heme pocket becomes more crowded. The crowded heme distal pocket would repress the axial ligand from leaving from the heme iron by its steric inhibition. Probably, it is

preferred for CooA to inhibit the axial ligand from dissociating from the heme iron to prevent activation in the absence of CO. These would lead to a more crowded heme distal pocket and larger geminate yield of CooA.

Discrimination of the CO Binding. The distal sites of the hemoproteins have inherent features related to their functions. Geminate yields for CO rebinding to heme protein are related to the discrimination of toxic CO. Geminate yield of CO binding to myoglobin is too small (~5%) at 20 °C in aqueous solution (Henry et al., 1983). Myoglobin bearing a larger heme pocket has a ligand docking site, which traps the dissociated ligand, within a few angstrom from the heme iron. This docking site facilitates inhibition of toxic CO ligands from rebinding by orientational and spatial constrains (Lim et al., 1995, 1997). The trapped CO in the docking site does not bind to the heme iron, but escape to the solvent. This leads to a slight geminate yield of myoglobin. Geminate rebinding to P450 in the presence of camphor is the similar case to that of myoglobin. In the presence of the camphor, P450 showed only ~2% geminate yield. On the other hand, 90% geminate yield was observed in the absence of camphor (Tian et al., 1995). When camphor is present, P450 combines with molecular oxygen and incorporates one of the atoms of molecular oxygen into substrates (Ullrich, 1979; White & Coon, 1980; Guengerich & Macdonald, 1984). Since CO binding competes with O_2 binding and inhibits the reaction, P450 in the presence of substrates should require the CO discrimination mechanism as myoglobin, resulting in a quite small geminate yield *via* alternation of the heme distal pocket (Tian et al., 1995).

The CO discrimination mechanism using such ligand docking sites may be dispensable for CooA, since CooA can grow under anaerobically condition and utilizes CO. However, it is required that CooA discriminates O_2 and CO to avoid the initiation for the transcription by O_2. Resonance Raman spectra revealed that CooA has a O_2 discrimination mechanism (Uchida et al., submitted). Indeed, stable oxy-CooA cannot be formed (Aono et al., 1996), which is related to the distal structure of CooA. IR spectra of CO-bound CooA mainly consist of the A_0 conformer, which means the absence of interaction between the iron-ligated CO and amino acid within the heme pocket (Morikis et al., 1989; Ray et al., 1994; Li et al., 1994). Most oxygen carrier or storage proteins, such as hemoglobin and myoglobin, have a histidine in the distal pocket which is hydrogen bonded to the iron-bound oxygen and stabilized O_2 binding form (Phillips et al., 1980; Phillips & Schoenborn, 1981). Disruption of the hydrogen bond

between the distal amino acid and the iron-coordinated O_2 leads to a decrease in O_2 dissociation and autooxidation rates (Olson et al., 1988; Mathews et al., 1989; Rohlfs et al., 1990). The lack of the interaction between the iron-bound ligand and distal amino acid results in the unstable O_2 bound form of CooA.

Comparing with CooA and CRP. CooA is a family of the transcriptional regulators, cAMP receptor protein (CRP), and shows high homology with CRP (28% identical, 51% similar) (Kerby et al., 1995). Comparing the activity of the CooA with that of CRP, the most prominent difference between CooA and CRP was the specific DNA-binding activity in the absence of effector. CooA can bind the specific DNA only in the presence of CO and cannot bind to the DNA in the absence of CO (He et al., 1996; Shelver et al., 1997), while CRP can slightly bind to the specific binding site even in the absence of cAMP (Fried & Crothers, 1984). This difference may originate from the structure of the effector binding site and a manner of the effector binding. In CooA, CO is recognized by the heme iron through a single covalent bond, and CO binding site is stoppered by the axial ligand when the effector is absent. In addition, as described above, the five-coordinated heme of CooA is quite unstable and cannot be observed at the physiological condition. These properties of CooA is useful to the distinct switch for turning on and off the transcription of genes. On the other hand, cAMP in the CRP is recognized by the several amino acids (Gly71, Glu72, Ser83, Thr127, and Ser128) through many non-covalent bonds (Weber & Steitz, 1984; Gronenborn et al., 1988; Belduz et al., 1993; Lee et al., 1994). It is likely to be difficult to fill such a large cavity and may form a vacant pocket when cAMP is absent. Therefore, the distinction between the presence and absence of cAMP for CRP is more ambiguous than that of CooA. These features of CRP may lead to the slight DNA binding affinity even in the absence of cAMP.

In summary, the present data indicate that the five coordinated heme of CooA is quite unstable. In the CO association reaction to ferrous six-coordinated CooA, five-coordinated intermediate was not observed by stopped flow spectrophotometer at a resolution of 100 ms. Since the five-coordinated heme is ambiguous whether it means turning on or off the switch for transcription of genes, it does not preferred for function of CooA. More crowded heme pocket, revealed by large geminate yield and resonance Raman spectra, may inhibit the axial ligand from dissociating from the heme iron and forming the five-coordinated heme.

FOOTNOTES

[1] The abbreviations used are: CO, carbon monoxide.

[2] Although quite a slow phase (~1 s^{-1}) was observed within a few percent of the total photolysis, we neglected this phase because of small amplitude and discussed only the other faster three components.

[3] The residuals form the three-exponentials showed a little deviation from the random distribution due to the contribution of the forth, slowest phase.

REFERENCES

Adachi, S., & Morishima, I. (1989) *J. Biol. Chem. 264*, 18896-18901.

Adachi, S., Sunohara, N., Ishimori, K., & Morishima, I. (1992) *J. Biol. Chem. 267*, 12614-12621.

Antonini, E., & Brunori, M. (1971) *Hemoglobin and Myoglobin in Their Reactions with Ligands*, North Holland Publishing Co., Amsterdam.

Aono, S., Nakajima, H., Saito, K., & Okada, M. (1996) *Biochem. Biophys. Res. Commun. 228*, 752-756.

Aono, S., Matsuo, T., Shimono, T., Ohkubo, K., Takasaki, H., & Nakajima, H. (1997) *Biochem. Biophys. Res. Commun.* in press.

Belduz, A. O., Lee, E. J., & Harman, J. G. (1993) *Nucleic. Acids. Res. 21*, 1827-1835.

Berinstain, A. B., English, A. M., Hill, B. C., & Sharma, D. (1990) *J. Am. Chem. Soc. 112*, 9649-9651.

Campbell, B. C., Sharma, V. S., & Magde, D. (1984) *J. Mol. Biol. 179*, 143-150.

Campbell, B. C., Magde, D., & Sharma, V. S. (1985) *J. Biol. Chem. 260*, 2752-2756.

Carver, T. E., Rohlfs, R. J., Olson, J. S., Gibson, Q. H., Blackmore, R. S., Springer, B. A., & Sligar, S. G. (1990) *J. Biol. Chem. 265*, 20007-20020.

Coletta, M., Ascoli, F., Brunori, M., & Traylor, T. G. (1986) *J. Biol. Chem. 264*, 9811-9814.

Fried, M. G., & Crothers, D. M. (1984) *J. Mol. Biol. 172*, 241-262.

Gibson, Q. H., Olson, J. S., McKinnie, R. E., & Rohlfs, R. J. (1986) *J. Biol. Chem. 261*, 10228-10239.

Gronenborn, A. M., Sandulache, R., Gartner, S., & Clore, G. M. (1988) *Biochem. J. 253*, 801-807.

Guengerich, F. P., & Macdonald, T. L. (1984) *Acc. Chem. Res. 17*, 9-16.

He, Y., Shelver, D., Kerby, R. L., & Roberts, G. P. (1996) *J. Biol. Chem. 271*, 120-123.

Henry, E. R., Sommer, J. H., Hofrichter, J., & Eaton, W. A. (1983) *J. Mol. Biol. 166*, 443-451.

Hofrichter, J., Sommer, J. H., Henry, E. R., & Eaton, W. A. (1983) *Proc. Natl. Acad. Sci. U.S.A. 80*, 2235-2239.

Jongeward, K. A., Magde, D., Taube, D. J., & Traylor, T. G. (1988) *J. Biol. Chem. 263*, 6027-6030.

Kerby, R. L., Ludden, P. W., & Roberts, G. P. (1995) *J. Bacteriol. 174*, 5284-5294.

Lee, E. J., Glasgow, J., Leu, S. F., Belduz, A. O., & Harman, J. G. (1994) *Nucleic. Acids. Res. 22*, 2894-2901.

Li, T., Quillin, M. L., Phillips Jr., G. N., & Olson, J. S. (1994) *Biochemistry 33*, 1433-1446.

Lim, M., Jackson, T. A., & Anfinrud, P. A. (1995) *Science 269*, 962-966.

Lim, M. H., Jackson, T. A., & Anfinrud, P. A. (1997) *Nature Struct. Biol. 4*, 209-214.

Mathews, A. J., Rohlfs, R. J., Olson, J. S., Tame, J., Renaud, J.-P., & Nagai, K. (1989) *J. Biol. Chem. 264*, 16573-16583.

Meunier, B., Rodriguezlopez, J. N., Smith, A. T., Thorneley, R. N. F., & Rich, P. R. (1995) *Biochemistry 34*, 14687-14692.

Olson, J. S., Rohlfs, R. J., & Gibson, Q. H. (1987) *J. Biol. Chem. 262*, 12930-12938.

Morikis, D., Champion, P. M., Springer, B. A., & Sligar, S. G. (1989) *Biochemistry 28*, 4791-4800.

Oldfield, E., Guo, K., Augspurger, J. D., & Dykstra, C. E. (1991) *J. Am. Chem. Soc. 113*, 7537-7541.

Olson, J. S., Mathews, A. J., Rohlfs, R. J., Springer, B. A., Egeberg, K. D., Sligar, S. G., Tame, J., Renaud, J.-P., & Nagai, K. (1988) *Nature 336*, 265-266.

Olson, J. S., & Phillips Jr, G. N. (1996) *J. Biol. Chem. 271*, 17593-17596.

Phillips, S. E. V. (1980) *J. Mol. Biol. 142*, 531-554.

Phillips, S. E. V., & Schoenborn, B. P. (1981) *Nature 292*, 81-82.

Quillin, M. L., Li, T. S., Olson, J. S., Phillips Jr, G. N., Dou, Y., Ikeda-Saito, M., Regan, R., Carlson, M., Gibson, Q. H., Li, H. Y., & Elber, R. (1995) *J. Mol. Biol. 245*, 416-436.

Ray, G. B., Li, X.-Y., Ibers, J. A., Sessler, J. L., & Spiro, T. G. (1994) *J. Am. Chem. Soc. 116*, 162-176.

Rohlfs, R. J., Mathews, A. J., Carver, T. E., Olson, J. S., Springer, B. A., Egeberg, K. D., & Sligar, S. G. (1990) *J. Biol. Chem. 265*, 3168-3176.

Shelver, D., Kerby, R. L., He, Y., & Roberts, G. P. (1995) *J. Bacteriol 177*, 2157-2163.

Shelver, D., Kerby, R. L., He, Y., & Roberts, G. P. (1997) *Proc. Natl. Acad. Sci. U.S.A. 94*, 11216-11220.

Springer, B. A., Sligar, S. G., Olson, J. S., & Phillips Jr., G. N. (1994) *Chem. Rev. 94*, 699-714.

Tian, W. D., Wells, A. V., Champion, P. M., Diprimo, C., Gerber, N., & Sligar, S. G. (1995) *J. Biol. Chem. 270*, 8673-8679.

Uchida, T., Unno, M., Ishimori, K., & Morishima, I. (1997) *J. Biol. Chem. 272*, 30108-30114.

Ullrich, V. (1979) *Top. Curr. Chem. 83*, 67-104.

Unno, M., Ishimori, K., & Morishima, I. (1990) *Biochemistry 29*, 10199-10205.

Unno, M., Ishimori, K., Morishima, I., Nakayama, T., & Hamanoue, K. (1991) *Biochemistry 30*, 10679-10685.

Weber, I. T., & Steitz, T. A. (1984) *Proc. Natl. Acad. Sci. U.S.A. 81*, 3973.

White, R. E., & Coon, M. J. (1980) *Annu. Rev. Biochem. 49*, 315-356.

PART V.

SUMMARY AND GENERAL CONCLUSIONS

In the present thesis, the author aimed to clarify the role of the protein dynamics in ligand binding to heme proteins. To understand the protein dynamics, most of the attention was focused on the ligand binding kinetics of myoglobin. The author utilized various techniques of the spectroscopies and site-directed mutagenesis to characterize the protein dynamics in ligand binding of myoglobin and CooA, and the results of the studies are highlighted below.

In Part II, the author described the effects of perturbation of protein dynamics by introducing an artificial linkage into myoglobin and by hydrostatic pressure on the ligand binding kinetics. In chapter 1, an intramolecular S-S bond was introduced at the EF corner of myoglobin. Although NMR, IR, and electronic absorption spectroscopies revealed that the introduction of the disulfide bond only induced minor structural deviations of the heme environmental structure, the CO rebinding rate obtained by laser photolysis was increased 0.98 to 1.8 $\mu M^{-1}s^{-1}$ by the S-S bond. The kinetic analysis based on the three-state model clearly showed that the ligand entry barrier was preferentially increased as compared with the bond formation barrier, suggesting that the fluctuation at the EF corner is one of the crucial determinants of the ligand entry barrier.

In chapter 2, hydrostatic pressure was applied to the ligand binding to wild type and the mutant myoglobins bearing a less hydrophobic amino acid residue (Ala, Gly, Ser) at position 29. The activation volumes ($\Delta V^{\neq}$) for CO binding to the three Leu29 mutants were positive (10–15 cm^3mol^{-1}), which is in sharp contrast to that of wild type myoglobin (-20 cm^3mol^{-1}). Previous studies reported that the prominent change in the activation volume form negative to positive value corresponds to the switch of the rate-determining step from the bond formation to the ligand migration. However, analysis of the unusual positive activation volume for the Leu29 mutants on the basis of the three-state model proposed that the positive $\Delta V^{\neq}$ was attributed to the large partial volume of the geminate state, not to the change of the rate-determining step. The perturbation of protein dynamics by hydrostatic pressure revealed that the volume of the geminate state for the Leu29 mutants particularly increased, indicating the presence of extra water molecules in the heme pocket. Comparison of the hydrophobicity at position 29 and the activation volume, the author proposed that the reduced hydrophobicity in the heme environment for the Leu29 mutants would facilitate the invasion of water molecules into the heme cavity and would result in an increase in the volume of the geminate state.

Part III is dealt with the roles of the amino acid constituting the heme pocket in the ligand binding kinetics. In chapter 1, the ligand binding kinetics for the three Leu29 (L29A, L29G, and L29S) mutants were investigated. The rate constants for CO and O_2 association were decreased by 3–5-fold, which were correlated with the hydrophobic index of the amino acid residue. Electronic absorption and infrared spectroscopies suggested the presence of water molecules in the heme pocket of these proteins, which might inhibit the ligand binding. As suggested in chapter 2 of Part II, these results also imply that the hydrophobicity of the heme pocket is one of the key factors in regulating the ligand binding to the heme iron to avoid invasion of the water molecules into the heme pocket.

In chapter 2, to further investigate the role of the amino acid within the heme pocket in ligand binding to myoglobin, we focused on the electrostatic interaction between the distal histidine and Thr67 in the protein dynamics. Although NMR, IR, and laser photolysis of the Val mutant showed that the electrostatic interactions of Thr67 and the distal histidine are not essential for the heme environmental structure and ligand binding process, Thr67→Asn or Asp substitutions changed the IR spectra of carbonmonoxy forms, indicating that some electrostatic interactions to the distal histidine can be formed by the amino acid located at position 67. The kinetic barrier for ligand entry was increased by the mutation to Asn or Asp, while that for bond formation was decreased. These observations suggest that the amino acid residue at position 67 can affect the position and/or electronic structure of the distal histidine by the electrostatic interactions with the distal histidine, which would be one of the perturbation to the hydrophobicity of the heme environment and would result in the change of the ligand binding property in myoglobin.

The approach the author has applied to myoglobin was also useful to examine the dynamics of other proteins. Part IV described the CO binding properties of CooA, a novel hemoprotein of transcriptional activator. In chapter 1, resonance Raman spectra revealed that in both ferrous and CO-bound CooA, the heme was six-coordinate low spin and histidine is one of the axial ligands. The C-O stretching frequency at 487 cm^{-1} corresponds to an "open" conformer as found for myoglobin, in which the replaced axial ligand in the ferrous state does not interact with the iron-bound CO due to the large structural alteration by binding CO to the heme iron. The finding that the CO binding to the heme iron induces such structural changes near the CO binding site suggests that the CO

binding can be utilized as a trigger for the conformational transition into the DNA binding form.

The CO binding kinetics for CooA was examined in chapter 2. The overall CO association reaction to ferrous CooA was monophasic and the rate constant was 3.6×10^{-5} $\mu M^{-1}s^{-1}$, which depended on CO concentration. The five-coordinate heme produced by dissociation of the axial ligand cannot be observed by stopped flow and resonance Raman spectra at millisecond time resolution. The transient five-coordinate heme was only detected by photolysis and its a half-life was in the order of 20 ns. The geminate recombination rate for CooA protein was quite fast and the geminate yields was also extremely high. Such unstable five-coordinate state would have some advantages in the quick structural changes by CO binding, which is crucial for the gene regulation.

In the present thesis, the author examined the ligand binding reaction for myoglobin and CooA to shed new light on the role of the protein dynamics in its biological function. As discussed in this thesis, dynamic properties of the protein are one of the crucial key factors for protein functions. The author disclosed several new aspects of the dynamical features of myoglobin, such as hydrophobicity of the heme pocket, the electrostatic interaction between the distal histidine and Thr67, and the structural change at the EF corner. The author hopes that the results and discussion in this thesis will contribute to the better understanding of protein dynamics.